Paper ID: KL-01

Advances in Magnetic Suspension Technology --- Towards Smart Mechatronics ---

Takeshi MIZUNO
Saitama University
E-mail: mizar@mech.saitama-u.ac.jp

Abstract

Several recent advances in magnetic suspension technology leading to smart mechatronics are reported. The magnetic suspension system using the attractive force of an electromagnet needs servo action to achieve stable suspension. It gives advantages and drawbacks to such magnetic suspension systems. Recent works making the use of the advantages and/or overcoming the drawbacks are presented.

Keywords: magnetic suspension, magnetic bearing, mechatronics

1. Introduction

Magnetic suspension generates force for suspension through magnetic fields. There is no contact between stator and floator so that no mechanical friction and wear are expected in operation even without lubrication. This advantage has already given rise to a lot of industrial applications such as Maglev system [1, 2], and active magnetic bearing (AMB) for complete contact-free suspension of a rotating object [3-6]. The most successful application is turbomolcular pump. In this application, AMB-based instruments are dominant.

However, the full potential of industrial applications has not been acheived yet. To fully utilize this unique technology, technical innovations and advances are still necessary althogh some people may consider this technology to be rather mature.

This report presents several recent innovations and advances in magnetic suspension technology. Because it is far beyond the author's ability to cover the whole aspects of magnetic suspension technology, an overview of technological fundamentals is presented first, which is followed by reports on the recent works of the author and a comment on *"toward smart mechatronics"*.

2. Fundamentals

There are various combinations of material in supporting magnet and suspended body to achieve magnetic suspension [1, 6]. The method mostly used in industrial applications utilizes the attractive force of an electromagnet. Figure 1 shows a basic actively controlled magnetic suspension system that consists of the following components:

- object to be suspended (floator)
- electromagnet to produce suspension force
- sensor to detect the displacement of the floator
- electronic analog or digital controller
- power amplifier to feed current to the windings of the electromgnet

This system is inherently unstable in the normal direction. Stable action can be achieved by sensing the position of the rotor and controlling the force fields to prevent the floator from departing from its desired position with sufficient rapidity; increase the current when the air gap is too large, decrease the current when the air gap is too small. The necessity of such servo action gives advantages and drawbacks to active magnetic suspension system.

One of the advantages is the capability of achieving various functions that are impossible for conventional mechanical suspension. For example, unbalance compensation is one of the unique characteristics of magnetic bearings; harmonic forces due to the imbalance are effectively compensated by the magnetic forces [7, 8]. Applicability to measurement systems is another advantage; when the integral-like action is implemented, the force acting on the floator can be estimated from the control input. This function is utilized in the identification of rotor dynamics and wind tunnels (see Section 3) [9, 10]. It is also possible to combine other functions with

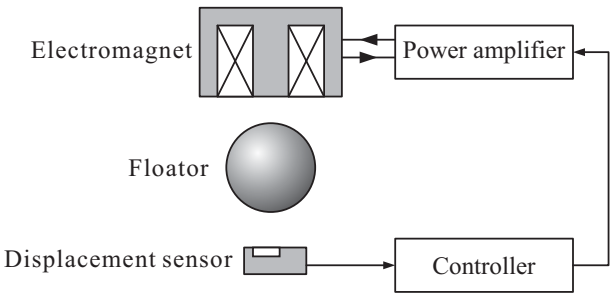

Fig.1. Basic structure of active magnetic suspension system

suspension. One of them is to combine motor function, which is called as self-bearing motor or bearingless motor [6]. We apply such system to wind tunnel suspension that is treated in Section 3.

One of the drawbacks is high cost as compared to conventional mechanical suspensions. To achieve hardware savings for cost reduction, *self-sensing* or *sensorless* magnetic suspension been proposed [11]. It is based on the property that voltage-controlled magnetic suspension system is controllable and observable even if only the coil current is the output (variable to be measured). Because the displacement and velocity of the floator can be estimated by an observer, the hardware of displacement sensing can be removed. It has been studied extensively as one of the most promising methods of reducing the cost of hardware [11-14]. Nevertheless, the reduction of cost is still insuffient. The authors have proposed quite a different approach of hardware reduction with an attention to another key component: *power amplifier*. This component is indispensable for the operation of a *single* suspension system so that it is impossible to omit the amplifier itself. The key point of the proposal is to reduce the *number* of power amplifier to float *multiple* floators, for example, with a *single* power amplifier [15]. It will give another promising method of reducing the hardware. Such magnetic supension is named as *multiple magnetic suspension* that is treated in Section 4.

Another drawback is the necessity of external energy to operate servomechanism. When the suspension force is supplied only by an electromagnet, a steady current flowing the electromagnet is necessary to counterbalance the gravitational force. It causes energy consumption and heating up of the electromagnet. An effective way of solving such a problem is zero-power magnetic suspension using hybrid magnet [16-18]. Recently, a energy harvesting technique such as solar power generation has been introduced and combined with magnetic suspension technology [19], which is treated in Section 5.

3. Wind Tunnel

Magnetic suspension provides an ideal way of supporting a model for wind tunnel tests because there is no support interference problem arising with mechanical model-support [21, 21]. The forces and moments to support the model are generated by electromagnets arranged outside the test section. In addition, aerodynamic forces acting on the model are estimated from the control current of the electromagnets.

Aerodynamics around a spinning body such as golf ball is still an intriguing topic in both academic and industrial fields. Although simulation-based analysis has been making very rapid progress, the details of the dynamics have not been clarified sufficiently. The main difficulty is that the target phenomenon is a complex mix of macro-scale and micro-scale dynamics. Therefore, ideal wind tunnel tests are still required for more precise and reproducible observation. However, conventional wind tunnels using magnetic suspension were not designed to test a spinning body so that they lacked the function of rotating the body [20, 21].

We have proposed a wind-tunnel system for spinning body to measure hydrodynamic forces acting on the body [9]. In the proposed system, the body is suspended and rotated by electromagnets. The forces acting on the body are measured from the control signal for suspension. An apparatus with a 60×60 mm wind tunnel has been developed [10]. It uses a 3-axis optical sensor operating in a fully-differential mode. This apparatus achieves stable suspension and rotation. The hydrodynamic forces acting on the spinning body are measured actually.

Figure 2 shows a photograph of the fabricated apparatus. The size of the total system is $360 \times 1200 \times 440$ mm, approximately. It consists of a magnetic suspension mechanism, a three-axis displacement sensor, a controller and a wind-tunnel. The outline of Each component will be explained in the following. A schematic drawing of

the mechanism for magnetic suspension is shown in Fig.3 where the nearest electromagnet is removed for a better view of the inside poles. The size is $244 \times 244 \times 296$ mm. The suspension system has eight electromagnets for controlling the three-dimensional position of a sphere body made of ferromagnetic material. Each electromagnet has five 300-turn coils. The impedance of the electromagnet can be adjusted by the connections of the coils. The distance of the poles are kept long enough for a 60×60 mm wind tunnel to be inserted.

The operation of the fabricated 3-axis optical sensor is illustrated in Fig.4. It combines a pair of unit with a LED (light source), four collecting lens and four phototransistors. It can detect the three-dimensional positions of the body in the full-differential mode.

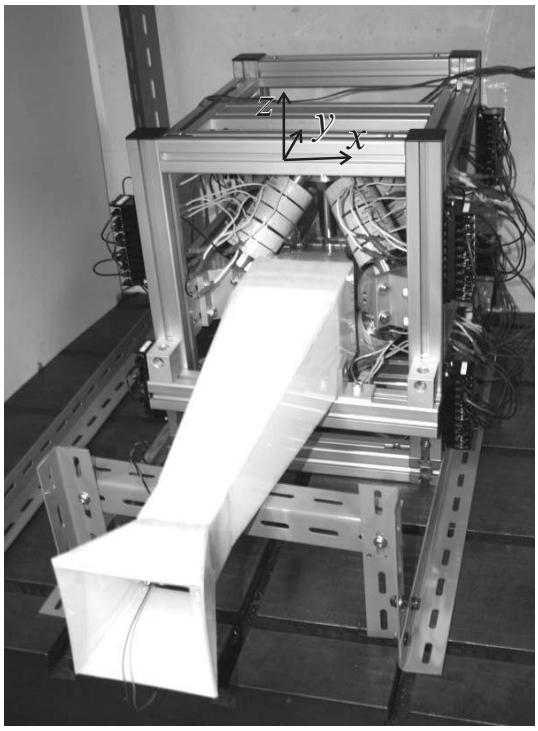

Fig.2. Fabricated wind tunnel with a magnetic suspension mechanism

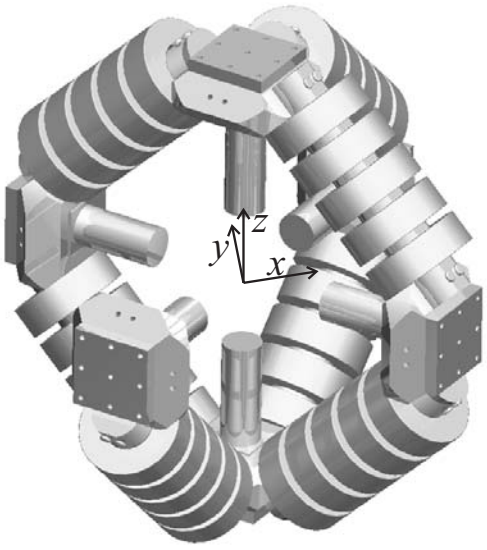

Fig.3. Schematic drawing of the magnetic suspension mechanism

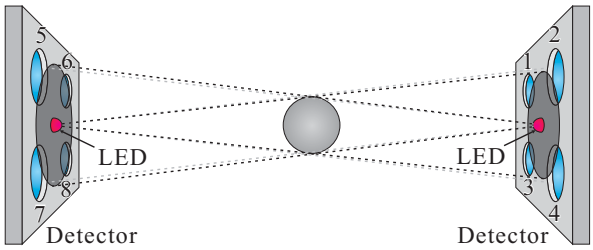

Fig.4. Three-dimensional differential optical displacement sensor

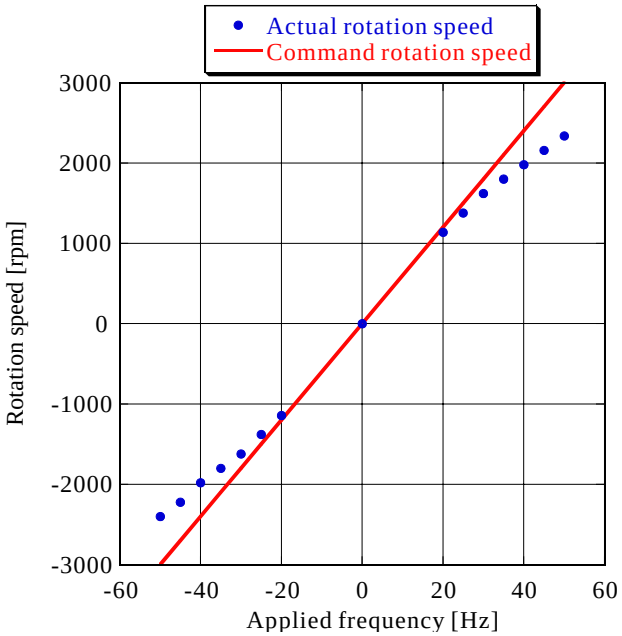

Fig.5. Relation between driving frequency and rotation Speed

Because the suspension system is inherently unstable, stabilization using active control is required. The outputs of the sensors are inputted into a DSP-based digital controller. The controller calculates control signals and send them together with excitation signal for rotation to eight power amplifiers for the electromagnets through D/A converters. The aerodynamics forces acting on the body are estimated from the control signals for maintaining the position of the body.

Stable suspension was achieved by applying PID control. The rotation of the body was realized by superimposing two-phase AC signals on the control signals for the *x*- and. *y*-directions. The rotation about the vertical axis (z-axis) was achieved. The relation between the excitation frequency and the rotational speed was studied experimentally. The results are summarized in Fig.5. The body is driven up to 3000rpm. Since the principle of rotation is same as that of induction motor, the slip is observed in higher frequency regions.

Several wind tunnel tests were successfully carried out. The fluid drag and lift forces were measured from the control input. It was observed from the measurement results that the drag force was proportional to the square of the wind speed approximately and the lift force also increased as the wind speed increased [10].

4. Multiple Magnetic Suspension

A basic magnetic suspension system has a single floator (object to be suspended) and electromagnet that is controlled with a single power amplifie as shown in Fig.1. Multiple magnetic suspension is a unique approach of hardware reduction with an attention to *power amplifier* [15]. In multiple magnetic suspension, multiple floators

are controlled with a single power amplifier. Multiple magnetis suspensions are classified into series and parallel.

Series magnetic suspension

The basic concept of *series* multiple magnetic suspension is illustrated by Fig.6(a) in which three floators are suspended with a single electromagnet. In the following, a series-type multiple magnetic suspension system with *n* floators is referred to as *n*-series magnetic suspension system. The floator 1 is suspended by the electromagnet and magnetized. Then, the floator 2 is also magnetized through the floator 1. In the same manner, all the floators are magnetized. Therefore, they can be suspended by the single electromagnet. However, the attractive forces between the floators obtained by the magnetization are frequently insufficient to suspend the successive floator(s). To obtain sufficient attractive force, permanent magnetic (pre-magnetized) floators are used instead of ferromagnetic floators as shown by Fig.6(b). Yamamoto *et al.* [22] has proposed *indirect suspension*, which corresponds to 2-series magnetic suspension, and achieved stable noncontact suspension.

It can be shown analytically that both current-controlled and voltage-controlled *n*-series magnetic suspension systems are controllable [23]. It can be shown analytically that both current-controlled and voltage-controlled *n*-series magnetic suspension systems are observable when one of the displacements is detected. It is obvious that the systems are observable when multiple displacements are detected. The voltage-controlled *n*-series magnetic suspension system is also observable even if only the current of the electromagnet is detected. It indicates that the self-sensing control of series multiple magnetic suspension systems is feasible theoretically.

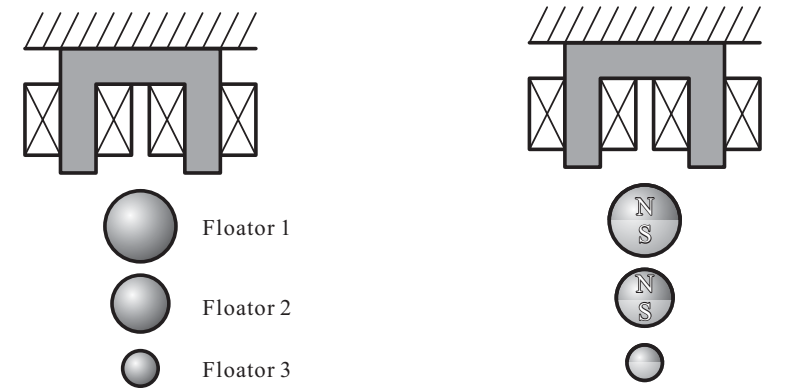

(a) Ferromagnetic floators (b) Pre-magnetized floators

Fig.6. Series multiple magnetic suspension system with three floators

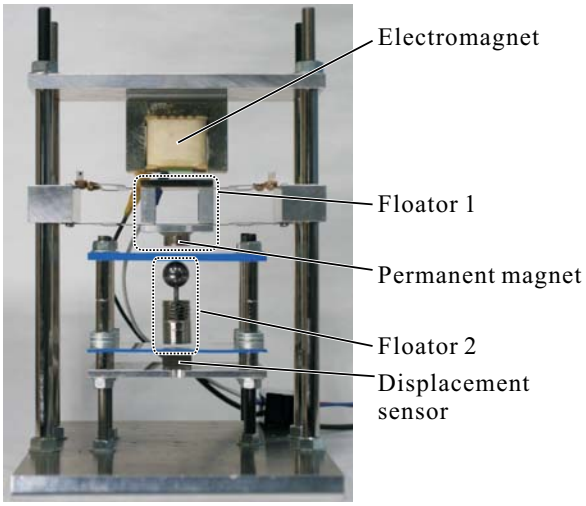

Fig.7. Photo of force measurement apparatus using double series magnetic suspension

One application of *2*-series magnetic suspension is force measurement; the proposed system can measure force without any displacement of the point of force actuation [24]. When PID control is applied to the displacement of the floator 2, the floator 1 displaces in proportion to the force applied to the floator 2 whereas the position of the floator 2 is maintained at the original position. Therefore, the force can be estimated for the displacement of the floator 1.

The proposed method has an advantage over conventional methods that the distance between the operating point of force (second floator) and the source of force is kept invariant. In addition, when the stiffness between the first and second floators is low, even small force leads to large displacement. Therefore, the proposed measurement method is suitable for the noncontact measurement of micro force. Figure 7 shows an apparatus fabricated based on this concept and the effectiveness of the proposed method has been studied experimentally [24]. The measurement results suggest that the proposed force measurement method will achieve higher resolution than conventional servo-type force measurement method.

Parallel magnetic suspension

A schematic drawing of a parallel magnetic suspension system is shown by Fig.8 in which *three* floators and electromagnets controlled with a *single* power amplifier. Based on this principle, the number of floators and

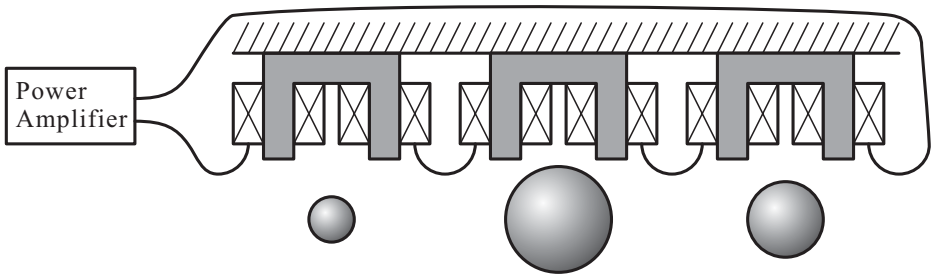

Fig.8. Parallel multiple magnetic suspension system with three floators and series-connected coils

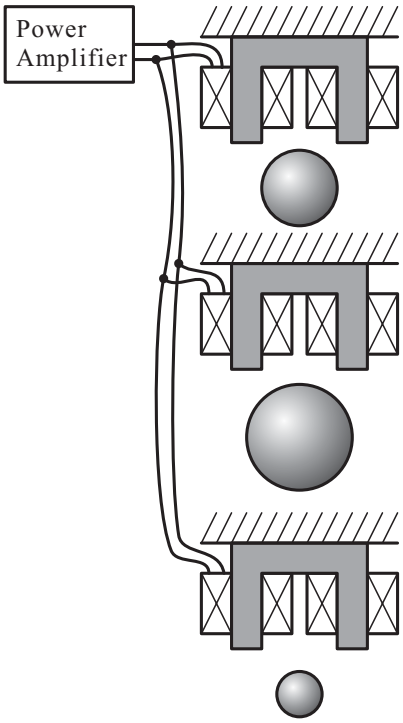

Fig.9. Parallel multiple magnetic suspension system with three floators and parallel-connected coils

electromagnets controlled by a single electromagnet can be set two or more arbitrarily. When the number is *n* and the connection of the coils is series as shown in Fig.4, we call it as *n*-parallel magnetic suspension system with *series connection*. Another connection of the coils is parallel as shown in Fig.9. Such system is referred to as *n*-parallel magnetic suspension system with *parallel connection* [15].

The controllability and observability of parallel magnetic suspension systems have been studied and the conditions under which the parallel magnetic suspension system are controllable and observable are clarified [15]. For example, The state equation of a current-controlled double parallel suspension system with series connection is given by

$$\dot{\boldsymbol{x}}_{cpt2}(t) = \boldsymbol{A}_{cpt2}\boldsymbol{x}_{cpt2}(t) + \boldsymbol{b}_{cpt2}i(t)\,, \tag{1}$$

where

$$\boldsymbol{x}_{cpt2} = \begin{bmatrix} x^{(1)} \\ \dot{x}^{(1)} \\ x^{(2)} \\ \dot{x}^{(2)} \end{bmatrix}, \quad \boldsymbol{A}_{cpt2} = \begin{bmatrix} 0 & 1 & 0 & 0 \\ a_{21}^{(1)} & 0 & 0 & 0 \\ 0 & 0 & 0 & 1 \\ 0 & 0 & a_{21}^{(2)} & 0 \end{bmatrix}, \quad \boldsymbol{b}_{cpt2} = \begin{bmatrix} 0 \\ b^{(1)} \\ 0 \\ b^{(2)} \end{bmatrix}, \quad a_{21}^{(k)} = \frac{k_s^{(k)}}{m^{(k)}}, \quad b^{(k)} = \frac{k_i^{(k)}}{m^{(k)}}$$

x : displacement of the floator, i : control current (common), m : mass of the floator, k_s : force to displacement factor, k_i : force to current factor, and a parenthetic superscript "(*k*)" indicates that the quantity is related to the *k*th subsystem consisting of a floator and the corresponding electromagnet (*k*=1 or 2). The factors k_s and k_i are usually nonzero. The controllability matrix of this system is given by

$$\boldsymbol{M}_C^{cpt2} = \begin{bmatrix} 0 & b^{(1)} & 0 & a_{21}^{(1)}b^{(1)} \\ b^{(1)} & 0 & a_{21}^{(1)}b^{(1)} & 0 \\ 0 & b^{(2)} & 0 & a_{21}^{(2)}b^{(2)} \\ b^{(2)} & 0 & a_{21}^{(2)}b^{(2)} & 0 \end{bmatrix} \tag{2}$$

Calculating the determinant gives

$$\det \boldsymbol{M}_C^{cpt2} = \left\{(a_{21}^{(1)} - a_{21}^{(2)})b^{(1)}b^{(2)}\right\}^2 \tag{3}$$

Therefore, the system (1) is controllable if and only if

$$a_{21}^{(1)} \neq a_{21}^{(2)} \tag{4}$$

This implies that the open-loop *mechanical* dynamics must be different among the subsystems for controllability [15].

The feasibility of parallel magnetic suspension has already been demonstrated experimentally in the case of $n = 2$ (double parallel suspension system) [25]. The zero-power control has also been achieved in the same system [26]. In addition, the concept of *multiple suspension* has been extended to *electrostatic* suspension [27].

5. Solar Magnetic Suspension

The necessity of external energy is one of the critical problems of active magnetic suspension system in widening its application fields. Recently, a energy harvesting technique such as solar power generation has been introduced and combined with magnetic suspension technology [19].

Figure 10 shows a photograph of a fabricated solar magnetic suspension appratus. The height of the apparatus is 310 mm, and the diameter of the central part is 88 mm. The central part has two arms and each arm carries four solar cells. The floator is made of soft iron and a hollow sphere having an outer diameter of 43 mm. A disk-shaped ferrite magnet is attached to the top of the floator for the zero-power suspension. In this apparatus, the single-degree-of-freedom vertical translational motion of the floator is actively controlled while the other motions are passively stabilized by the edge effects.

Figure 11 shows the outline of the fabricated solar magnetic suspension system including solar power generation. In this figure, solid and dashed lines represent signal and power supply, respectively. The fabricated solar magnetic suspension system has solar cells, a power storage device and a voltage stabilizing circuit for the peripheral devices in addition to the components of conventional magnetic suspension system. The electric power generated by solar cells supplies current to the electromagnet and the peripheral devices of the fabricated system via buffered capacitors. The buffered capacitors are used for reducing the power fluctuation caused by the variation of luminance and instantaneous power consumption just after a disturbance acts in the floator.

To maintain levitation for a long time by solar energy solely, significantly dedicated low-power peripheral devices are developed. Figure 12 shows a photograph of the circuits of the peripheral devices that is placed in the cylindrical part of the apparatus at the top. The peripheral devices consists of a storage circuit, a displacement sensor, a controller, a stabilizing power supply and a power amplifier.

The average power consumption of the fabricated magnetic suspension system is 33 mW in stable suspension.

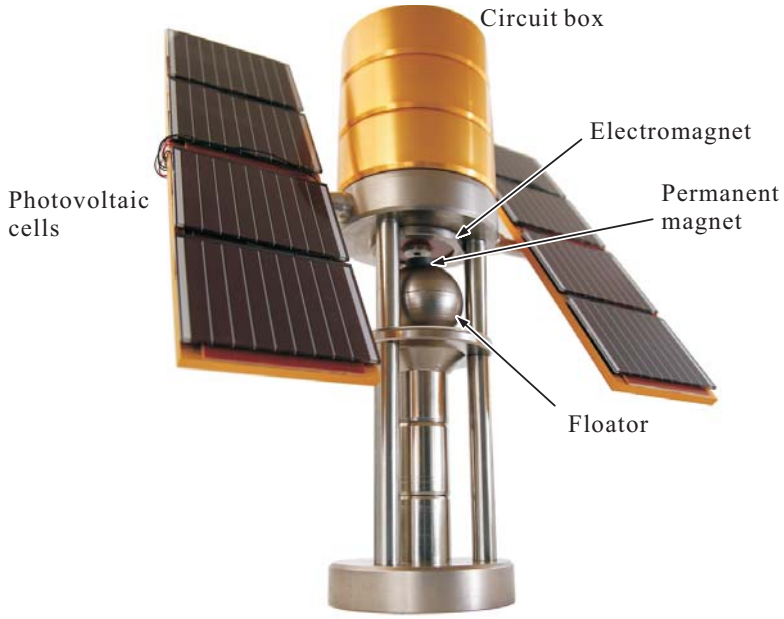

Fig.10. Photo of the fabricated solar magnetic suspension apparatus

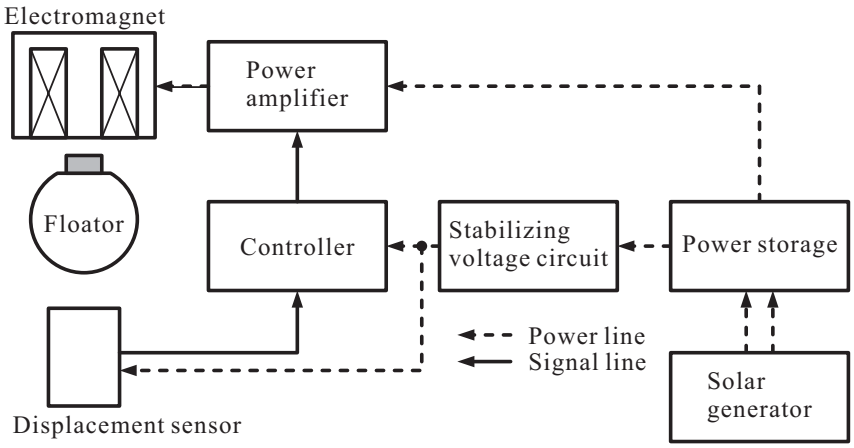

Fig.11. Outline of the solar magnetic suspension system

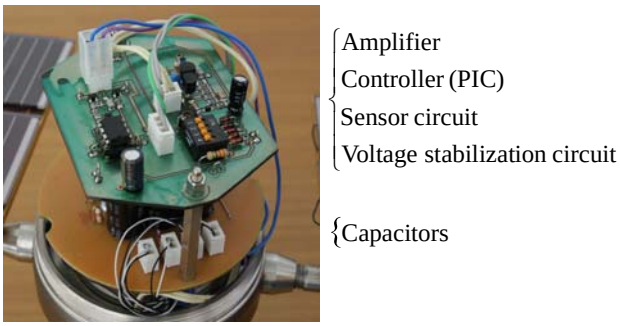

Fig.12. Photo of the circuits for peripheral devices (inside the circuit box).

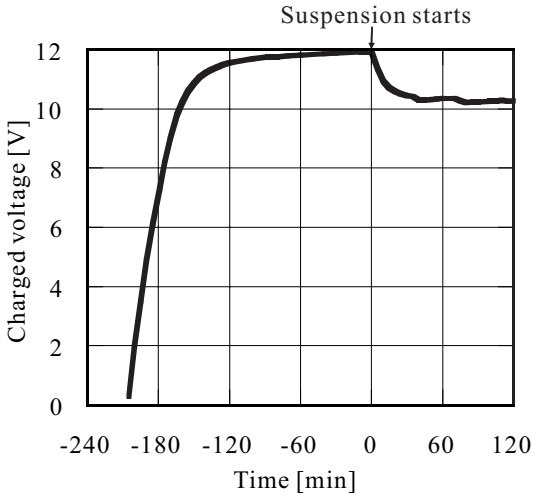

Fig.13. Time-history of the charging voltage under a low luminance.

This power consumption is almost equal to that of a super luminosity LED of red-to-green wavelength. When commercial peripheral devices were used, the suspension system consumed 500 mW. A conventional magnetic suspension system of the same dimensions supplied by a commercial power source consumes more than a few watts. In contrast, the fabricated system can achieve stable suspension even under a 5klx-illuminance of a fluorescent lamp.

Figure 13 shows a time history of the charged suspension voltage under such low luminance. The initial value of the capacitors was zero (discharged). The charged voltage is risen by the power supplied from the solar generator during -205 to 0 min. The charged voltage approaches to 12 V at the time of 0 min just before the suspension starts. The charged voltage decreased to 10.3 V until the supply and demand power were balanced (after 60 min).

6. Toward Smart Mechatronics

Mechatronics is an interdisciplinary area of engineering based on classical fields of mechanical and electrical engineering and on information technology [6]. A typical mechatronic system takes in signals, process them and puts out signals to produce forces and/or motions. Such a system detects changes in environment and reacts to them according to a suitable strategy through information processing. Therefore, mechatronic systems are more or less *smart*. For innovations in mechatronics, however, qualitative changes or evolutions will be necessary. One of the candidates is the introduction of energy harvesting technology to mechatronic systems because it will lead to clean and tidy (another sense of smart) machines. I hope that the advances described above will be clues to future *smart mechatronics*.

7. References

[1] B.V.Jayawant, “Electromagnetic Levitation and Suspension Techniques”. Rdward Arnold, pp.1-31, 1981.

[2] M. Morishita, T. Azukizawa, S. Kanda, N. Tamura. and T. Yokoyama, “A New Maglev System for Magnetically Levitated Carrier System”, *IEEE Trans. on Vehicular Technology*, Vol.38, No.4, pp.230-236, 1989.

[3] G. Schweitzer, H. Bleuler and A. Traxler, “Active Magnetic Bearings”, *Hochschulverlag AG an der ETH Zürich*, 1994.

[4] H. Bleuler, C. Gaehler, R. Herzog, R. Larsonneur, T. Mizuno, R. Siegwart and S.J. Woo, “Application of Digital Signal Processors for Industrial Magnetic Bearings”, *IEEE Trans. on Control Systems Technology*, Vol.2, No.4, pp.280-289, 1994.

[5] T. Mizuno and T. Higuchi, “Design of the Totally Active Magnetic Bearings ---Structures of the Optimal Regulator---”, *Proc. International Symposium on Design and Synthesis*, pp.534-538, 1984.

[6] G. Schweitzer and E.H. Maslen (eds.), “Magnetic Bearings”, *Springer*, pp.1-68, 2009.

[7] T. Mizuno and T. Higuchi, “Compensation for Unbalance in Magnetic Bearing Systems”, *Trans. Society of Instrument and Control Engineers (SICE)*, Vol.20, No.12, pp.1095-1101, 1984 (*in Japanese*).

[8] T. Mizuno, “Analysis on the Fundamental Properties of Active Magnetic Bearing Control Systems by a Transfer Function Approach”, *JSME International Journal*, Series C, Vol.44, No.2, pp.367-373, 2001.

[9] T. Mizuno, M. Furutachi, Y. Ishino and M. Takasaki, “Proposal of Wind Tunnel for Spinning Body using Magnetic Suspension”, *Proc. 12th International Symposium on Magnetic Bearings*, pp.232-236, 2010.

[10] T. Mizuno, Y. Sakai, Y. Ishino and M. Takasaki, “Fabrication of a New Wind Tunnel for Spinning Body Using Magnetic Suspension”, *Proc. 13th International Symposium on Magnetic Bearings*, Paper 23, 2012.

[11] D. Vischer and H. Bleuler, “Self-Sensing Active Magnetic Levitation”, *IEEE Trans. on Magnetics*, Vol. 29, Vol.2, pp.1276-1281, 1993.

[12] T. Mizuno and H. Bleuler, “Self-Sensing Magnetic Bearing Control System Design Using the Geometric Approach”, *Control Engineering Practice*, Vol.3, No.7, pp.925-932, 1995.

[13] T. Mizuno, K. Araki and H. Bleuler,”Stability Analysis of Self-Sensing Magnetic Bearing Controllers”, *IEEE Trans. on Control Systems Technology*, Vol.4, No.5, pp.572-579, 1996.

[14] T. Mizuno, H. Bleuler, H. Tanaka, H. Hashimoto, F. Harashima. and H. Ueyama, “Industrial Application of Position Sensorless Active Magnetic Bearings”, *Electrical Engineering in Japan*, Vol.117, No.5, pp.124-133, 1996.

[15] T. Mizuno, M. Takasaki and Y. Ishino, “Multiple Magnetic Suspension Systems (1st report: Basic Concepts and Theorems)”, *Trans. JSME*, Series C, Vol.76, No.761, pp.76-83, 2010 (*in Japanese*).

[16] A.V. Sabnis, J.B. Dendy and F.M. Schmitt, “A Magnetically Suspended Large Momentum Wheel”, *J. Spacecraft*, Vol.12, pp.420-427, 1975.

[17] M. Morishita and T. Azukizawa, “Zero Power Control Method for Electromagnetic Levitation System”, *Trans. IEE Japan*, Vol.108-D, No.5, pp.447-454. 1988 (*in Japanese*).

[18] T. Mizuno and Y. Takemori, “A Transfer-Function Approach to the Analysis and Design of Zero-Power Controllers for Magnetic Suspension System”, *Electrical Engineering in Japan*, Vol.141, No.2, pp.67-75, 2002.

[19] Y. Ishino, T. Mizuno and M. Takasaki, “Fabrication of Power Saving Solar Magnetic Suspension System”, *Trans. JSME*, Series C, Vol.79, No.800, pp1056-1065, 2013 (*in Japanese*).

[20] R.P. Boyden, C.P. Britcher and P. Tcheng, “Status of Wind Tunnel Magnetic Suspension Research”, *SAE Technical Paper Series* 851898, pp.1-9, 1985.

[21] H. Sawada, H. Suenaga, T. Suzuki and N. Ikeda, “Status of MSBS study at NAL”, *Proc. 2nd International Symposium on Magnetic Suspension Technology*, Part 1, p 275-289, 1994.

[22] A. Yamamoto, M. Kimura. and T. Hikihara, “A Study on Indirect Suspension of Magnetic Target by Actively Controlled Permanent Magnet”, *Proc. 11th International Symposium on Magnetic Bearings*, pp.182-188 2008.

[23] T. Mizuno, Y. Maruyama, M. Takasaki, Y. Ishino, and Y. Oshiba, “Series-Type Multiple Magnetic Suspension System”, *Journal of System Design and Dynamics*, Vol.5, No.5, pp1017-1029, 2011.

[24] T. Mizuno, D. Sekine, Y. Ishino and M. Takasaki, “Proposal of Force Measurement Using Series Magnetic Suspension”, *Proc. JSME 2012 11th Motion and Vibration Conference (MOVIC2012)*, 8560, 2012.

[25] T. Sakurada, T. Mizuno, M. Takasaki and Y. Ishino, “Multiple Magnetic Suspension Systems (2nd report: Realization of Double Parallel Magnetic Suspension)”, *Trans. JSME*, Series C, Vol.77, No.779, pp765-776, 2011 (*in Japanese*).

[26] T. Mizuno, T. Sakurada, Y. Ishino and M. Takasaki, “Zero-Power Control of Parallel Magnetic Suspension Systems”, *Journal of System Design and Dynamics*, Vol.5, No.5, pp765-776, 2011.

[27] T. Mizuno, T. Kato and M. Takasaki, “Proposal and Fundamental Properties of Parallel Electrostatic Suspension Systems”, *SICE Journal of Control, Measurement, and System Integration (JCMSI)*, Vol.3, No.5, pp.346-351, 2010.

Paper ID: KL-02

Tissue Engineering of Aortic Heart Valve: New Directions

Yosry (Yos) Morsi
Research Leader and Advisor PhD London FEA
Biomechanical and Tissue Engineering Laboratory
Swinburne University of Technology, Hawthorn, Melbourne, Victoria, Australia
Email: ymorsi@swin.edu.au

Abstract

In this talk Professor Morsi will summarize the experience gained in the last 15 years at Swinburne University of Technology to develop a tissue engineered aortic heart valve. In doing so a complete analysis of principle and fundamental of heart valves are presented and discussed. Initially an introduction and discussion on the research questions related to current heart valve problems and the issues related to development of tissue engineering aortic heart valve are given, followed by background information on the clinical aspects of heart valve diseases treatments and diagnostics. The types of heart valves replacements and their limitations are then discussed followed by a full account of the design and manufacturing of the scaffolds from natural and synthetics materials. In vitro conditioning and Swinburne's experience is then given and the presentation is concluded with a full discussion on the research questions related to tissue engineering aortic heart valves to date and recommendations for future research to create a functional tissue-engineered aortic heart valve.

Keywords:

1. Introduction

Natural heart valves are remarkably adapted to allow unidirectional flow without regurgitation or trauma to the blood and do not permit any excessive development of local stress in the valve leaflets and supporting surrounding tissues. Moreover, healthy valves are biologically dynamic structures that are capable of repairing injury that could result from any excessive cyclic pressure loading (70 beats per minute, more than 100,000 beats per day, and more than 36 million beats per year) [1].

Valvular heart disease is a major health problem causing significant indisposition and death worldwide [2]. The incidence of valvular disease increases with age, ranging from 0.7% in the 18-44 year old group to 13.3% in the 75 years and older group [3,4], and this percentage is expected to increase due to an older and larger population in near future. Dysfunctional heart valve could result from inherited heart pathology, leading to stenosis or inefficiency of the valve or could part of diseases such as calcification, regurgitation, degeneration and stenosis or endocarditis. Endocarditis is a disease allied with the inflammation of endocardium, due to bacteria or an infection with rheumatic fever and has a significant adverse effect on the functionality and long-term life of the patient. Aortic valveis the most affected by these diseases as it carries the maximum load of the heart. In general, however, the treatment of a dysfunctional heart valve is either repair of or replacement with artificial ones.

Prosthetic heart valves are instigated regularly to replace damaged natural ones, and they are widely instigated in ventricular assist devices (VAD) and in total artificial hearts (TAH). These valves are of two types, mechanical ones with components manufactured of non-biologic materials (e.g., carbon, metal, polymeric materials) or tissue valves, which are constructed of either animal or human tissue, at least in part. Literature suggests that over 285,000 substitute valves are employed per year, and approximately 40% of these are tissue valves [5]. Subsequently, due to

a recent increase in the aging population, there has been a shift toward the increased use of tissue valves. However, in general, these artificial valves suffer from a number of drawbacks that are different for mechanical and tissue valves. Nevertheless, the composite rate of valve-related complications is similar for both types.

The principal disadvantages of mechanical valves are associated with a substantial risk of systemic thromboembolism and thrombosis (largely due to abnormal flow past the rigid occluder and the use of non-physiologic surfaces) and serious complications from hemorrhage associated with the necessary use of chronic anti-coagulation therapy.

Oppositely, tissue valves maintain a low rate of thromboembolism without anti-coagulation therapy. However, these bio-prostheseswhich are partly biologic tissue and partly synthetic, are normally subject to progressive tissue deterioration leading to structural dysfunction. Nevertheless, tissue valves demonstrate, in general, a beneficial potential of acclimatization to the patient's cardiovascular environment [6]. Nonetheless, the key factors limiting the development of tissue valve replacements include changes induced by preservation, fabrication, and methods of implantations. For example, it is known that the functional/structural characteristics of tissues used in bio-prostheses are modified by glutaraldehyde cross-linking. Moreover, the choice of fixation technique is vital, as using the wrong technique could adversely affect the microstructural of the valve, particularly leaflets, and subsequently the degree of compliance compared to the biological tissue [7, 8, 9]. Generally, the degree to which the tissues are affected depends upon the fixation technique adopted and the method of fabrication. Moreover, the major cause of bio-prosthetic valve dysfunction is deterioration of cuspal tissue,which is primarily due to the inability of artificial materials to mimic the natural tissue. Calcification contributes to failure of tissue valves leading to regurgitation through tears in calcified cusps. This deterioration originates from mineralisation, often deep within the tissue (intrinsic) or at the surface (extrinsic) that are influenced by the host, the design of the implant and/or by the induced mechanical stresses. Non-calcified damage to the valvular structure that could accrue through constrained abnormal valve motion is also a major mechanism of degradation in porcine and pericardial prosthetic valves. Clearly, the maintenance of tissue structural integrity is critical to extending durability of tissue heart valves [10].

Conversely, the main drawbacks of artificial heart valves are the physical barriers and the restricted lifespan associated with them. The types and configurations of current artificial heart valves are well documented in literature, and a number of alternative designs have been suggested and examined structurally and hydrodynamically. Although the results from these studies revealed satisfactory correlation between *in vitro* measurements and *in vivo* clinical and pathological findings, they serve to highlight the continuing need for the development of long-term replacement valves [11]. In general, it is highly desirable that valve designs have durable membranes or leaflets and support structures that resist degradation due to *in vivo* environmental factors and mechanical stressing while retaining the functional characteristics and hemodynamics associated with the natural human heart valves. More importantly, no currently used valvular replacement devices provide growth potential, which is a major restriction for younger patients.

2. The Concept of Tissue Engineering

Full account of this concept is given by Morsi [12]. Recently, it has been recognized that an alternative to the fabrication of prosthetic valves is tissue engineering (TE) of an anatomically appropriate scaffold containing cells and controlling the development of normal functional valve architecture in vivo. This is indeed an exciting concept.

Figure 1 shows one concept of tissue engineering heart valves (TEHVs). This notion focuses on the development of a functional identical copy of a healthy heart valve to overcome all the disadvantages associated with the current clinical use of mechanical and bio-prosthetic heart-valves. However, existing results are still preliminary, and various issues remain to be addressed before the clinical application of a tissue-engineered heart valve will be possible for replacement [4, 13]. The three most important parts of tissue engineering are cells, biomaterialsand

conditioning techniques such as in vitro and in vivo. Out of these three components, cells are the only living part, and hence the other two parts need to be optimized to suite the cells used for tissue regeneration.

Overall, TE of heart valves can be divided in two general strategies. The first strategy uses decellular(not made up of or divided into cells) natural biomatrices.With this decellularization (remove cells or cellular material from an organ or tissue) approach, the Extra Cellular Matrix (ECM) of say porcine heart valve is used as a scaffold (after elimination of their cellular antigens to reduce their immunogenicity) to guide the repopulation of the new cells after implementation in the patient. With this repopulation technique, various methods for decellularization have been proposed to ensure that the mechanical properties of the biomatrices or the reconstitution of the tissue in vivo is not affected. In general, as will be discussed in Chapter 7, various concerns regarding the stability and resorption of the natural biomatrices have to be addressed. Nevertheless, it has been argued that in contrast to biodegradable polymer scaffold TEHVs (the second approach), decellularbiomatrices maintains natural ligands and Extra Cellular Matrix (ECM) constituents that could be more suitable for cell adhesion and proliferation [9, 14].

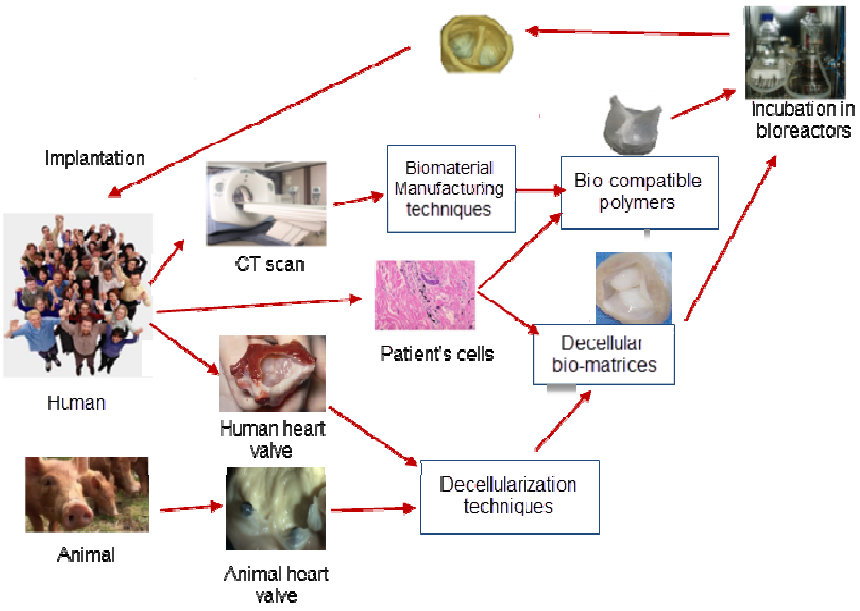

Figure.1. Illustration of the general concept of tissue engineeringheart valve.With permission (Yosry S Morsi, Tissue Engineering of the Aortic Herat Valve: Fundamentals and Developments, Book, Nova Science Publishers, 2011. http://www.amazon.com/Tissue-Engineering-Aortic-Heart Valve/dp/161942939X:

The second strategy is to use biocompatible degradable nature or polymeric scaffoldsmoulded into heart valve geometry. Generally, cells isolated from donor tissue are cultured and then seeded onto these scaffolds, resulting in constructs that can be implanted in vivo after a specific cultivation period in vitro. The cells grow, develop, and produce Extra Cellular Matrix (ECM) as the polymer degrades, ultimately leaving a natural tissue heart valve without any synthetic or natural component. Ideally, eliminating immunological responses to the TE-construct and facilitating the growth and remodeling processes, autologous cells should be used. However, other types of cells such as stem cells have been proposed [15, 16].With this approach, the cell-polymer interaction is also critical because the quality and extent of ECM formation will determine the overall structure and mechanical properties of

the newly developed tissue. Moreover, with this approach, biological materials have been also used as scaffolds for TEHV alone or with various types of polymers.

Still, degradable nature or polymeric scaffolds approach became very popular recently and currently is the most favorable one by most researchers. Morsi et al. [8, 17] accentuated the urgent need to develop new materials for heart valves scaffolds, particularly leaflets that are capable of mimicking the deformation and coaptation of natural heart valves and called for hybrid approach, i.e., using artificial and natural materials, which will be discussed in Chapter 7. Moreover, further development is required in the areas of scaffold design, fabricationtechnology and biomaterials with suitable mechanical properties. However, while improvements are progressing, the manufacturing processes available to date still need to be optimized so that the scaffolds produced are suitable for tissue engineering of aortic heart valve. The use of harsh organic solventsfor dissolving polymers and other chemicals required by the conventional fabrication process may produce toxic by-products. This in turn affects the biocompatibility of the scaffold and raises concern about safety of patients [18]. Rapid prototyping technology, on the other hand, may offer an attractive and cost-effective approach. Nevertheless, it can be expected that continual research into the fabrication process will lead to advancements and breakthroughs in addressing the complex requirements of manufacturing scaffolds for tissue engineering of heart valve. Moreover, the developed scaffold must continually withstand the physiological conditions that natural valves are subjected to (engineering simulation and in vitro conditioning play important roles in this). Other issues that need to be addressed include understanding the factors that control cell adhesion, differentiation and proliferation, the optimal period of culture and its environment (static or dynamic) and methods of cell seeding (selective cell or mixed cell population seeding), which are vital for the development of a complex, tri-layered, flexible structure of the aortic valve that can function as a viable and efficient one. All these issues are fully discussed in this presentation.

3. Conclusion

In a nutshell, tissue-engineered heart valves clearly have the potential to improve our ability to treat valvular heart disease and to abolish many of the undesirable physical properties observed in the present heart valve substitutes. In addition, research and improvements are called for TEHVs scaffold from both polymeric and decellularized biometrics. Clinical use of TEHVs within the next decade is believed to be perceptible. In essence, tissue engineering can utilize the existing and future information and data in the field of biology, biochemistry and molecular biology to formulate the correct concept of generating new tissue. Likewise, progress in the science of bioengineeringsimulation and numerical modelling as well as advancement in biomaterials would, in principle, provide the right platform to engineer tissues of the required chracteristics, which will compliment the realistic application of engineering principles to human implementations. Equally, developments of genetic engineering, cloning and stem cell biology, which are dependent on each other,can further enhance our understaing of various tissue human diseases and greatly assist the development of correct treatments.

4. References

[1] Thubrikar, M. J., The aortic valve, Boca Raton, Florida, CRC Press, 1990.

[2] Jones, D. L., R. Adams, M. Carnethon, G. De Simone, T. B. Ferguson, K. Flegal, E. Ford, K. Furie, A. Go, K. Greenlund, N. Haase, S. Hailpern, M. Ho, V. Howard, B. Kissela, S. Kittner, D. Lackland, L. Lisabeth, A. Marelli, M. McDermott, J. Meigs, D. Mozaffarian, G. Nichol, C. O'Donnell, V. Roger, W. Rosamond, R. Sacco, P. Sorlie, R. Stafford, J. Steinberger, T. Thom, S. Wasserthiel-Smoller, N. Wong, J. Wylie-Rosett and Y. Hong, Writing group members,Heart Disease and Stroke Statistics—2009 Update: A Report From the American Heart Association Statistics Committee and Stroke Statistics Subcommittee, *Circulation,* 2009. 119(3): pp 480-486.

[3] Nkomo, V. T., J. M. Gardin, T. N. Skelton, J. S. Gottdiener, C. G. Scott and M. E. Sarano, Burden of valvular heart diseases: a population-based study, *Lancet.* 2006.368(9540): pp 1005-1011.

[4] Mol, A., A. I. P. M. Smith, C. V. C. Bouten and F. P. T. Baaijens, Tissue engineering of heart valves: Advances and current challenges, *Expert Revof. Med. Devices.* 2009.6(3): pp 259-275.

[5] Mikos, A. G., S. W. Herring, P. Ochareon, J. Elisseeff, H. H. Lu, R. Kandel, F. J. Schoen, M. Toner, D. Mooney, A. Atala, M. E. V. Dyke, D. Kaplan and G. V. Novakovic, Engineering Complex Tissues, *Tissue Engineering*, 2006.12(12): pp 3307-3339.

[6] Berry J. L., J. A. Steen, J. K. Williams, J. E. Jordan, A. Atala and J. J. Yoo, Bioreactors for development of tissue engineered heart valves, *Annals of Biomedical Engineering*, 2010. 38(11): pp. 3272-3279.

[7] Lin, Q., Y. S. Morsi, B. Smith and W. Yang, Numerical simulationand structure verification of Jellyfish heart valve, *International Journal of Computer Applications in Technology*, 2004.21(1-2): pp 2-7.

[8] Morsi, Y. S. and I. Birchall, Tissue engineering a functional aortic heart valve: an appraisal, *Future Cardiol.* 2005.1(3): pp 405-411.

[9] Brody, S. and A. Pandit, Approaches to heart valve tissue engineering scaffold design, *J. Biomed. Mater Res. B Appl. Biomater.*, 2007. 83(1): pp. 16-43.

[10] Schoen, F. and R. Levy, Tissue heart valves: Current Challenges and future research perspectives, *Founders Aw 25th Annual Meeting Soc. Biomaterials.* 1999. Pp: 441-65.

[11] Morsi Y. S., W. W. Yang, C. S. Wong and S. Das, Transient fluid-structure coupling for simulation of a trileaflet heart valve using weak coupling, *J. Artif. Organs.* 2007. 10(2): pp. 96-103.

[12] Yosry S Morsi, Tissue Engineering of the Aortic Herat Valve: Fundamentals and Developments, Book, Nova Science Publishers, 2011. *http://www.amazon.com/Tissue-Engineering-Aortic-Heart Valve/dp/161942939X:*

[13] Mendelson, K. and F. J. Schoen, Heart valve tissue engineering: concepts, approaches, progress, and challenges, *Ann. Biomed. Eng.* 2006.34(12): pp 1799-1819.

[14] O'Brien, M. F., S. Goldstein, S. Walsh, K. S. Black, R. Elkins and D. Clarke, The SynerGraft valve: a new acellular (nonglutaraldehyde-fixed) tissue heart valve for autologous recellularization first experimental studies before clinical implantation, *Semin. Thorac. Cardiovasc. Surg.* 1999.11(4 Suppl 1): pp 194-200.

[15] Shinoka, T., C. K. Breuer, R. E. Tanel, G. Zund, T. Miura, P. X. Ma, R. Langer, J. P. Vacanti and J. E. Mayer, Jr., Tissue engineering heart valves: valve leaflet replacement study in a lamb model, *Ann. Thorac. Surg.* 1995.60(6 Suppl): pp S513-516.

[16] Hoerstrup, S. P., R. Sodian, S. Daebritz, J. Wang, E. A. Bacha, D. P. Martin, A. M. Moran, K. J. Guleserian, J. S. Sperling, S. Kaushal, J. P. Vacanti, F. J. Schoen and J. E. Mayer, Jr., Functional Living Trileaflet Heart Valves Grown In vitro, *Circulation*, 2000.102(90003): pp III-44-49.

[17] Morsi, Y. S., I. E. Birchall and F. L. Rosenfeldt, Artificial aortic valves: an overview, *Int. J. Artif. Organs*. 2004. 27(6): pp 445-451.

[18] Morsi, Y.S., Wong, C.S. and Patel, S.S., Conventional manufacturing process for three-dimensional scaffolds, *Virtual Prototyping of Biomanufacturing in Medical Applications*, 2008, Chapter7: pp. 129-148.

Paper ID: KL-03

Natural Fiber Reinforced Polymer Composites: a Green Alternative

S. M. Sapuan[1,2], Y.A. El-Shekeil[1]
[1]Department of Mechanical and Manufacturing Engineering, Universiti Putra Malaysia, 43400 UPM Serdang, Selangor, Malaysia
[2]Laboratory of Biocomposite Technology, Institute of Tropical Forestry and Forest Products (INTROP), Universiti Putra Malaysia, 43400 UPM Serdang, Selangor, Malaysia
E-mail: drsapuan@yahoo.com

Abstract

Composites are materials that consist of two or more materials; one of them serves as a matrix and one or more serve as fillers or reinforcing agents. Polymers are divided into petroleum based and biobased. Biobased polymers come to replace petroleum based once to reduce the impact of synthetic polymers on the environment. Fibers can be synthetic (e.g. carbon and glass fiber) or natural fibers such as kenaf, jute and sisal. Due to huge amount of plastics and synthetic fiber-plastic composites, and their negative effect on environment, shortage of landfill space, depletion of petroleum resources –which is needed to produce plastics- the need of biobased plastics and composites is growing. The importance of natural fiber composites has become more apparent due to their numerous benefits such as low cost and density. They have less abrasiveness to equipment and they need less energy for processing if compared to synthetic fiber composites. They are also renewable and biodegradable. This paper overviews the natural fiber reinforced polymer composite; its background, polymers, natural fibers, composite mechanical properties and natural fiber composites.

Keywords: Natural fiber composites, eco-friendly materials, renewable fibers.

1. Background

Composites are materials that consist of two or more materials; one of them serves as a matrix and one or more serve as fillers or reinforcing materials. The properties of the composite material vary from the properties each individual component. By 1960s fiber reinforced polymers were too expensive, therefore used in the niche market only. By the 1980s and 1990s decreased to be used in broad applications [1]. Polymers are divided into petroleum which is popular and biobased polymers that come to replace petroleum based once to reduce the impact of synthetic polymers on the environment. Fibers can be synthesis such as; carbon, and glass fibers and can be natural fibers such as kenaf, jute and sisal. Due to huge amount of plastics and synthetic fiber-plastic composites, and their negative effect on environment, shortage of landfill space, depletion of petroleum resources –which is needed to produce plastics- the need of biobased plastics and composites is growing. The new trend of biobased plastics and composites is based on renewable plant and agricultural stock [2]. It will be difficult to substitute petroleum-based products with 100% biobased ones. A viable solution is to combine petroleum and bioresources to produce useful products [2].

The importance of natural fiber composites has become more apparent due to their numerous benefits such as low cost and density. They have less abrasiveness to equipment and they need less energy for processing if compared to synthetic fiber composites. They are also renewable and biodegradable. On the other hand there are some obstacles facing today's very promising natural fiber composites industry. The first point raises when natural fiber composites are discussed is the fiber-polymer incompatibility. The reason behind incompatibility is the hydrophilic nature of natural fibers vs. hydrophobic nature of most polymers used in this field. In the trail to reduce incompatibility many methods have been used including but not limited to chemical and physical treatments for natural fibers, using coupling agents in the interface between fibers and polymers etc.

2. Polymers

Polymers and polymer composites are gaining more importance as structural materials and replacing materials for metals in applications within the aerospace, automotive, marine, sporting goods and electronic industries. Polymers are divided into two main groups; thermoplastics and thermosets.

Molecular structure of thermoplastics is simple. Their macromolecules are independent. Thermoplastics can be softened or melted by heating; therefore they can be shaped, formed and solidified when cooled. Thermoplastics can be recycled and reprocessed without sever damage [3].
Thermosets have independent macromolecules before hardening, just like thermoplastics, however hardening creates three dimensional structures by chemical cross linking during processing.
Using thermoplastic composite in structural application will need the help of fiber reinforcement in order to have more stiffness to withstand the load. Fiber reinforced polymers started after World War II. Combining fibers with polymers resulted in better mechanical properties than either the components alone. By 1960s fiber reinforced polymers were too expensive, therefore used in the niche market only. By the 1980s and 1990s decreased to be used in broad applications [1].
Based on chemical structure types of thermoplastics can reach more than 50. There are thermoplastic in the group of polyolefins (e.g polyethylene, polypropylene), vinyls (e.g, poly-vinylchloride), styrenics (e.g polystyrene), fluoropolymers (e.g polychlorotrifluoro-ethylene), acrylics (e.g polymethylmetacrylate), polyesters (polyethylene terephthalate), polyimides (e.g polyetherimide), polyamides (e.g nylon 66), Sulfur-containing polymers (e.g polysulfone), Polyethers (e.g polyacetal), and others like thermoplastic polyurethane [4].

Advantages of thermoplastics compared to thermosets [3, 5, 6]:

It is rational to justify using thermoplastic despite their higher cost rather than using thermoset polymers:

- Thermoplastics can be melted, reformed and reshaped without losing its properties, while thermosets are cross-linked after the first curing and cannot be reformed or remelted.
- Thermoplastic processing time is a fraction of the long curing time of thermosets.
- Thermoplastics have near infinite shelf life with less cost to be stored, while shelf life of thermosets is less than six months with added refrigerating expenses.
- Thermoplastics have greater toughness than thermosets, which means a better impact strength.
- Thermoplastics can be completely recycled, and little to no volatile organic compounds (VOCs) are released during processing. Thermosets materials, on the other hand, can only be ground filled.
- Reduction in cycle time at temperature, the processing energy of the thermoplastics is less than processing energy for thermosets.

Disadvantages of thermoplastics compared to thermosets

The biggest disadvantage of thermoplastics compared to thermoset is that viscosity of thermoplastics is higher than viscosity of thermosets. Thermoplastics can have melt viscosities from 500 to 1000 times more than thermosets [7]. Therefore; it will need higher pressure in processing. High matrix viscosity of thermoplastics can cause other problems during processing thermoplastic composites such as de-alignment of reinforcing fibers during consolidation and the formation of voids within the final composite product. Another disadvantage of thermoplastics is the creep and relaxation of the material if the temperature rises. This is because thermoplastics have no chemical links between macromolecules [3]. Policies to use recyclable materials are increasing, therefore, in some applications industry is going towards using thermoplastics despite its disadvantages.

3. Natural fibers

Natural fibres are considered as composites of hollow cellulose fibrils with lignin and hemicelluloses as matrix. [8]. Natural fibers are divided into three main divisions based on their origins; plants, animals and minerals as shown in Figure 1. The term “natural fibers” in this research will be directed to plant (lignocellulosic) fibers. Plant fibers include straw, bast, leaf, seed, or grass fibers. Properties of natural and synthetic fibers are shown in Table 1. Typical structure of a natural fiber is shown in Figure 2.

The main component of plant fibers is cellulose followed by hemicelluloses and lignin. Cellulose is a linear macromolecule consisting of ($C_6H_{11}O_5$) repeating units. Chemical structure of cellulose is shown in Figure 3.

Cellulose has an average molecular weight between 130,000 and 190,000 with an average degree of polymerization of approximately 800 to 1200. Hemicelluloses consist of polysaccharides of comparatively low molecular weight built up from hexoses, pentoses, and uronic acid residues [9]. Lignin is a complex chemical compound –it’s thought to have three-dimensional copolymer of aliphatic and aromatic constituents with very

high molecular weight. It gives the rigidity to the plants [2, 9]. Chemical composition of some natural fibers is shown in Table 2

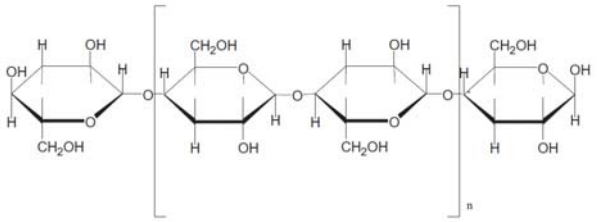

Fig. 3. Chemical structure of cellulose

Table.

Cellulose is the main component of natural fibers. Main component of cellulose is anhydro-d-glucose, which contains three hydroxyl groups. These hydroxyl groups make natural fibers hydrophilic in nature [10, 11]. Natural fibers are increasingly being used due to their lightweight, non-abrasiveness, combustibility. They are also non-toxic, lower in cost than synthetic fibers with biodegradable properties.

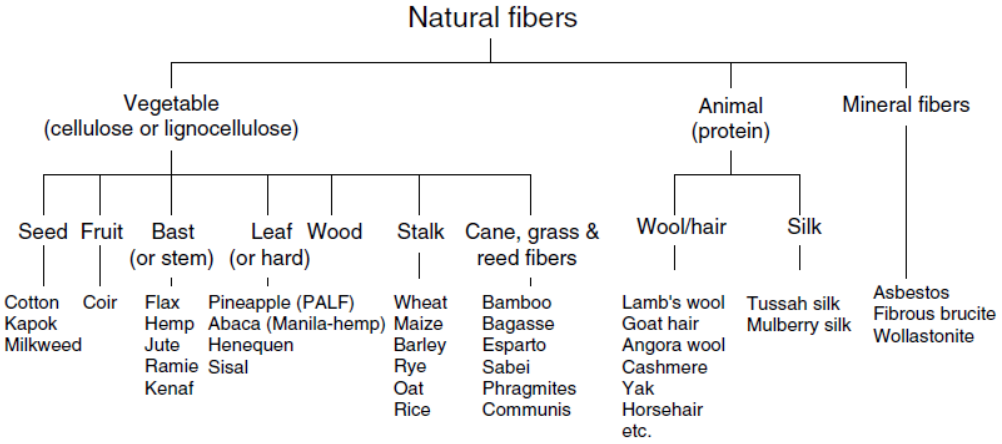

Fig. 1. Classification of natural fibers [12].

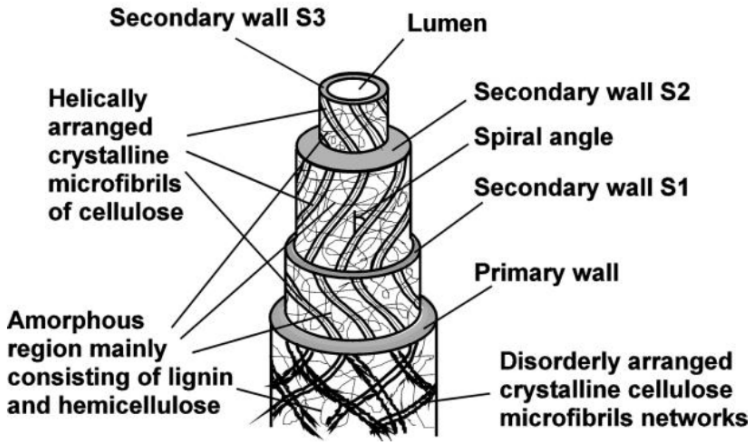

Fig. 2. Typical structure of natural fiber [8]

Table 1. Properties of natural and synthetic fibers [16]

Fiber	Density (g cm^{-3})	Diameter (μm)	Tensile Strength (MPa)	Young's Modulus (GPa)	Elongation at Break (%)
Flax	1.5	40–600	345–1500	27.6	2.7–3.2
Hemp	1.47	25–500	690	70	1.6
Jute	1.3–1.49	25–200	393–800	13–26.5	1.16–1.5
Kenaf			930	53	1.6
Ramie	1.55	—	400–938	61.4–128	1.2–3.8
Nettle			650	38	1.7
Sisal	1.45	50–200	468–700	9.4–22	3–7
Henequen					
PALF		20–80	413–1627	34.5–82.5	1.6
Abaca			430–760		
Oil palm EFB	0.7–1.55	150–500	248	3.2	25
Oil palm mesocarp			80	0.5	17
Cotton	1.5–1.6	12–38	287–800	5.5–12.6	7–8
Coir	1.15–1.46	100–460	131–220	4–6	15–40
E-glass	2.55	<17	3400	73	2.5
Kevlar	1.44		3000	60	2.5–3.7
Carbon	1.78	5–7	3400[a]–4800[b]	240[b]–425[a]	1.4–1.8

[a] Ultra high modulus carbon fibers.
[b] Ultra high tenacity carbon fibers.

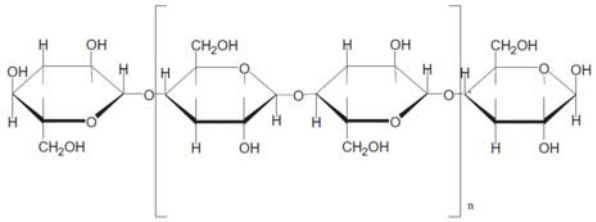

Fig. 3. Chemical structure of cellulose

Table 2. Chemical compositions of some plant fibers [13]

Type of fiber	Cellulose	Lignin	Pentosan	Ash	Silica	Spiral Angle (deg)
Stalk Fiber						
Straw						
Rice	28-48	12-16	23-28	15-20	9-14	-
Wheat	29-51	16-21	26-32	4.5-9	3-7	-
Barley	31-45	14-15	24-29	5-7	3-6	-
Oat	31-48	16-19	27-38	6-8	4-6.5	-
Rya	33-50	16-19	27-30	2-5	0.5-4	-
Cane fiber						
Bagasse	32-48	19-24	27-32	1.5-5	0.7-3.5	-
Bamboo	26-43	21-31	15-26	1.7-5	0.7	-
Grass fiber						
Esparto	33-38	17-19	27-32	6-8	-	-
Sabai	-	22	24	6	-	-
Reed fiber						
Phragmites						
Communis	44-46	22-24	20	3	2	-
Bast Fiber						
Seed flax	43-47	21-23	24-26	5	-	8-10
Kenaf	44-57	15-19	22-23	2-5	-	8
Jute	45-63	21-26	18-21	0.5-2		8
Hemp	57-77	9-13	14-17	0.8	-	6
Ramie	89-91	-	5-8	-	-	8

Core fiber						
Kenaf	37-49	15-21	18-24	2-4	-	-
Jute	41-48	21-24	18-22	0.8		-
Leaf fiber						
Abaca (Manila)	56-63	7-9	15-17	1-3	-	-
Sisal						
(agave)	43-62	7-9	21-24	0.6-1	-	10-25
Seed Hull fiber						
Cotton	85-96	0.7-1.6	1-3	0.8-2	-	-
Wood fiber						
Coniferous	40-45	26-34	7-14	<1	-	-
Deciduous	38-49	23-30	19-26	<1	-	-

4. Composite materials

A composite material can be defined as a material containing two or more materials which after mixing in a controlled manner can produce a new material with new properties. These properties are unique and superior in some respects to the properties of individual components [14]. Composites can be classified into three of the following: ceramics, metals and polymeric composites. This research is concerned only about the polymeric composites. From another point of view the composite material can be defined as a material that consists of fibers or fillers plus a resin. Fibers work as carriers of the load, therefore increase the stiffness of the composite. Fillers serve to reduce the cost. Sometimes additives are added to the composites to enhance mechanical and physical properties. Composite materials can be classified based in two main categories: based on size of fibers, or type of fibers. First, by size: short or long fiber size. Second, synthetic or natural fibers. This research is concerned about a short natural fiber composite.

4. Composite mechanical properties

Composite mechanical properties are considered the most important even though the composite may not be designed for load bearing applications. At least shape of the composite product should be maintained stable during usage [13]. Mechanical properties for short fiber reinforced composites are not easy to be estimated. There are some reasons behind that such as: (1) fiber dispersion, (2) fiber orientation distribution, (3) fiber volume fraction and (4) the quality of interface between fiber and matrix that influence the composite properties [13]. These factors, due to variation in fiber length and fiber length distribution in short fibers, along with inherent process variability, cannot be controlled precisely during manufacturing from part to part or from batch to batch [13, 15, 16]. Significant change in properties of the composite can be achieved by changing factors like aspect ratio and volume fraction [17]. If the aspect ratio is too small there will be insufficient stress transfer to fibers and thus the reinforcement is improper and sometimes fiber will act as a filler. In contrast if the aspect ratio is too high, the fibers may get entangled during processing leading to poor mechanical properties, due to poor dispersion. At low level of fiber loading the fibers are not able to transfer the load to one another leading to decrease in the strength. At higher levels of fiber content the fibers are not sufficiently wetted by the matrix, and the increased population of fibers leads to agglomeration and stress transfer gets blocked [18-20].

5. Natural fiber composites

Natural fiber reinforced polymers are gaining more and more awareness due to benefits such as renewability, biodegradability and reduction in weight and cost. Further advantages of natural fibers are [21]:

- As plants they contribute to CO2 consumption;
- At the end of natural fiber's life if burned or landfilled, the amount of CO2 is neutral;
- The abrasive nature of natural fiber is low which make it easy to process and more recyclable.

Factors like worldwide environmental concern, very fast consumption of petroleum, since plant resources 100,000 times faster than petroleum resource can be renewed [22], these factors are forcing the whole world to "go green".

Joshi et al. [23] have studied the life cycle of natural and glass fiber composites and found that natural fibers are environmentally superior to glass fibers in most cases. The following reasons justify this conclusion: 1- processing natural fibers has less impact into the environment; 2- an application requires a higher percentage of natural fiber than glass fiber to get the same performance, which reduces the percentage of polymer needed. This contributes to lower the cost and reduce the pollution caused by the polymers; 3- less density of natural fiber composites results in a better efficiency, and less emission in the usage stage -in the automotive applications; 4- burning the natural fibers at the end of its life results in energy and carbon credits. However,

fertilizer use in natural fiber cultivation results in higher nitrate and phosphate emissions which can lead to a negative effect on local water [24]. Energy consumed to produce a glass fiber is much more than the energy of producing a natural fiber. The energy needed to produce a fiber like flax is approximately 17% of the energy needed to produce the same amount of glass fiber [25].

Research by Mohanty et al. [26] has shown that natural fiber composites show comparable or even better mechanical properties over glass fiber reinforced plastics. However, utilizing natural fibers and replacing glass fibers is still challenging. Lots of work needs to be done in order to overcome the shortcomings of natural fibers. Some of the common drawbacks of utilizing natural fibers with polymer composites are: high moisture sorption, which affects the properties of the final product and low processing temperature due to the degradation of natural fibers at high temperature. The high moisture sorption limits the applications of the composites, and the low processing temperature limits the matrix selection to the low melted matrices. Another problem facing natural fiber reinforced polymers is the poor adhesion (i.e. incompatibility) between fibers and polymers due to the hydrophilic nature of cellulose and the hydrophobic nature of polymers. There are three main solutions for the poor adhesion; pre-treating natural fibers to enhance their properties, using coupling agents or compatiblizers to modify the polymers, and selecting suitable processing methods for producing the composites [26].

Uniformity and shape of natural fibers gives them another challenge to be produced. Along the length of the fiber different there are always different cross-sections. This makes difficulty in the prediction of the mechanical properties of the composites. Natural fiber composites are not considered totally green unless growth, separation and processing of the fibers are well controlled. Durability of the composite product is another issue where it should be comparable to glass fiber composites [24].

6. Acknowledgment

Parts of this paper have been published in Yousuf El-Shekeil, 2012 *Properties of Short Kenaf Bast Fiber-Reinforced Thermoplastic Polyurethane Composites,* Doctoral Thesis, Universiti Putra Malaysia.

6. References

[1] Bakis CE, Cosenza E, Lesko JJ, Machida A. Fiber-reinforced polymer composites for construction—state-of-the-art review. Journal of Composites for Construction. 2002;6:73-.

[2] Mohanty AK, Misra M, Drzal LT. Natural Fibers, Biopolymers, and their Biocomposites. Boca Raton: CRC Press; 2005.

[3] Biron M. Thermoplastics and thermoplastic composites: technical information for plastics users. Oxford: Elsevier; 2007.

[4] Wirawan R. Thermo-mechanical properties of sugarcane bagasse-filled polyvinyl chloride composites. PhD Thesis: Universiti Putra Malaysia; 2011.

[5] Greco A, Musardo C, Maffezzoli A. Flexural creep behaviour of PP matrix woven composite. Composites Science and Technology. 2007;67:1148-58.

[6] Mohd Ishak ZA, Leong YW, Steeg M, Karger-Kocsis J. Mechanical properties of woven glass fabric reinforced in situ polymerized poly (butylene terephthalate) composites. Composites Science and Technology. 2007;67:390-8.

[7] Thermoplastic Composites Explained. 2010.

[8] Rong MZ, Zhang MQ, Liu Y, Yang GC, Zeng HM. The effect of fiber treatment on the mechanical properties of unidirectional sisal-reinforced epoxy composites. Composites Science and Technology. 2001;61:1437-47.

[9] Rowell RM, Stout HP. Jute and Kenaf, in" A Handbook of Fiber Chemistry," Lewin and Pearce, Eds: Marcel Dekker, Inc., New York; 1998.

[10] Habibi Y, El-Zawawy WK, Ibrahim MM, Dufresne A. Processing and characterization of reinforced polyethylene composites made with lignocellulosic fibers from Egyptian agro-industrial residues. Composites Science and Technology. 2008;68:1877-85.

[11] Aji IS. Mechanical and thermal characterization of hybridized short kenaf/ pineapple fiber reinforced high density polyethylene composites. PhD Thesis: Universiti Putra Malaysia; 2011.

[12] Anuar H, Zuraida A. Improvement in mechanical properties of reinforced thermoplastic elastomer composite with kenaf bast fibre. Composites Part B: Engineering. 2011;42:462-5.

[13] Ichhaporia PK. Composites from natural fibers. PhD Thesis: Carolina State University; 2008.

[14] Hull D, Clyne TW. An introduction to composite materials. Cambridge: Cambridge University Press; 1996.

[15] Arnold CA, Hergenrother PM, McGrath JE. An overview of organic polymeric matrix resins for composites. Composite Applications: The Role of Matrix, Fiber, and Interface, TL Vigo and BJ Kinzig (eds), VCH, New York. 1992.
[16] De SK, White JR. Short fibre-polymer composites. Boca Raton: CRC; 1996.
[17] Shalin RE. Polymer matrix composites. London: Chapman & Hall; 1995.
[18] El-Shekeil YA, Salit MS, Abdan K, Zainudin ES. Development of a new kenaf bast fiber-reinforced thermoplastic polyurethane composite. BioResources. 2011;6:4662-72.
[19] Jacob M, Thomas S, Varughese KT. Mechanical properties of sisal/oil palm hybrid fiber reinforced natural rubber composites. Composites Science and Technology. 2004;64:955-65.
[20] Özturk S. Effect of fiber loading on the mechanical properties of kenaf and fiberfrax fiber-reinforced phenol-formaldehyde composites. Journal of Composite Materials. 2010;44:2265-.
[21] Bledzki AK, Gassan J. Composites reinforced with cellulose based fibres. Progress in Polymer Science. 1999;24:221-74.
[22] Netravali AN, Chabba S. Composites get greener. Materials today. 2003;6:22-9.
[23] Joshi SV, Drzal LT, Mohanty AK, Arora S. Are natural fiber composites environmentally superior to glass fiber reinforced composites? Composites Part A. 2004;35:371-6.
[24] Summerscales J, Dissanayake N, Virk A, Hall W. A review of bast fibres and their composites. part 2 – composites. Composites Part A: Applied Science and Manufacturing. 2010;41:1336-44.
[25] Holbery J, Houston D. Natural-fiber-reinforced polymer composites in automotive applications. JOM Journal of the Minerals, Metals and Materials Society. 2006;58:80-6.
[26] Mohanty AK, Misra M, Drzal LT. Sustainable bio-composites from renewable resources: opportunities and challenges in the green materials world. Journal of Polymers and the Environment. 2002;10:19-26.

Paper ID: KL-04

Fluid Dynamic Behaviors of Cylindrical Structures

Md. Mahbub Alam
Institute for Turbulence-Noise-Vibration Interaction and Control, Department of Mechanical Engineering and Automation, Shenzhen Graduate School
Harbin Institute of Technology
Shenzhen, China

E-mail: alamm28@yahoo.com; alam@hitsz.edu.cn

Abstract

Multiple cylindrical structures are widely seen in engineering. Flow interference between the structures leads to a very high fluctuating forces, structural vibrations, acoustic noise, or resonance, which in some cases can trigger failure. Recently circular pins in various arrays have been used as fins to enhance the cooling effect. While the enhancement is directly connected to nature of flow around the pins, not much is known about the physics of flow around the pins. The knowledge of flow around two cylinders is insightful for understanding the flow around an array of structures/pins. This paper comprises an in-depth physical discussion of the flow-induced vibration of two circular cylinders in view of the time-mean lift force on stationary cylinders and interaction mechanisms. The gap-spacing ratio T/D is varied from 0.1 to 5 and the attack angle α from 0° to 180° where T is the gap width between the cylinders and D is the diameter of a cylinder. Six interaction mechanisms and five instabilities were observed. While the six interaction mechanisms are connected to six different responses, the five instabilities are responsible for multistable flows. Though a single non-interfering circular cylinder does not correspond to a galloping following quasi-steady galloping theory, two circular cylinders experience violent galloping vibration due to shear-layer/wake and cylinder interaction as well as boundary layer and cylinder interaction. A larger magnitude of fluctuating lift communicates to a larger amplitude vortex excitation.

Keywords: fluid dynamics, structures, forces, instabilities, interactions, flow-induced vibrations.

1. Introduction

Cylindrical structures in a group are frequently seen on land and in the ocean, for example, chimney stacks, tube bundles in heat exchangers, high-rise buildings, harvesting wave and tide energy from ocean, overhead power-line bundles, bridge piers, stays, masts, chemical-reaction towers and offshore platforms. Mutual flow interaction between the structures makes the wake very excited or tranquil depending on the spacing between the structures. The excited wake-enhancing forces in some cases cause a catastrophic failure of the structures. Naturally, it is important to understand the proximity effect on aerodynamics associated with multiple closely spaced cylindrical structures. While much is known of the flow physics around a single isolated cylinder, not much is known of the fluid dynamics around a cylinder neighbored by another. There is no doubt that flow physics around two cylinders is much more complex and more complicated than that around a single cylinder, because of interference between the cylinders [1, 2]. The study of the aerodynamics of two closely separated structures is thus of both fundamental and practical significance. Cross-flow-induced vibration problems are frequently encountered for cylindrical structures such as electric power lines, cooling towers, flow sensor tubing, cables of suspension bridges, etc. The resulting vibrations depend strongly on cylinder configuration (relative to flow), pitch spacing, cylinder diameters and flow conditions. The cross-flow-induced vibration is the most important problem in various fields, and is known to have caused many failures in various industrial components.

Time-mean drag and lift forces acting on two staggered cylinders have been examined in the literature (e.g. [3-5]), with most of the emphasis being on the downstream cylinder. Only a few studies have reported force measurements for the upstream cylinder [6-9]. Furthermore, fluctuating force measurements in the literature are very scant, though the fluctuating lift and drag forces acting on structures are a major cause of the fatigue failure of the structures and are used for predicting flow-induced responses. Most literature sources are connected to

one of the three arrangements, tandem ($\alpha = 0°$) or side-by-side ($\alpha = 90°$) or staggered ($0° < \alpha < 90°$). See Fig. 1 for definitions of symbols. Furthermore, flow classifications in the literature are based on either theoretical treatment [10], or experimental measurement of forces, *St* and pressure (e.g. [4]) or flow visualization image (e.g. [11]).

The instability of slender structures has received the attention of many scientists during decades [12-15]. One of the reasons for such studies is the fact that buildings and other slender structural elements are built more and more frequently using new techniques that involve weight-saving materials (thus reducing the overall stiffness) and innovative cross-sectional geometries. In consequence, when designing certain structures such as particularly high and slender buildings, one may find that critical velocities of aeroelastic instabilities such as vortex-induced excitation and galloping are within the design wind speed.

Practically no structure is perfectly rigid, hence it is worthy to gain physical insight into the flow-induced response of the structure. Bokaian and Geoola [16] investigated the case of two identical cylinders in tandem and staggered arrangements where the downstream one was fixed and the upstream one both-end-spring-mounted, allowing both ends to vibrate at the same amplitude (two-dimensional model) in the cross-flow direction only. They reported galloping vibration generated at a spacing ratio of $T/D < 0.8$ ($\alpha = 25°$), $T/D \leq 0.75$ ($\alpha = 0°$) and vortex excitation (VE) at other T/D and α. Bokaian and Geoola [17] also investigated the other case where the upstream cylinder was fixed and the downstream one was free to oscillate. Depending on T/D, the cylinder exhibited either only galloping ($T/D = 0.59$, $\alpha = 0°$) or only VE ($T/D > 1.5$, $\alpha = 0°$) or a combined VE and galloping ($T/D > 0.5$, $\alpha = 0°$), or a separated VE and galloping ($1.0 \leq T/D \leq 1.5$). Note that the vibration always occurs at the natural frequency f_n of the cylinder. The VE corresponded to vibration occurring near the reduced velocity U_r ($= U_\infty/f_nD$, U_∞ is the free-stream velocity) where the natural vortex-shedding frequency f_v is close to f_n. On the other hand, the galloping vibrations persist for higher U_r corresponding to a higher f_v than f_n. In Bokaian and Geoola [16-17], the investigated ranges of T/D, α and mass-damping factor $m^*\zeta$ were 0.09 ~ 4, 0° ~ 70° and 0.018 ~ 0.2, respectively, where m^* is the mass ratio and ζ is the damping ratio.

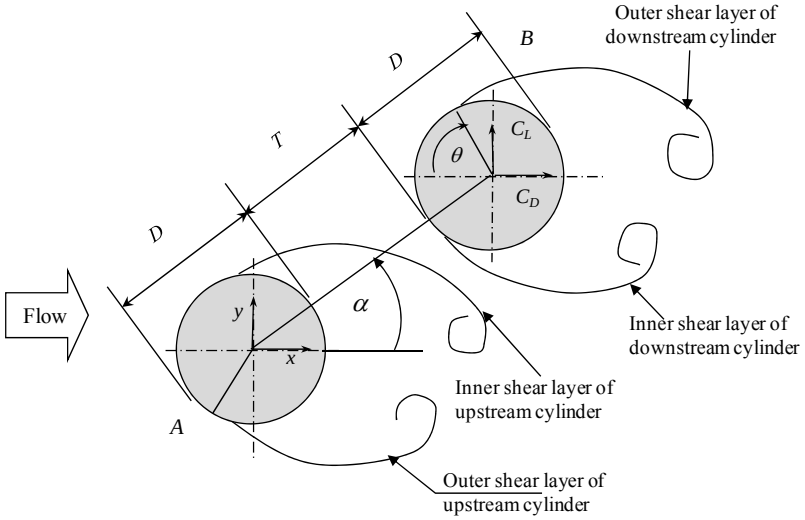

Fig. 1. Arrangement of cylinders and definitions of symbols.

Laneville and Brika [18] coupled two identical cylinders ($T/D = 7 \sim 25$, $m^*\zeta = 0.00007$) mechanically by thin wires, allowing them to vibrate in in-phase and out-of-phase mode. They found that the response of the cylinder is more complex and dependent on the coupling mode. Huera-Huarte and Bearman [19] conducted experiments on flow-induced responses of two tandem cylinders for $L/D = 1$ to 3 at $m^*\zeta = 0.043$. The upstream cylinder experienced larger vibrations than the rear one for small gap distances at small U_r, when the shedding frequency was close to its natural frequency. The downstream cylinder exhibited galloping with large amplitudes at high U_r for the largest gap separations.

Alam and Kim [20] and Kim et al. [21] conducted a systematic investigation on flow-induced response characteristics of two circular cylinders at $\alpha = 0° \sim 90°$, $T/D = 0.1 \sim 3.2$. Dependence of vibration-amplitude-to-diameter ratio a/D on reduced velocity U_r was examined.

The objectives of this study were to (i) classify possible interaction mechanisms and instability for two stationary rigid cylinders, and (ii) correlate interaction mechanisms, lift forces and flow-induced responses of

the cylinders mounted elastically. The possible range of α = 0° ~ 180° was considered with T/D = 0.1 ~ 5.0. Flow-induced response results are incorporated from literature published by the current author and others.

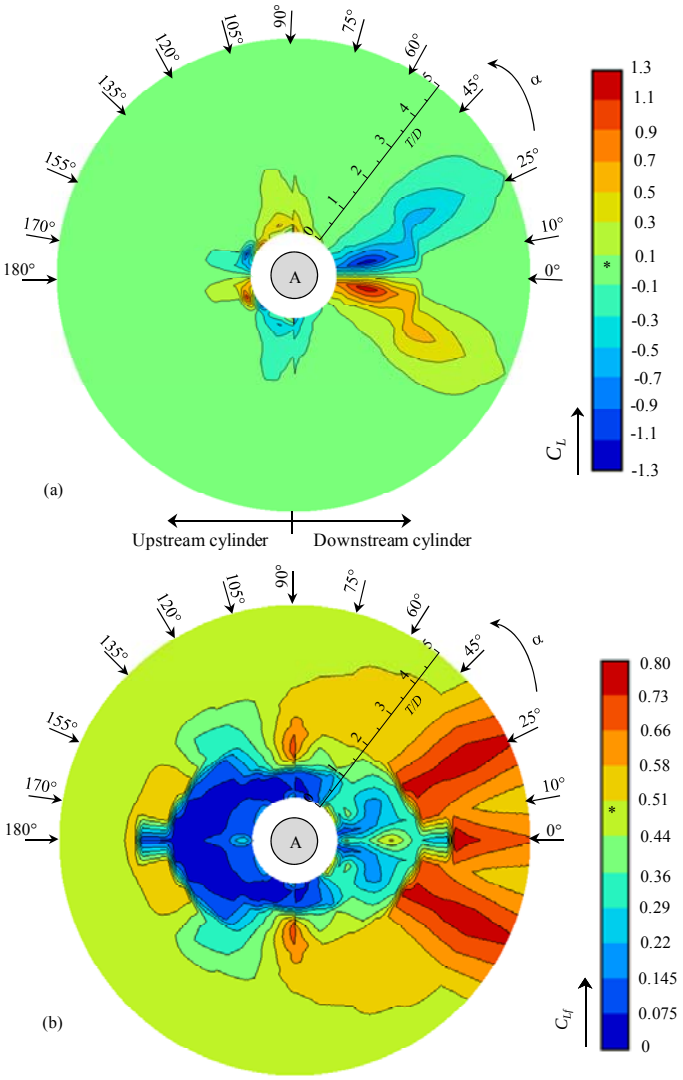

Fig. 2. Contour maps of (a) time-mean lift coefficient C_L and (b) fluctuating lift coefficient C_{Lf} of cylinder *B*. [1]. Points marked by '*' denote values of coefficients of an isolated cylinder.

2. Experimental details

Fluid force measurements were conducted in a closed-circuit wind tunnel with a 2.2-m-long test section of 0.3 m in width and 1.2 m in height at Kitami Institute of Technology. Two circular cylinders of the same diameter D = 49 mm, made of brass, spanned horizontally across the test section width. The free-stream velocity, U_∞, was 17 m/s, resulting in Reynolds number Re ($\equiv U_\infty D/\nu$) = 5.5 × 10^4, where ν is the kinematic viscosity of air. The flow non-uniformity was within ± 0.2% (rms) inside the central cross-sectional area of 0.24 m × 0.95 m in the test section, and the longitudinal turbulence intensity was less than 0.5% in the absence of the cylinders. A schematic diagram of the cylinder arrangement appears in Fig. 1, along with the definitions of symbols. The Cartesian coordinate system was defined such that the origin was at the center of Cylinder *A*, with the *x*- and y-axis along the streamwise and lateral directions, respectively.

Fluid forces were measured over a small spanwise length of the cylinders using load cells. Measurements were done for α = 0° ~ 180°, T/D = 0.1 ~ 5. Tuning of T/D was T/D = 0.1, 0.2, 0.3, 0.5, 0.6, 0.7, 0.8, 0.9, 1.1, 1.2, 1.5, 1.8, 2.1, 2.4, 2.7, 3.0, 3.5, 4.0, 4.5 and 5.0.

Flow visualization was carried out in a water channel with a 300 × 350 mm working section and 1.5 m in length. Two circular tubes with identical diameters of 20 mm were used. The Reynolds number in the water channel experiment was 350. The flow was visualized by using the hydrogen bubble technique, involving a platinum wire of 0.02 mm in diameter.

3. Results and discussion

3.1. Fixed cylinders

Lift forces

Time-averaged lift coefficient (C_L) and fluctuating (rms) lift coefficient (C_{Lf}) are measured for the whole ranges of α and T/D mentioned in section 2. Contours of time-averaged lift coefficient (C_L) and fluctuating (rms) lift coefficient (C_{Lf}) measured on the C_L and C_{Lf} in a T/D - α plane are presented in Fig. 2. In the scale bars, the color or the range marked by black '*' indicates the value of a single isolated cylinder. The result can be described with reference to Fig. 1 in which Cylinder A is fixed, and traversing of Cylinder B is done with variations of the two parameters T/D and α, which suffice to determine the possible arrangement of the two cylinders. It may be noted that Cylinder B acts as the downstream cylinder for $|\alpha| < 90°$ and the upstream cylinders for $|\alpha| > 90°$, i.e. the left and right sides of a contour map show the values of coefficient of the upstream and downstream cylinders, respectively. At the peripheries of the middle and outer circles, the values of T/D are 0.0 and 5.0, respectively. Upward (+ve y-direction) C_L is considered as positive.

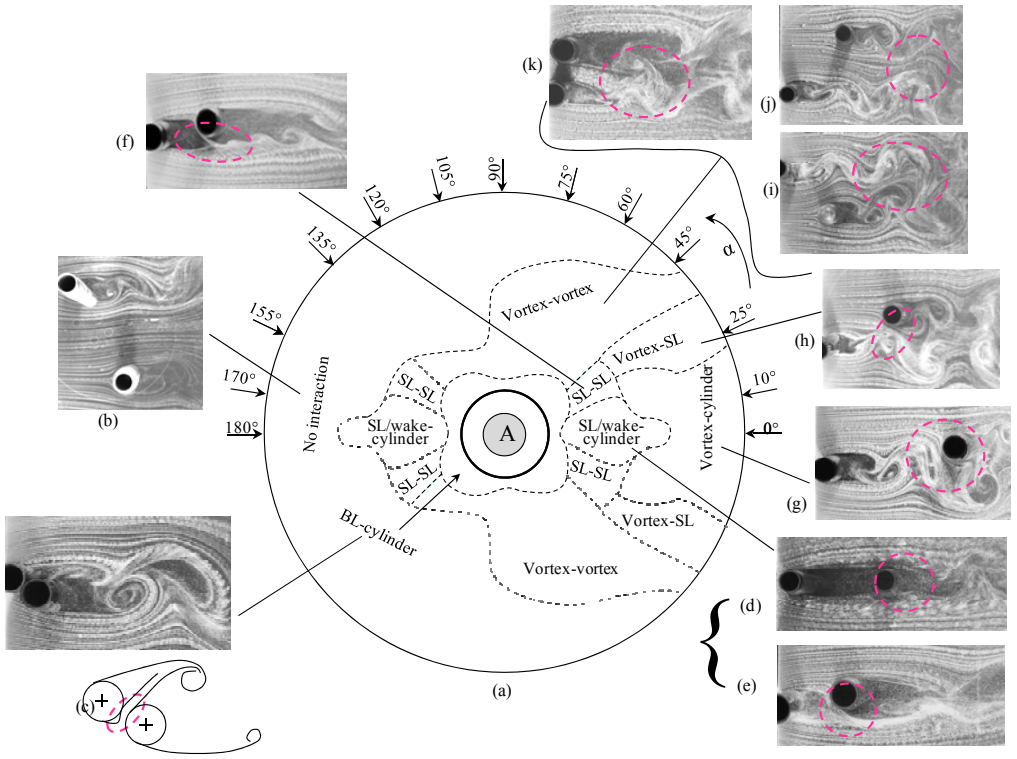

Fig. 3. Interaction regimes in T/D - α plane. SL : shear layer, BL : boundary layer.

The C_L in the downstream region (right half) is highly sensitive to T/D and α; however, that in the upstream region (left half) retains single-cylinder values except for $|\alpha| = 135°$-$180°$, $T/D < 0.4$ - 1.0, and $|\alpha| = 90°$ - 135°, $T/D < 1.3$ - 0.4. The C_L around the cylinder for $T/D < 0.5$ varies greatly with change in α from 0° to 360°. The minimum (most negative) values of $C_L = -1.03$ and - 1.15 ~ - 1.25 occur at $\alpha = 155°$, $T/D = 0.3$ and $\alpha = 10°$, $T/D = 0.8 \sim 1.1$, respectively. At the respective conjugate positions, C_L increases to a maximum. On the other hand, C_{Lf} is extremely small for smaller spacing, i.e., $T/D < 2$ - 3 depending on α (Fig. 2b) and remarkably high for α = - 35° to 35°, $T/D > 2.5$ - 3.0. Hence the interference between the cylinders not only has a negative effect by

increasing forces, but also a positive effect by reducing forces on the cylinder. Its effect, however, depends on α and *T/D*. It is expected that at different values of *T/D* and α, interaction mechanisms between the cylinders will be different, hence C_L and C_{Lf} are strong functions of *T/D* and α.

Flow-structure interaction

When one cylinder is neighbored by another, the two cylinders may be connected to or interacted by boundary layers, shear layer, vortex and wake. Therefore it is possible that a cylinder may experience complex interaction mechanisms where cylinder, boundary layer, shear layer, vortex and wake are the five physical interacting parameters. Based on interaction mechanisms, the whole region of α and *T/D*, can be classified into six regimes as illustrated in Fig. 3, viz, boundary-layer (BL) and cylinder interaction regime, shear-layer/wake and cylinder interaction regime, shear-layer (SL) and shear-layer (SL) interaction regime, vortex and cylinder interaction regime, vortex and shear-layer (SL) interaction regime, vortex and vortex interaction regime. The flow structures given explicate the difference between the interactions.

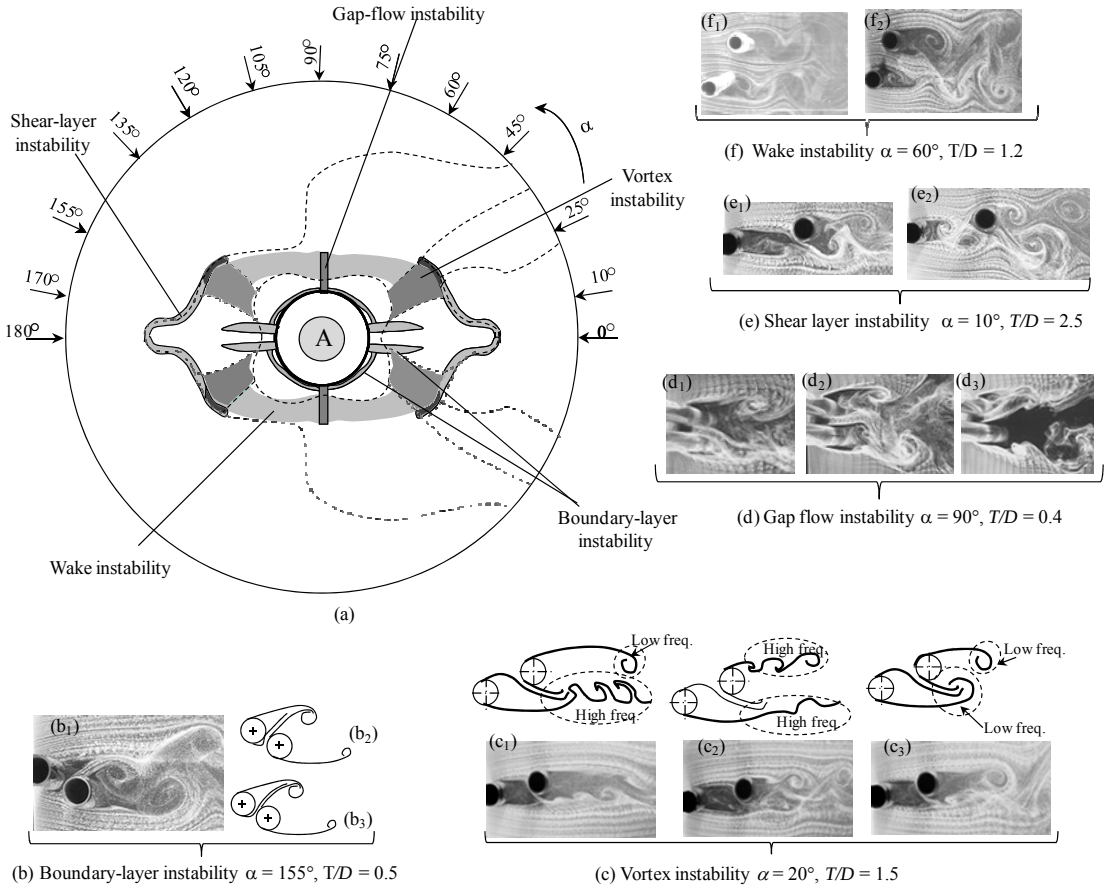

Fig. 4. (a) Types of instability and their regimes. (b-f) Multistable flow caused by the instabilities.

Flow instability

When two cylinders interact each other in the above six mechanisms, instabilities were observed in the boundary-layer, vortex, gap-flow, shear-layer and wake. The regimes where the instabilities appear are shadowed as in Fig. 4. The boundary-layer instability occurring when *T/D* is small causes formation and burst of a separation bubble (Fig. 4b_2, b_3), responsible for bistable flow. Hence a discontinuous jump/drop in lift or drag forces is afoot. When the outer shear layers of the two cylinders shed vortices at different frequencies at an intermediate α, vortex instability may result in lock-in between the vortices from the two sides, generating a tristable wake of low-high, high-high and low-low frequencies (Fig. 4c). Being very unstable, the gap flow at α

≈ 90° switches from a side to the other, engendering bistable or tristable flow (Fig. 4d). While the gap flow is biased downward (Fig. $4d_1$), it becomes straight (Fig. $4d_2$) and then swerves upward (Fig. $4d_3$). Mutual switch between reattachment (Fig. $4e_1$) and coshedding flow (Fig. $4e_2$) occurs due to instability of the upstream-cylinder shear layer when two cylinders are nearly tandem ($\alpha < 25°$). For larger α, the two wakes may have the different vortex frequencies (Fig. $4f_2$) but intermittently they become locked-in having the same frequency of vortices (Fig. $4f_1$).

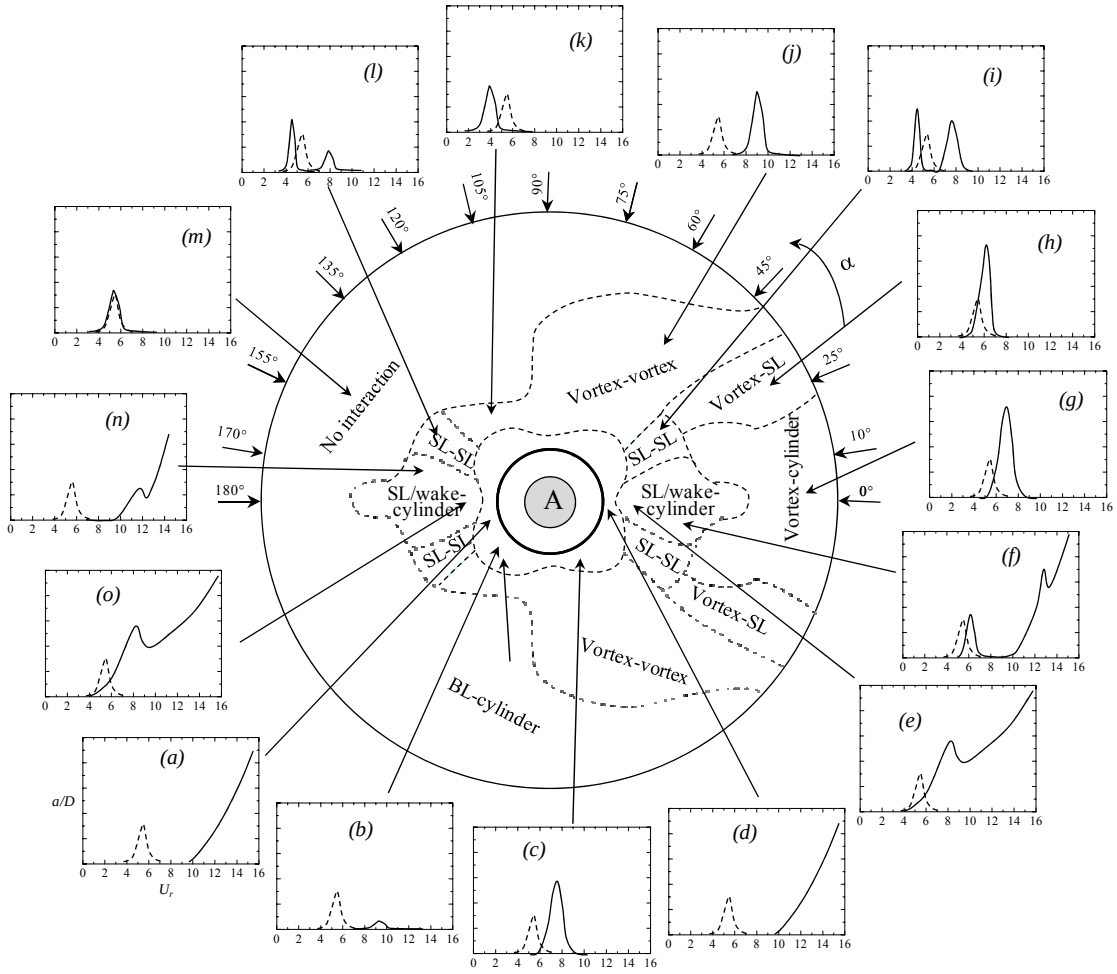

Fig. 5. Nature of flow-induced vibration responses at different interaction regimes. Dashed line represents a single isolated cylinder response. The vertical and horizontal axes of the response graphs are the vibration amplitude ratio a/D and reduced velocity U_r ($= U_\infty/f_n D$). The response curves are based on the results in [17-18 20].

3.2. Flexible cylinders

Flow-induced vibrations

How the interactions affect flow-induced instability of the two cylinders - compared to a single isolated (non-interfering) cylinder - is of great interest to researchers in science and engineering. This section includes an overview of flow-induced vibration results for two elastically mounted cylinders. The detailed results of cylinder responses at different interaction regimes are presented in Fig. 5. While the vertical axis of the response curves represents the vibration amplitude a normalized by D, the horizontal axis is U_r. The response curves were incorporated from Refs. [16-17], and Alam and Kim [20]. The dashed line in the response graphs stands for single isolated cylinder response, insinuating VE at $U_r \approx 5.4$ (≈1/St = 1/0.186). While both cylinders experience divergent galloping vibration for $U_r > 10$ at $0 < \alpha < 25°$ (Fig. 5a, d) in the boundary layer and cylinder interaction regime, they experience VE between $U_r = 7$ to 10 for $25° < \alpha < 155°$ (Fig. 5b, c). For the latter case, the downstream cylinder vibration amplitude is larger than the upstream one. Divergent violent vibrations of

both cylinders are generated in the regime of shear-layer/wake and cylinder interaction (Fig. 5e, f, n, o). VE and galloping are combined at smaller *T/D* (Fig. 5e, o) and separated for larger *T/D* (Fig. 5f). High amplitude VE is afoot in the regimes of vortex and cylinder interaction (Fig. 5g) and vortex and shear-layer interaction (Fig. 5h), where C_{Lf} on stationary cylinders is high (Fig. 2b). In the SL and SL interaction regime, VE occurs at two regimes of U_r (Fig. 5i, l). Each cylinder sheds vortices at two frequencies [22], hence experiences two VE. In the vortex and vortex interaction regime, VE intervenes at a high U_r for the downstream cylinder (Fig. 5j) and at a low U_r for the upstream cylinder (Fig. 5k). This is due to the fact that the downstream and upstream cylinders generally shed vortices at a low and at a high frequency, respectively. The no interaction regime corresponds to VE at the same U_r as that of a single cylinder (Fig. 5m).

It is worth mentioning that a larger C_{Lf} (Fig. 2b) corresponds to larger amplitude VE (Fig. 5c, g, h). The most striking feature is that divergent galloping vibration is generated at shear layer/wake and cylinder interaction (Fig. 5e, f, n, o) and at boundary layer and cylinder interaction (Fig. 5a, d) regimes where there is a large variation in C_L in the cross-flow direction (Fig. 2a). Based on galloping theories it is an acknowledged fact that galloping is not generated on an axis-symmetric body, e.g. a circular cylinder. Hence the question arises, why do two circular cylinders in close proximity experience galloping? In the regimes of boundary layer and cylinder interaction as well as shear -layer/wake and cylinder interaction, the two cylinders are connected by boundary layer or shear layer, and the combined shape of the two cylinders is not longer axis symmetric, hence the two cylinders may be prone to generating galloping vibrations. Furthermore, due to having non-uniform velocity between the cylinders, the downstream cylinder is again not axis symmetric with respect to local approaching flow. In other words, the galloping generation for two circular cylinders at close proximity is not violating the galloping theories. Details of the instability mechanism are discussed in the next section with reference to the lift force and interaction mechanisms.

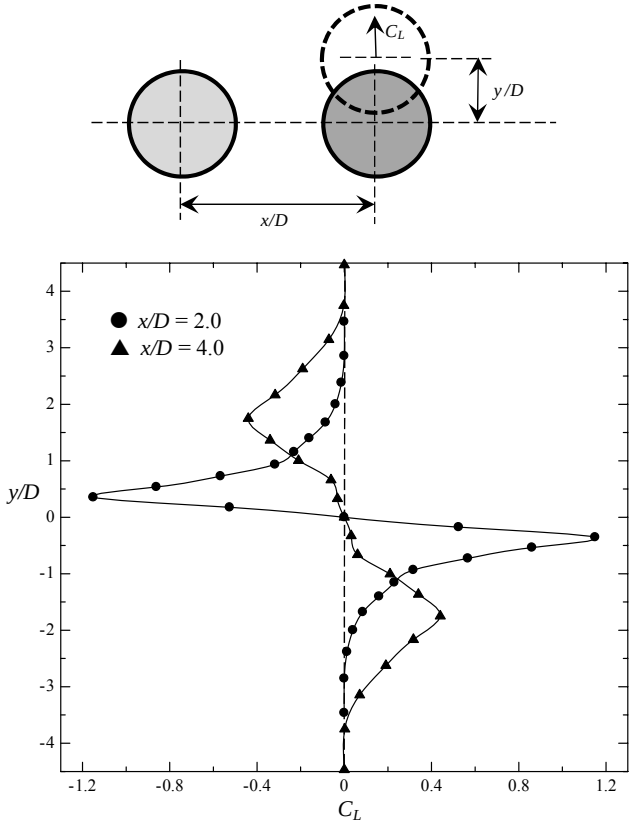

Fig. 6. Variations in C_L with *y/D* at *x/D* = 2.0 and 4.0.

Galloping mechanism

Figure 6 shows C_L variation with change in *y/D* at *x/D* = 2 and 4. C_L is maximum and minimum at *y/D* = - 0.4 and 0.4, respectively for *x/D* = 2 and at *y/D* = - 1.8 and 1.8 for *x/D* = 4. These two *y/D* values correspond to the locations of positive and negative peaks in the C_L contour map (Fig. 3a). The figure suggests that when the cylinder position is below the center line (*y/D* = 0), C_L is in an upward direction; and when the cylinder position

is above the center line, C_L is in a downward direction. Now it is possible to get $\partial C_L / \partial(y/D)$. Figure 7 shows how $\partial C_L / \partial(y/D)$ varies with *y/D*. It is clear that the system is stable for *y/D* = -0.4 ~ 0.4 and unstable for | *y/D*| > 0.4 (Fig. 7a). In the former region, our intuition is confirmed: in the case of the tandem cylinder (*y/D* = 0), when the downstream cylinder is displaced in the transverse direction away from *y/D* = 0 line, there is a restoring lift force that is acting to return the cylinder to its original position (see Fig. 6). Hence quasi-steady arguments, as used in galloping theory, suggest stability of the downstream cylinder rather than instability. Galloping type response however occurs at *y/D* = - 0.4 ~ 0.4 (Fig. 5). Why and how? At *y/D* = 0, C_L = 0 (Fig. 6), there is no force to displace the cylinder in a transverse direction. But for *y/D* ≠ 0, $C_L \neq 0$, i.e., a force exists to displace the cylinder from its neutral position. Cylinder motion is thus generated, though displacement may be very small. It does not matter in which direction the displacement occurs.

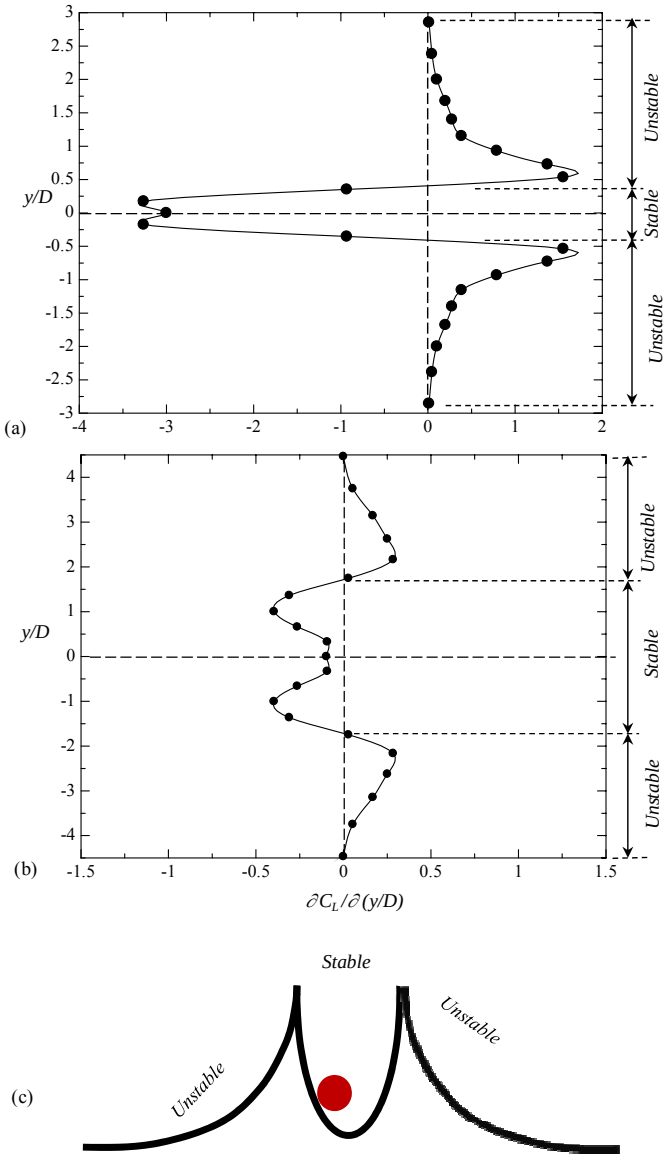

Fig. 7. Dependence of lift-force gradient $\partial C_L / \partial(y/D)$ on *y/D* at (a) *x/D* = 2.0 and (b)) *x/D* = 2.0 . (c) Sketch showing stability and instability. In fact, the $\partial C_L / \partial(y/D)$ variation corresponds to an extremely slow motion, i.e., f_n = very low.

The question that now arises is how an initial displacement for *y/D* = 0 occurs. Indeed, *y/D* = 0 is the critical geometry between staggered configurations of *y/D* = 0+ and *y/D* = 0-. For *y/D* = 0+, only the upper shear layer of the upstream cylinder reattaches onto the upper surface of the downstream cylinder; for *y/D* = 0-, only the lower shear layer of the upstream cylinder reattaches onto the lower surface of the downstream cylinder. Hence,

for y/D = 0, the upper and lower shear layers of the upstream cylinder reattach alternately onto the upper and lower surfaces of the downstream cylinder, respectively, especially for T/D smaller than critical spacing. This alternating reattachment generates fluctuating forces to displace the cylinder. When the cylinder is slightly displaced (Fig. 8a), the reattached shear layer is in a hesitating position, critically hovering to go on the upper side or the lower side. Instability is thus generated. For a cylinder spacing larger than critical, the oncoming vortex also has two options of where to go, on the upper side and lower side (Fig. 8b). This hesitation is responsible for generating the instability.

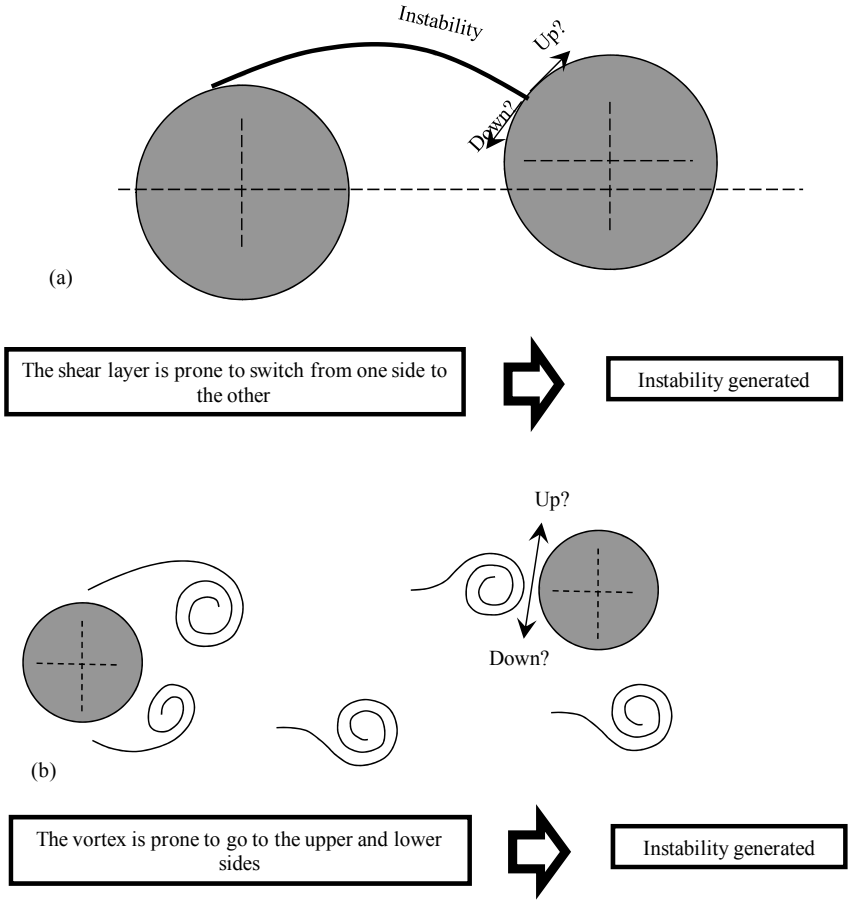

Fig. 8. Instability generation for (a) T/D < critical, (b) T/D > critical.

4. Conclusions

Time-mean lift, fluctuating lift, flow structures and the flow-induced responses of two circular cylinders are hooked up with mechanisms of interaction between the cylinders for all possible arrangements. The current investigation has led to the conclusions below.

Fluid dynamics around two cylinders is classified into six based on how the two cylinders interact with each other. The six occur at six different interaction regimes, namely, boundary layer and cylinder interaction regime; SL/wake and cylinder interaction regime; SL and SL interaction regime; vortex and cylinder interaction regime; vortex and SL interaction regime; and vortex and vortex interaction regime. Each of them has different traits and is connected to a different flow-induced response. While the boundary layer and cylinder interaction intensifies the lift force and generates galloping vibration, the SL/wake and cylinder interaction make changes in lift forces briskly with α or y/D, reduces fluctuating lift and generates both VE and galloping vibration. Two VEs occur at two different reduced velocities in the SL and SL interaction regime. Both vortex and cylinder interaction and vortex and shear layer interaction causes extensively high fluctuating lift, generating relatively high amplitude VE. The VE-reduced velocity is slightly higher for the vortex and cylinder interaction than for the vortex and shear layer interaction. Vortex and vortex interaction results in a slightly higher fluctuating lift and generates VE

only.

Though a single non-interfering circular cylinder does not experience galloping, two circular cylinders incur violent galloping vibration due to SL/wake and cylinder interaction as well as boundary-layer and cylinder interaction. A stronger fluctuating lift corresponds to a larger amplitude VE.

5. Acknowledgments

The author wishes to acknowledge supports given to him from Shenzhen Government through grant CB24405004 and from China Govt through '1000-young-talent-program'.

6. References

[1] M.M. Alam, and J.P. Meyer, "Two Interacting Cylinders in Cross Flow", *Physical Review E*, Vol. 84, 056304, pp. 16, 2011.

[3] J. Price, "The Origin and Nature of the Lift Force on the Leeward of Two Bluff Bodies", *Aeronautical Quarterly,* Vol. 26, pp. 154–168, 1976.

[4] M.M. Zdravkovich, and D.L. Pridden, "Interference between Two Circular Cylinders; Series of Unexpected Discontinuities", *Journal of Industrial Aerodynamics*, Vol. 2, pp. 255-270, 1977..

[5] S.J. Price, and M.P. Paidoussis, "The Aerodynamic Forces acting on Groups of Two and Three Circular Cylinders when Subject to a Cross-Flow", *Journal of Wind Engineering and Industrial Aerodynamics,* Vol. 17, pp. 329-347, 1984.

[6] M.M. Alam, M. Moriya, K. Takai, and H. Sakamoto, "Fluctuating Fluid Forces acting on Two Circular Cylinders in a Tandem Arrangement at a Subcritical Reynolds number", *Journal of Wind Engineering and Industrial Aerodynamics*, Vol. 91, pp. 139–154, 2003.

[7] M.M. Alam, M. Moriya, and H. Sakamoto, 2003 "Aerodynamic characteristics of two side-by-side circular cylinders and application of wavelet analysis on the switching phenomenon", *Journal* of *Fluids and Structures*, Vol. 18, pp. 325-346.

[8] Z. Gu, and T. Sun, "On Interference between Two Circular Cylinders in Staggered Arrangement at High Subcritical Reynolds Numbers", *Journal of Wind Engineering and Industrial Aerodynamics,* Vol. 80, pp. 287-309, 1999.

[9] M.M. Alam, H. Sakamoto, and Y. Zhou, "Determination of Flow Configurations and Fluid Forces acting on Two Staggered Circular Cylinders of Equal Diameter in Cross-Flow," *Journal* of *Fluids and Structures*, Vol. 21, pp. 363-394, 2005.

[10] M.M. Zdravkovich, "The Effects of Interference between Circular Cylinders in Cross Flow", *Journal* of *Fluids and Structures*, Vol. 1, pp. 239-261, 1987.

[11] I. Peschard, and P. Le Gal, "Coupled Wakes of Cylinders", *Physical Review Letters*, Vol. 77, pp. 3122–3125, 1996.

[12] G. Parkinson, and J. Smith, "The Square Cylinder as an Aeroelastic Non-Linear Oscillator", *Journal of Mechanics and. Applied mathematics*, Vol.17, pp. 225–239, 1964.

[13] M. Novak, "Aeroelastic Galloping of Prismatic Bodies", *Journal of Engineering Mechanics Division, Proc.* ASCE, Vol. 9, pp. 115–142, 1969.

[14] E. Simiu, and R.H. Scanlan, "Wind Effects on Structures. Fundamentals and Applications to Design, Wiley, New York, 1996.

[15] M. Novak, "Galloping Oscillations of Prismatic Structures", *Journal of Engineering Mechanics Division, Proc.* ASCE, Vol. 98, pp. 27–46, 1972.

[16] A. Bokaian, and F. Geoola, "Proximity-Induced Galloping of Two Interfering Circular Cylinders", *Journal of Fluid Mechanics*, Vol. 146, pp. 417-449, 1984.

[17] A. Bokaian, and F. Geoola, "Wake-Induced Galloping of Two Interfering Circular Cylinders. *Journal of Fluid Mechanics*, Vol. 146, pp. 383-415, 1984.

[18] A. Laneville, and D. Brika, "The Fluid and Mechanical Coupling between Two Circular Cylinders in Tandem Arrangement", *Journal* of *Fluids and Structures*, Vol. 13, 967-986, 1999.

[19] F.J. Huera-Huarte, and P.W. Bearman, "Vortex and Wake-Induced Vibrations of a Tandem Arrangement of Two Flexible Circular Cylinders with Near Wake Interference", *Journal* of *Fluids and Structures*, Vol. 27, pp. 193 – 211, 2011.

[2] M.M. Alam, Y. Zhou, and X.W. Wang, "The Wake of Two side-by-side Square Cylinders", *Journal of Fluid Mechanics*, Vol. 669, pp. 432-471, 2011.

[20] M.M. Alam, and S. Kim, "Free Vibration of Two Identical Circular Cylinders in Staggered Arrangement", *Fluid Dynamic Research*, Vol. 41, 035507, 17pp, 2009..

[21] S. Kim, M.M. Alam, H. Sakamoto, and Y. Zhou, "Flow-Induced Vibrations of Two Circular Cylinders in Tandem Arrangement, Part 1: Characteristics of Vibration", *Journal of Wind Engineering and Industrial Aerodynamics,* Vol. 97, pp. 304-311, 2009.

[22] M.M. Alam, and H. Sakamoto, "Investigation of Strouhal Frequencies of Two Staggered Bluff Bodies and Detection of Multistable Flow by Wavelets", *Journal* of *Fluids and Structures*, Vol. 20(3), pp. 425-449, 2005.

International Conference on Mechanical, Industrial and Materials Engineering 2013 (ICMIME2013)
1-3 November, 2013, RUET, Rajshahi ,Bangladesh.

Paper ID: KL-05

Utilization of Solar Energy and Waste Heat for Water Heating, Drying and Desalination of Seawater

M.N.A.Hawlader

Department of Mechanical Engineering, Faculty of Engineering,
International Islamic University Malaysia,Jalan Gombak,
53100 Kuala Lumpur, Malaysia
**e-mail:mehawlader@iium.edu.my*

Abstract

The population growth of the world has led to a greatly increased demand for energy. Due to this growing global energy demand and concern for environmental degradation, the potential of running thermal system usingsolar energy is receiving considerable attention in recent years. Solar energy is clean and most inexhaustible of all energy resources. The heat pump commonly used for space cooling, a low temperature application, makes it an excellent match for the use of solar energy. A solar assisted heat pump system has been fabricated and installed for space cooling, water heating, drying and desalination. Besides solar energy, the system makes use of waste heat available from heat pump, which is normally released to the atmosphere leading to global warming. An unglazed evaporator collector absorbs solar energy and ambient energy.On condenser side of the heat pump, desalination chamber, water heater and cloth dryer are connected to make use of waste heat available from the heat pump system.This system is particularly suitable for hotels and hospitals where cooling, water heating and drying are always needed and enormous amount of waste heat is available.

Keywords: Solar energy, heat pump, space cooling, water heating, drying and desalination

1. INTRODUCTION

It is impossible for life to survive without water and the severe crisis of fresh water in semi-arid and arid regions of the world has created significant importance to find alternative sources of potable water. Efficient management of ground water and surface water would be an option but these resources will not be able to meet entire requirements due to rapid growth of population. Also, pollution is deteriorating the conditions of the available sources and affecting the entire water scenario. Desalination of seawater is an option, as abundant supply of it exists in nature [1-3].

Energy is an essential component for most desalination processes. The unreliable prices of fossil fuels, tremendous growth in demand and global warming have created a new dimension to look for sustainable energy resources with reduced impact on environment. Solar energy, a clean, environment friendly and sustainable resources can play an important role [2]. There can be significant utilization solar energy particularly in areas where low temperatures, less than 100^{o}C, are involved [4-5].

A combination of solar energy, ambient energy and waste heat is considered for production of hot water, provide drying and perform desalination [6]. Evaporator collectors are used for the collection of solar energy and ambient energy [7]. Several experiments were conducted by Abou- Ziyan [8] to identify appropriate refrigerant.Hawlader et al. [9]and Chyng [10] conducted experiments using solar assisted heat pump (SAHP) to produce hot water. The evaporator collector absorbed both solar energy and ambient energy due to low operating temperature. For refrigerant R134a, the coefficient of performance (COP) of the heat pump system reached as high as 9.Huang and Lee [11] studied the long term performance of solar assisted heat pump water heater. Grossman [12] carried out experiments with a solar heat pump system to provide cooling, dehumidification and air-conditioning. In 2003, Hawlader et al. [13] conducted series of experiments on a solar assisted heat pump system (SAHPS) to provide water heating and drying.

More than half of the building energy consumption is attributed to air conditioning urban households, especially for those buildings running air-conditioner all the day, such as hotels and hospitals. Conventional vapor compression air conditioning system throws the heat from a heat source (air-con room) to the ambient air without making an effort to recover it. A solar assisted heat pump(SAHP) system for air-conditioning, water heating and drying was proposed by Hawladeret al. [14]. Based on the principle, a SAHP systemhas beendeveloped where solar energy, ambient energy, and air con waste heat are used to provide hot water, drying and desalination. This paper includes a brief description of the system and the results obtained from it.

2. THE SYSTEM AND EXPERIMENTS

A heat pump system has been built, as shown in Figure 1, and located on the roof top of a buildingto evaluate performance under outdoor meteorological conditions. The system consists of four major sections: a solar assisted heat pump, a desalination unit, a dryer and a hot-water storage tank. For the collection of solar energy, a solar collector and an evaporator collector are used. A solar assisted air conditioning (heat pump) system provides energy required for desalination, drying and water heating.

The hermetic reciprocating compressor is coupled with a three phase induction motor, whereby the speed of the motor is controlled by a frequency inverter. The evaporator-collector is made of copper absorber plate and coated with black paint. Serpentine copper tubes, with external diameter of 9.5mm, are brazed onto the bottom of the collector plate. The bottom part of the collector evaporator is insulated with polyurethane foam to reduce heat lost from the plate's bottom. The room evaporator is located in a space to be cooled to provide comfort condition. The evaporator collector and room evaporator are connected in parallel with individual expansion valve. The condensing coils for heating saline water and fresh water run in parallel using control valves, while the dryer is connected in series.

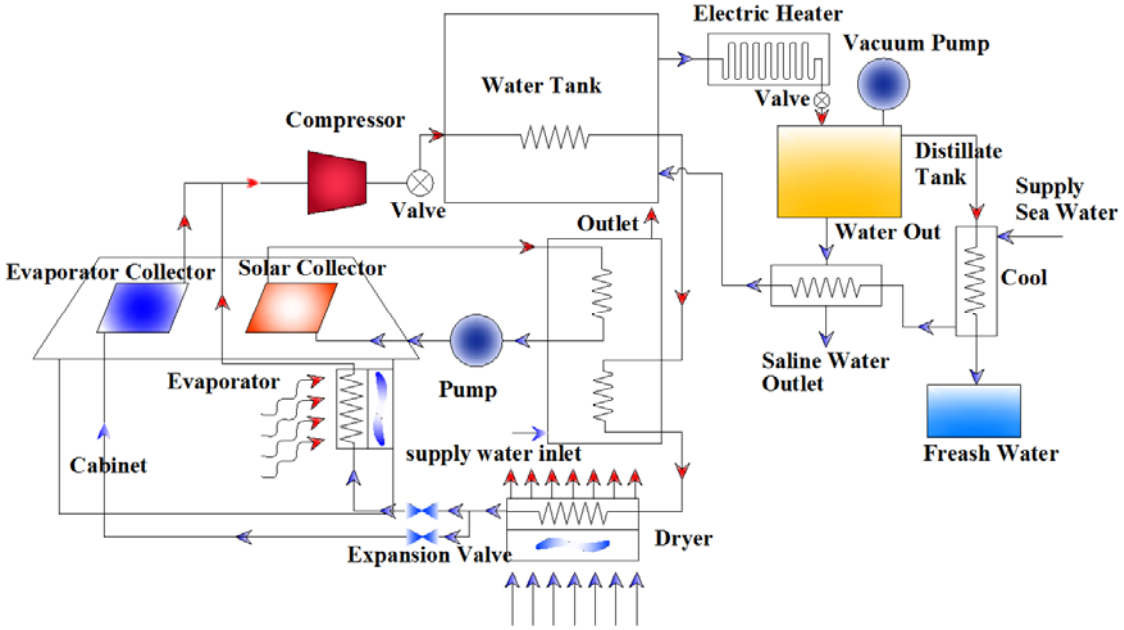

Figure 1. An integrated solar heat pump system for water heating, drying and desalination

Solar Assisted Heat Pump (SAHP)

The SAHP consists of a hermetic type reciprocating compressor, evaporators(evaporator-collector and room evaporator), condensers(condensing coil in lower portion of desalination chamber, water-cooled condenser, air-cooled condenser), and lastly expansion valves. The evaporator components are connected in parallel to each other, while the condensers are connected in parallel / series, with by-pass system.

In the compressor, saturated /slightly superheated refrigerant vapor at a lower pressure enters the inlet and is compressed to a high pressure and temperature. The superheated vapor first enter the condenser coil in the chamber filled with saline seawater, where it releases sensible and latent heat and raise the temperature to the

desired level. The condenser coil in seawater chamber and hot water tank are arranged in parallel with appropriate control to maintain the desired temperature level. Subsequently, to ensure total condensation of refrigerant before it reaches the expansion valve, the refrigerant will flow through the air-cooled condenser. Latent heat released from the condensation of refrigerant vapor is recovered by water and air in the water-cooled condenser and air-cooled condenser, respectively. In this system, the recovered heat in the water-cooled condenser and air-cooled condenser are used for water heating and drying purposes.

The saturated or sub-cooled liquid refrigerant from the condensers will then be split into two separate branches. Each branch will lead the refrigerant to separate evaporator components. Refrigerant mass flow rate in each branch is regulated by the thermostatic expansion valve before entering the evaporator components. In the evaporator-collector, collector plate gained solar energy from solar radiation, ambient energy from ambient air and latent heat due to condensation of water vapor present in the air. Energy gained by the collector plates is then transferred to vaporize the refrigerant in the serpentine tubes. In the room evaporator, refrigerant vaporizes by receiving thermal energy from room air, while the room air is cooled by releasing heat to the cold refrigerant flowing through finned tube. The mass flow rate of refrigerant in each evaporator is regulated to ensure refrigerant exit in each evaporator either in saturated or slightly superheated vapor state. The two streams of refrigerant vapor are then mixed together before entering the compressor inlet and the cycle continues.

The process of desalination

Although there are a number of ways to convert seawater to fresh water, a common overall processapplies to all schemes. Actual nature of each step would depend on the desalination method used. Figure 2 shows the steps involved in the process.

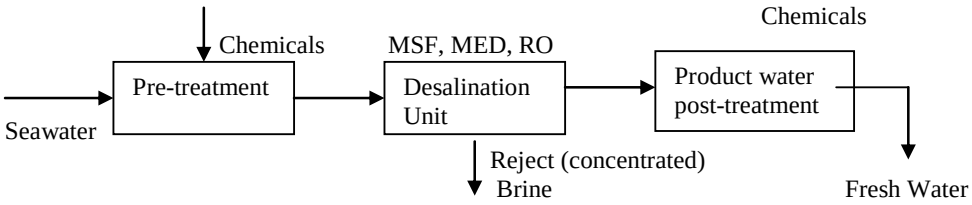

Figure 2. Schematic diagram of a desalination process

The nature of the pre-treatment depends to a great extent on the type of intake system and the nature of pollution in the surrounding sea. The supply of water directly from shallow bays near the shore may provide seawater with high contents of bacteria, algae and suspended solid. Normally, seawater drawn from the open ocean is cleaner and requires less pre-treatment steps. Pre-treatment of raw feed water is necessary to preserve the life and reliability of the desalination equipment. As stated earlier, there are a number of methods available for the conversion of seawater to fresh water. Irrespective of the method of conversion process, the product water should have a total dissolved solid (TDS) content of less than 500 ppm [15]. Table 1 shows the typical constituents of seawater and potable water. This product water is not suitable for direct human consumption and some form of post-treatment is necessary to control sodium and chloride ions and its pH. A treatment with acid, H_2SO_4, controls carbonate scale formation and convert any sulphides to H_2S. The acidified water is then sent to a stripping tower to remove excess CO_2 and H_2S gases. Chlorine is then added as a disinfectant. Finally lime, $Ca(OH)_2$, is added to increase water hardness and decrease corrosion risks, while fluoride is added to reduce dental cares.

In the desalination section, the system consists of a seawater tank, desalination chamber fitted with a vacuum pump, a condenser coil to cool vapor generated in desalination chamber, and a distillate tank. The saline feed-water is preheated by the condensing vapor and, subsequently, by the reject brine. In practice, the temperature of feed water before entering the desalination tank should not be below 70˚C. After passing through the electrical heater, the water will enter the desalination chamber. The desalination chamber will be evacuated to a pressure of about 0.12 bar, hence, the corresponding temperature of water will drop from 100^{o}C at standard atmospheric pressure to 50^{o}C at the pressure of 0.12 bar. Upon entering the desalination chamber, the water will undergo thermodynamic flashing and evaporation. The remaining part of the saline water passes through a coil and releases additional heat to feed water. Vapors produced from flashing and evaporation will rise to top of the chamber, pass through a cooling coil and the water is collected in a fresh water tank, as shown in the Figure 1.

Table 1. Typical constituents of seawater and potable water [15,16]

Constituents	Seawater[1] (mg/L)	Potable Water[2] (mg/L)
Barium	0.02	1.0
Calcium	412	75
Carbonates	28	150
Chloride	19500	250
Copper	$1x10^{-4}$	1.0
Fluoride	1.3	1.5
Iron	0.002	0.3
Lead	$5x10^{-7}$	0.05
Magnesium	1290	50
Manganese	$2x10^{-4}$	0.05
Mercury	$3x10^{-5}$	0.001
Nitrates/Nitrogen	11.5	10
Phosphates	0.06	0.4
Potassium	380	10
Silica	2	7.1
Sodium	10770	200
Sulphates	905	400
Total dissolved solid	33387 (ppm)	500 (ppm)
pH	8.0	6.5 - 8.5
Turbidity	3 - 15 NTU	5 NTU

Solar water heater

The hot water tank acts as a condenser for the heat pump and receives heat from the refrigerant as well as solar collector. Water condenser absorbs most of the heat from the superheated refrigerant. There is a phase change for refrigerant from superheated vapor to saturated two-phase mixture of vapor and liquid. Water absorbs bulk of latent heat of condensation of the refrigerant. Also, water from the storage tank is circulated through a conventional solar collector using a pump. This pump operates only when useful energy is collected from the sun.

Drying with hot air

After the water condenser, the refrigerant may be in a state of two-phase or saturated condition. The air condenser ensures complete condensation of refrigerant vapor and may be slightly sub-cooled before it reaches he expansion valve. The energy recovered from the air condenser is used for low temperature application, such as drying – it may be grain drying or cloth drying depending on the nature of applications.

3. RESULTS AND DISCUSSION

Meteorological conditions

Singapore and Johor Baru, Malaysia are located at about latitude $1^{o}22'$N and longitude $103^{o}55'$. There is hardly any seasonal variation of the meteorological conditions in Singapore or Johor Bahru. Figures 3 and 4, show the values of solar radiation, wind speed, ambient temperature, and relative humidity in 2008. It can be seen that the temperature generally reaches around 30 °C, with the maximum value of about 35 °C. Wind speed varies from around 1 to 4 m/s, with relative humidity between 65% and 85%, and solar radiation varies from 400 to more than 1000 W/m^2 for the condition considered.

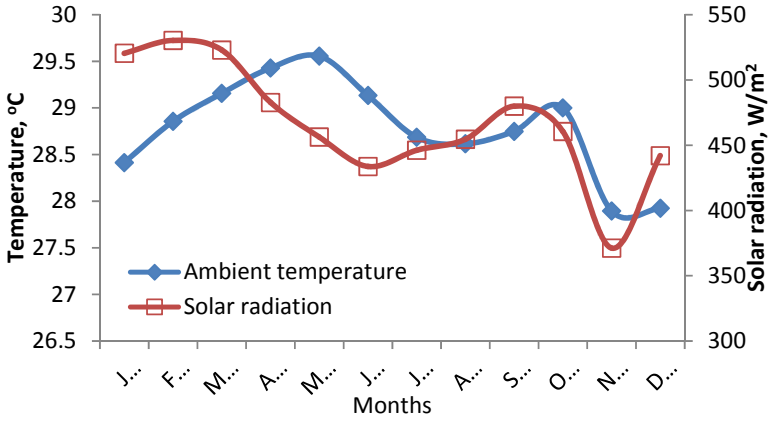

Figure 3.Variation of monthly ambient temperature and solar radiation

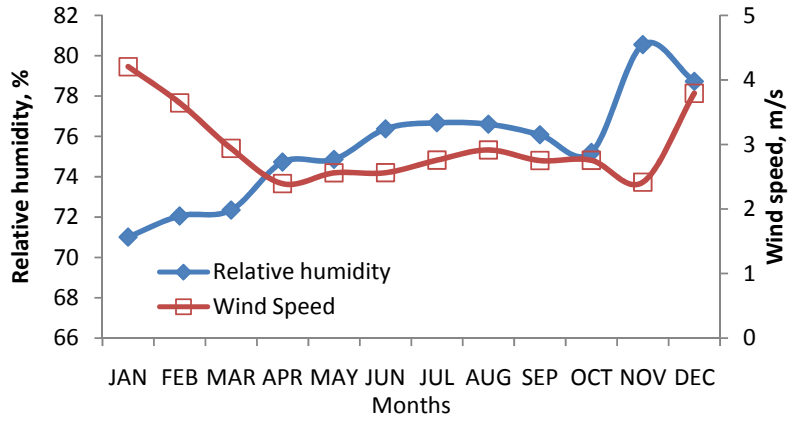

Figure 4.Variation of monthly relative humidity and wind speed

Performance of Water and Evaporator collectors

The evaporator collector uses refrigerant after the expansion valve. The operating temperature of the collector is much lower than the atmospheric air temperature. The collector is unglazed and coated with matt black paint. It absorbs allthe radiation incident upon it. As the operating temperature of the collector is lower than the atmospheric temperature, it also gains energy from the environment by convection. Due to low temperature of the collector surface, lower than the dew point, there is condensation of the water vapor in the air and the collector absorbs latent heat of condensation. Hence, the evaporator collector absorbs both solar energy and ambient energy.

The solar water collector is normally glazed to reduce heat losses. A part of the solar radiation is transmitted through the glass cover and absorbed by the absorber panel. As a result the panel will be heated and, normally, the operating temperature is much higher than the ambient temperature and there will be heat losses to the atmosphere. Figure 5 shows the efficiency of the water and evaporator collectors. Evaporator collector operates at a much higher efficiency than the water collector.

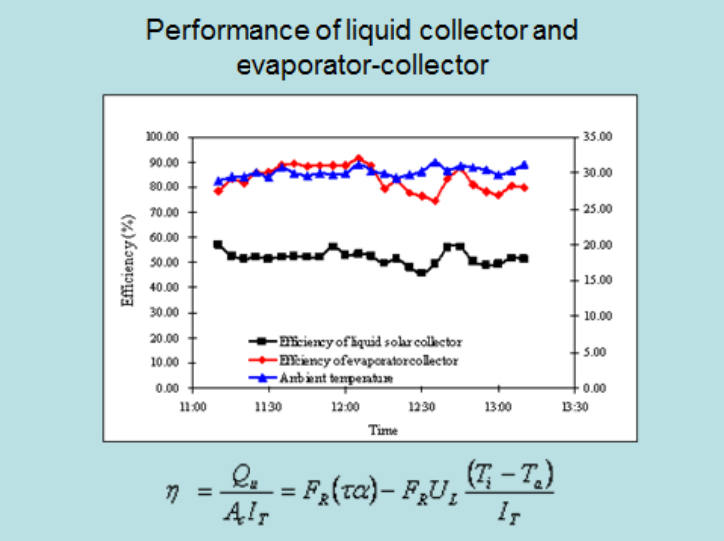

Figure 5: Efficiency of evaporator and water collectors.

Space cooling (Air-con)

As seen from Figure 6, room temperature was cooled from 27°C to 20°C in one hour and became stable. In the room evaporator, refrigerant after expansion valve absorbed heat from room air and became super-heated at the evaporator outlet. As seen from the Figure 7, evaporating heat of room evaporator dropped from 7.8kW to 6.6kW when then room temperature reduced from 27°C to 20°C. It is due to the fact that the temperature difference between air and refrigerant declined as a result of drop of room temperature.

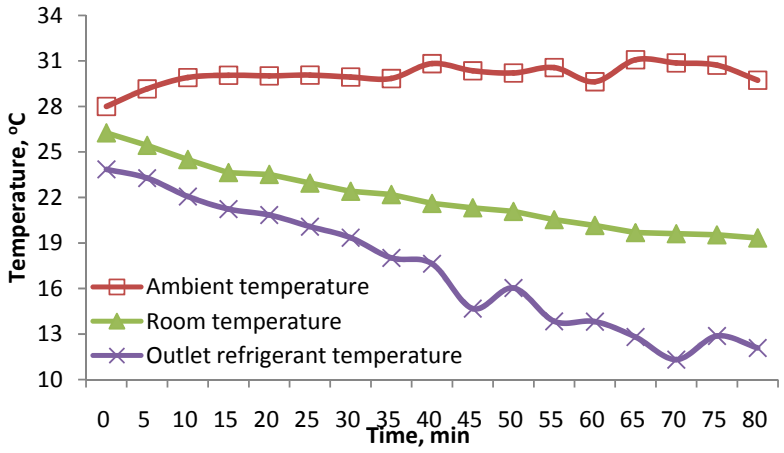

Figure 6 Variation of temperature of ambient, room and outlet refrigerant.

Water heating

Figure 8 shows the variation of temperatures of water and refrigerant. The temperature of the 400 liters of water in the tank increases in a steady manner and rises from 34°C to 60°C in about 65 minutes. With the rise of water temperature, the condensing heat released in water condenser declined due to the fact that the temperature deference between refrigerant and water decreases.

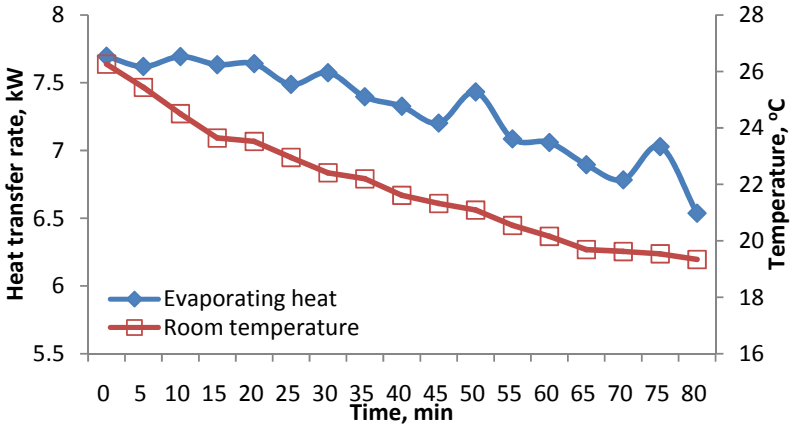

Figure 7 Variation of room temperature and evaporating heat with time.

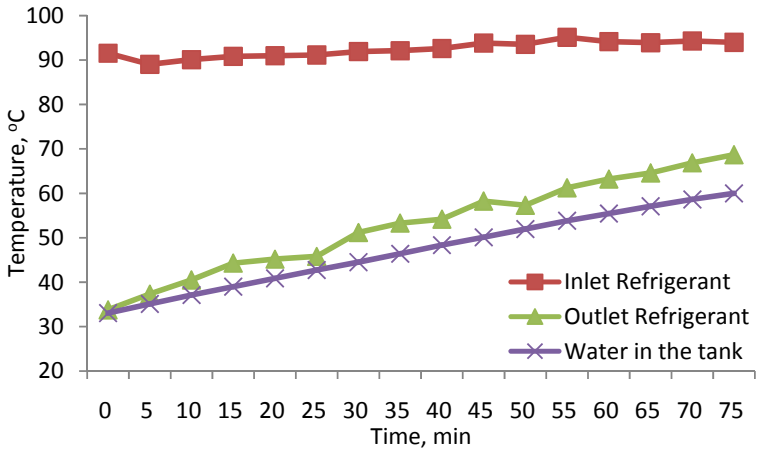

Figure 8. Variation of temperatures of water and refrigerant with time

Desalination

In the desalination chamber, thermodynamic flashing and evaporation occur almost simultaneously. Uniform flashing of water takes place when feed water enters the desalination chamber through the spray nozzle, at a temperature higher than water's saturation temperature. Condensing coil located at the bottom of the chamber, provides thermal energy to heat up and evaporates remaining feed water that does not vaporize during flashing. Vapor produced from flashing and evaporation will rise to the top of the chamber, where it will be condensed by the cooling coil, as shown in Figure 1.

The desalination is obtained by single stage MED technique. As shown in Figure 9, desalination rate increases with radiation and then as time passes it comes to a steady rate of 9.6 kg/hr.

Drying

Figure 10 shows the variation of air temperature and moisture content of material during the drying process. In this drying process, temperature of the water in the water condenser was maintained at 60℃ by controlling the water flow rate. It enabled the stabilization of the temperature of air for drying.

As seen fromFigure 10, the inlet air, with the temperature of around 30℃ and RH of 0.6, was heated to around 36℃ in air condenser. This warm airis allowed to flow through the drying chamber and discharged after releasing heat in the drying process. Textile with the bone dry weight of 1.5kg was wetted and hanged in the drying chamber. The moisture content of material was reduced from 0.9 to 0.09 in 60 minutes. The drying falls mostly in the falling rate region. With the declination of moisture content, the temperature difference between the inlet and outlet of the drying chamber declined gradually. In full mode operation, the heated air temperature is normally lower than 40℃ because the refrigerant from compressor condensed in water condenser and released most of condensing heat before it went through the air condenser to heat the ambient air. When the water is bypassed, the air temperature in the dryer can be as high as 55°C.

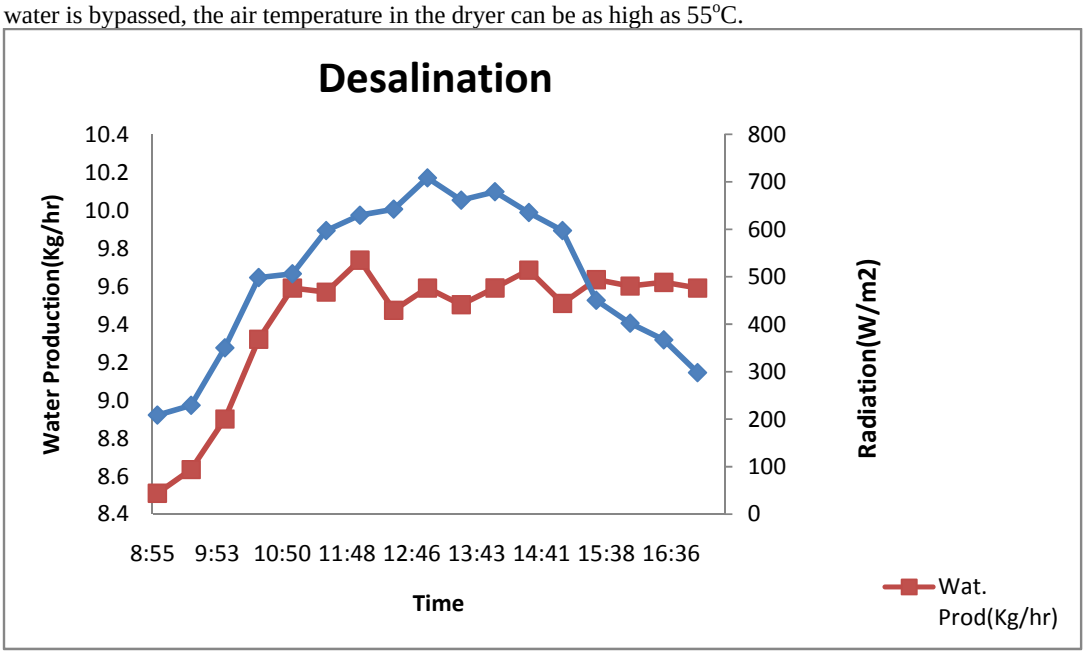

Figure9 Variation of Water desalination and solar radiation with time

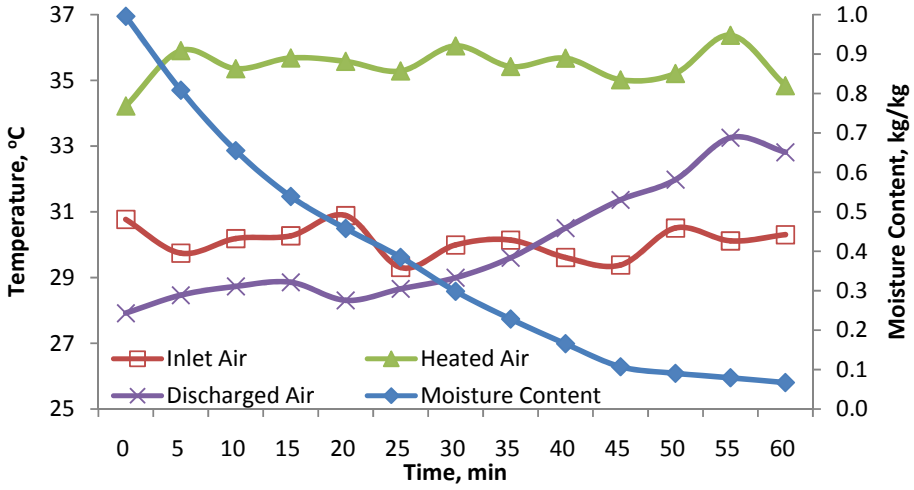

Figure 10 Variation of air temperature and moisture content with time [17]

4. CONCLUSIONS

The solar assisted heat pump system operates on Rankine cycle where one of the innovative featuresis the use of an inexpensive unglazed evaporator-collector, which enables collection of ambient energy.The energy absorption from evaporator collector and space cooling is 28% and 33%, respectively.This gives 14 kW (for a system where the compressor input is 3.5 kW) heat in the condenser side for desalination,water heating and drying. Due to the use of double condenser arrangement, the drying performance is limited and restricted by the water temperature in water condenser. It can be resolved by bypassing the water condenser leading to a constant drying air temperature as high as 55^{o}C.The system is considered environment friendly, encourage a reduction inglobal warming and offers a good potential for supporting basic human need, WATER.

REFERENCES

[1] A.Malek, M.N.A. Hawlader and J.C. Ho, 1992, "Large-scale seawater desalination: a technical and economic review", ASEAN Journal of Science Technology Development., 9(2), pp 41-61, 1992.

[2] L.G**.** Rodriguez, "Renewable Energy Applications in Desalination: State of The Art*"*, Solar Energy, Vol. 75, pp 381-393, 2003.

[3] M.N.A. Hawlader and K.A. Jahangeer, "Solar Heat Pump Drying and Water Heating in the Tropics*"*, Solar Energy, Vol. 80, pp. 492-499, 2006.

[4] Huang, B.J., J.P. Lee, and J. P. Chyng, "Heat-Pipe Enhanced Solar-Assisted Heat Pump Water Heater", Solar Energy, Vol. 78, pp. 375-381, 2005.

[5] Hawlader, M.N.A., S.K. Chou, and M.Z. Ullah, "The Performance of A Solar Assisted Heat Pump Water Heating System", Applied Thermal Engineering, Vol. 21, pp. 1049-1065, 2001.

[6] M.N.A. Hawladerand Zakaria M. Amin, "Desalination of seawater using solar, ambient energy and waste heat from air conditioning", Desalination and Water Treatment**,** 42, 235–240, 2012.

[7] M. N. A. Hawlader, S.M.A. Rahman and K.A. Jahangeer, "Performance of evaporator collector and air collector in solar assisted heat pump dryer". Energy Conversion and management, 49, 1612 -1619, 2008.

[8] H. Z. Abou-Ziyan, H. Z., "Solar-assisted R22 and R134a heat pump systems for low-temperature applications", *Applied Thermal Engineering*, 17(5), 455-469, 1997.

[9] Hawlader, M.N.A., Chou, S.K. and Ullah, M.Z., "The performance of a solar assisted heat pump water heating system", *Applied Thermal Engineering*, 21(10), 1049-1065, 2001.

[10] J.P. Chyng, "Performance analysis of a solar-assisted heat pump water heater", Solar Energy, 74(1), 33-44, 2003.

[11] B.J. Huang and C.P. Lee, C.P., "Long-term performance of solar-assisted heat pump water Heater", Renewable Energy, 29, 633–639, 2003.

[12] Gershon Grossman, "Solar-powered systems for cooling, dehumidification and air-conditioning", Solar Energy, 72(1), 53–62, 2002 .

[13] M.N.A. Hawlader, S.K. Chou, K.A. Jahangeer, S.M.A. Rahman, and Eugene K.W. Lau, "Solar-assisted heat-pump dryer and water heater", Applied Energy, 74(1-2), 185-193, 2003.

[14] M.N.A. Hawlader, K.A. Jahangeer, Ye Shaochun and Choy Tack Hoon, "A solar heat pump system for air-conditioning, water heating and drying", World Renewable Energy Congress, 28 August -03 September 2004, Denver, USA

[15] DeZuane, Hand book of drinking water quality: standards and controls, Van Nostrand Reinhold, New York, 1990.

[16] Seawater: It's coposition, properties and behaviour, Prepared by an Open University Team, Walton Hall, Milton Keynes, England, Pergamon Press, 1989.

[17] YeShaochun, “Integrated solar heat pump system for cooling, water heating and drying”, Ph D thesis, National University of Singapore, Singapore, 2009, p78.

Paper ID: KL-06

University Industry Linkage for Indigenous Development: A Case Study from Developing World

Abdul Ghafoor
School of Mechanical and Manufacturing Engineering
National University of Sciences and Technology
Islamabad 44000, Pakistan
Phone: +92 51 9085 6001, Email: aghafoor@smme.nust.edu.pk

Abstract

Universities around the globe are seen pursuing University-Industry Linkages (UILs) more aggressively in the recent years than ever. This indicates that the universities have assumed a new role of contributing in the nation buildings through helping the industry. There is no doubt about the role played by the universities in the world's developed countries. The key players in the industrialization of the nations are the Governments, Higher Educations Institutions (HEIs) and the Industry. Their role towards each other has been defined in Triple Helix Model. There are however cases in which countries like Norway and Australia still feel that UILs have to be strong and to be pursued objectively. Currently the leaders of higher education have also been given a new role and are being asked to have focus on research, innovation and commercialization. It has been realized that the role of (HEIs) should also include building of economies, communities and leadership. UILs bring the universities and the industry close to each and help repose the confidence among both the parties. These linkages have proved as a successful tool for finding Indigenous solutions to the industry and national problems through the involvement of the academia. On the other hand, the industry can also help universities with the R&D funding, commercialization of the innovations and helping in design of the university curriculum that are relevant to the industry. Cooperation between the universities and the industry is a win-win situation for both. At National University of Sciences and Technology (NUST), Pakistan, UILs were started under Corporate Advisory Council (CAC) that was specifically established for the purpose to bridge gap between industry and academia. CAC has leading industrialists as its members who work with the senior members of the academics. CAC forum has helped both parties understand strength and need of each other. This arrangement has worked effectively and some success has been achieved.

This paper discusses some of the UILs models being followed by the developed countries. The paper also discusses the initiative undertaken at NUST to establish UILs under the model of CAC and the success achieved under this arrangement.

Key Words: *University-Industry Linkages (UILs), Higher Education Institutions (HEIs), Corporate Advisory Council (CAC), research, innovation, development, commercialization, role of universities and higher education*

Acknowledgement: The author is thankful to the Corporate Advisory Council (CAC) secretariat officials for their help in providing the relevant data related to university-industry collaboration at the National University of Sciences and Technology (NUST).

Introduction

Growth and development of any nation are linked to the Government policies towards its industrialization. The industrialization on the other hand is strongly based on the trained human capital of the country. Nations have been striving to capitalize on the factors that include preparation of favorable policies by the Government to attract the investment and provision of resources for the training of required manpower. The industrialized nations worked hard, identified the key factors and exploited for the growth. They are progressing at a faster speed as compared to the developing nations who failed to mobilize their resources. The key components for the growth and the development are; the Government itself, the Industry and the Higher Education Institutions (HEIs). Each of these has a role towards others. Role of three towards each other has been defined in a term named Triple Helix Model. Triple Helix Model has been evolved about half a century ago and still evolving with new rolesof its components (Leydesdorff, L. and Etzkowitz, H.). The Triple Helix Model and its evolution stages are discussed in this paper.

In the HEIs, faculty is the brain and has the most important role to play in the social and economic development of the nations. World's leading nations have used this intellectual property in efficient and effective manners. On the other hand many could not exploit these resources and are lacking. During the past quarter of a century, some but limited activity is seen in developing nations where the professors have assumed the responsibilities of writing business plans, gaining expertise in raising funds for themselves and the institutions through various entrepreneurial activities.

University entrepreneurial activities of scientists can be traced back to couple of hundred years and hence cannot be termed by any means new phenomena (Etzkowitz, 1983). Over the period, the approach followed by the university professors was continuously refined across the globe. As a result, more focused and result oriented methodologies emerged (Shimshoni, 1970). More activities of the Professors are noticed in the recent past where they have established their own businesses and are managing full time besides their academic activities (Krim-sky et al., 1991 and Plewa et al., 2013). Different universities of the world are following various models to work with the industry. National University of Sciences and Technology (NUST) has established Corporate Advisor Council (CAC) to have a close liaison with the industry of the country. This approach has worked effectively and both the entities are interacting for benefit of each other. This model is discussed in detail in the paper.

Triple Helix Model and its Evolution

Triple Helix Model symbolizes the overlapping role of its three key components; Government, Industry and Academia. This name has been given to precisely explain the importance of the role of three entities towards each other and in the nation building. The nations that have developed well have very clear role of all the entities. They work hand in hand with clear understanding. The Government role remains of formulating policies and providing resources required for Human Resource (HR) development to the academia and industry while the industry has generate revenue for the country by employing the trained HR and following the policy guidelines. The academia responsibility has been to train manpower for the industry and government.

The evolution of Triple Helix Model can be categorized into four stages. During first stage, the role of its three components was only of formal nature with least virtual no interaction between academia and industry. Three components continued their function till somewhere middle of twentieth century. Second stage of evolution of cooperation between University, Industry and the Government can be seen in the third and partly fourth quarter of the twentieth century when the interaction between all of them was increased and the time when maximum progress in the industrialization of the nations can be seen. It was actually this interaction and the growth resulting from it that name of Triple Helix was realized. During last quarter of the century, the role of Triple Helix entities has been of overlapping and evolution of Science and Technology Parks (STPs) has been observed. The entities have moved out of their foothold and economies are seen being built as a result of functioning of STPs. This era can be named as third stage of evolution of Triple Helix. In current days, the key players in the socio-economic development of the nationsare working beyond their boundaries in the form of Global Think Tank Networks (GTTNs) and proving all kinds of support to each in the form of policies guidelines, advisory and consultancy services (e.g., Pires and Castro 1997; Gulbrandsen 1997). The stages of evolution of Triple Helix are depicted in the Figure 1.

Role of Universities in 21st Century

The Universities need to be ready to accept the challenging role in the current century. With the evolution of Triple Helix Model and revolution of industrialization across the globe, the Universities have to transform themselves from mere teaching and R&D role to the entrepreneurial ones. With the fast changing life styles, the Universities are expected to contribute in the building of economies, communities and the leadership. The managers of the Higher Education Commission (HEC) and leaders of HEIs of Pakistan have set the medium term development framework to have transformation through the establishment of Office of Research, innovation and Commercialization (ORIC) in the Degree Awarding Institutions (DAIs) of the country. NUST has moved a step ahead by institutionalizing the UILs under the CAC and increasing the interaction with the Government by launching GTTN. The changing role of HEIs over the period is shown in the Figure 2. The universities of the current era are expected to have moved up the ladder as shown in the figure. Those at the top of the ladder can be said contributing the most. Universities in the leading and industrialized nations have already adopted new roles of being entrepreneurial and giving advices to the Governments on policy guidelines. HEIs in the developing world need to move faster to catch up the ever changing demands of the society and industry otherwise the gap between developed and underdeveloped nations will be widened.

Example of UIL in NUST Pakistan

As mentioned above, university-industry need to join hands for mutual cooperation as well as provide a platform for policy guidelines to the Government on social and economic issues. Universities having the largest clusters of intellectuals have the leading role to be played. Specifically Science & Technology Universities all over the world make significant contributions to the development of technologies which are essential in an economy.

Fully realising the responsibilities, the academic programs of the NUST are designed to meet the national needs and challenges of the new millennium. Fields of Engineering, Life Sciences and Natural Sciences are continuously updated with emerging trends; at the same time, modern disciplines are being offered to prepare professionals to manage the ever-growing demands of a knowledge economy with requisite degree of expertise. NUST aims to develop itself into a Centre of Excellence for advanced scientific and technological research, and to emerge as a leader in academic research in Pakistan. These objectives are being fulfilled through the induction of the most brilliant and dynamic faculty, and providing their mental and creative abilities with a nurturing and enabling environment. This has facilitated excellence in R&D at the NUST schools.

Corporate Advisory Council; Model of UIL at NUST

In conjunction with the academic research, NUST has also laid emphasis on practical, solution-based, Industry-specific R&D, both for the training and development of our students, and for providing support to the local Industry. One of the advantages of NUST's location is its close vicinity to Islamabad's Industrial and Corporate Sectors. Through the combined and multi-disciplinary strengths of 18 constituent Schools, Colleges and Institutes, NUST is well-equipped to serve several Sectors of the economy with its intellectual capital (1000+ faculty and 12,000+ students) and state-of-the-art lab and research infrastructure. At the same time, it has been reported that currently there is at least a wastage of about 10-12%, which amounts to approximately USD 20-25 billions. It is also clearly understood that these wastages can be removed through knowledge input and technology, and the gaps can be filled through University-Industry linkages (UILs). The technical and academic strengths of NUST; combined with the needs of the Industry to find innovative, practical and cost-effective solutions; and the need of the economy to flourish through advancements in technologies; are the basis for the establishment of the Corporate Advisory Council (CAC) at NUST.

The CAC was formed in 2010, with the simple mandate of having a positive impact on the socio-economic development of Pakistan through active engagement with the Industry. The CAC has developed linkages with

industrial and business enterprises across 11 Sectors of the economy. The CAC is headed by the University and along with him is Professor Emeritus as the Co-chair having experience of working with the Industry within and outside Pakistan. Each Sector Committee is headed by an Industry Co-Chair and a NUST Co-Chair, and comprises members from the Industry and NUST schools. The CAC Partners in its 11 Sector Committees include the leading names from different Industries, including Indus Motor Company Ltd, Atlas Honda Litd., Huawei Technologies Pakistan, House of Habib, Asian Development Bank, National Bank of Pakistan, Fauji Foundation, Siemens Pakistan Engineering Company, Oil and Gas Development Company, NESPAK, Pakistan Atomic Energy Commission, Planning Commission of Pakistan, Ministry of Science & Technology Pakistan, and many others.Also part of the CAC are senior representatives from Government establishments, thereby creating a unique *triple-helix* combination of Academia, Industry and Government, engaging in advisory, consultation and R&D collaboration. Organizational structure of CAC is shown in Figure 3. The structure of each sector committee is given in Figure 4.

The CAC brings the NUST Institutes and the Industry together on a common platform, enabling them to join hands to find workable solutions, through R&D, to real-life problems encountered in product development, design and commercialization. The projects that NUST schools engage in with the Industry add value in terms of process efficiencies leading to cost reduction or quality improvements, product improvements, product or process innovation, etc.

In a period of less than 3 years, the CAC membership has grown to include more than 150 members from top-line local and international business and industrial firms, banking and investment houses, high-level public policy-makers, and intellectuals. Cooperation and collaboration between Industry and NUST Academia has led to innovative projects aimed at providing solutions to Industrial and Corporate partners. Coming together on the CAC platform has also enhanced inter-Industry linkages, which, in turn, is strengthening University-Industry linkages. Moreover, it has helped human capital development at NUST in more practical, Industry-specific, and meaningful terms, ranging from the curriculum, which is continuously revised to include Industry orientation, to student placements including internships, on-the-job training, and employment within the industry, creating an overall environment of Industry-specific human capital development. The CAC and NUST have several international collaborations including foreign universities, business councils, and corporate entities.

Conclusion

Today, there is more understanding in the Universities and the Industry than ever. Governments are also laying a lot of emphases for having collaborations in the form of UILs and establishment of STPs. It however needs to be understood that success of these models lies in having confidence in own institutions. The models have proved to be successful in the industrialized nations and therefore others must follow without wasting more time.

Reference

Etzkowitz, H., (1983), Entrepreneurial Scientists and Entrepreneurial Universities in American Academy Science, Minerva.

Krimsky, S., Ennis, J., Weissman, R., (1991), “Academic-corporate ties in biotechnology: a quantitative study” Science, Technology and Human Values 16(3),275-287,Summer.

Shimshoni, D., (1970), “The Mobile Scientists in the American Instrument Industry”, Minerva 8(1).

Plewa, C., Korff, N., Baaken, T. and Macpherson, G. (2013), “University-industry linkage evolution: an empirical investigation of relational success factors”, R&D Management 43:365-380. Doi: 10.1111/radm.12021.

Etzkowitz, Henry and Leydesdorff, Loet (1997), “Universities in the Global Economy: A Triple Helix of University-Industry-Government Relations”.

Pires, Artur da Rosa and Eduardo Anselmo de Castro (1997), “Can a strategic project for a university be strategic to regional development?”, Science and Public Policy 24(1) 15-20.

Gulbandsen, Magnus (1997), “Universities and Industrial Competitive Advantage”, pp.121-131 in:
Etzkowitz, Henry and Leydesdorff, Loet (1997).

Unlinked References

Ghafoor, A., (2013), “Role of Higher Education in the Socio-Economic Development” International Conference on Intellectual Capital Management, held in Zanjan, Iran, 11-12 Sep, 2013.

Higher Education Commission (HEC), Pakistan, Policy Documents.

National University of Sciences and Technology (NUST) Corporate Advisory Council (CAC), Pakistan Policy Documents.

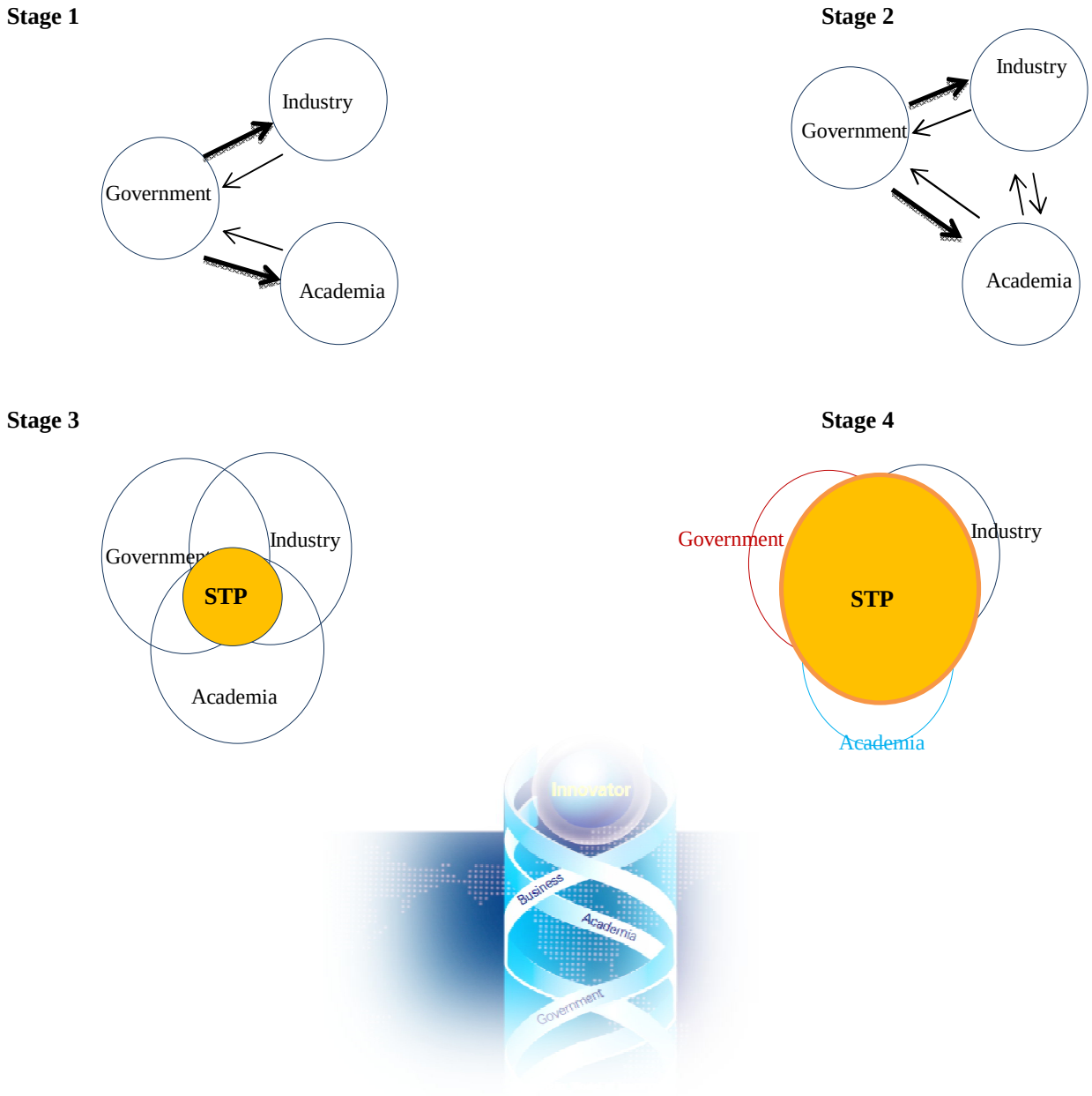

Figure1: Evolution of Triple Helix Model through various stages

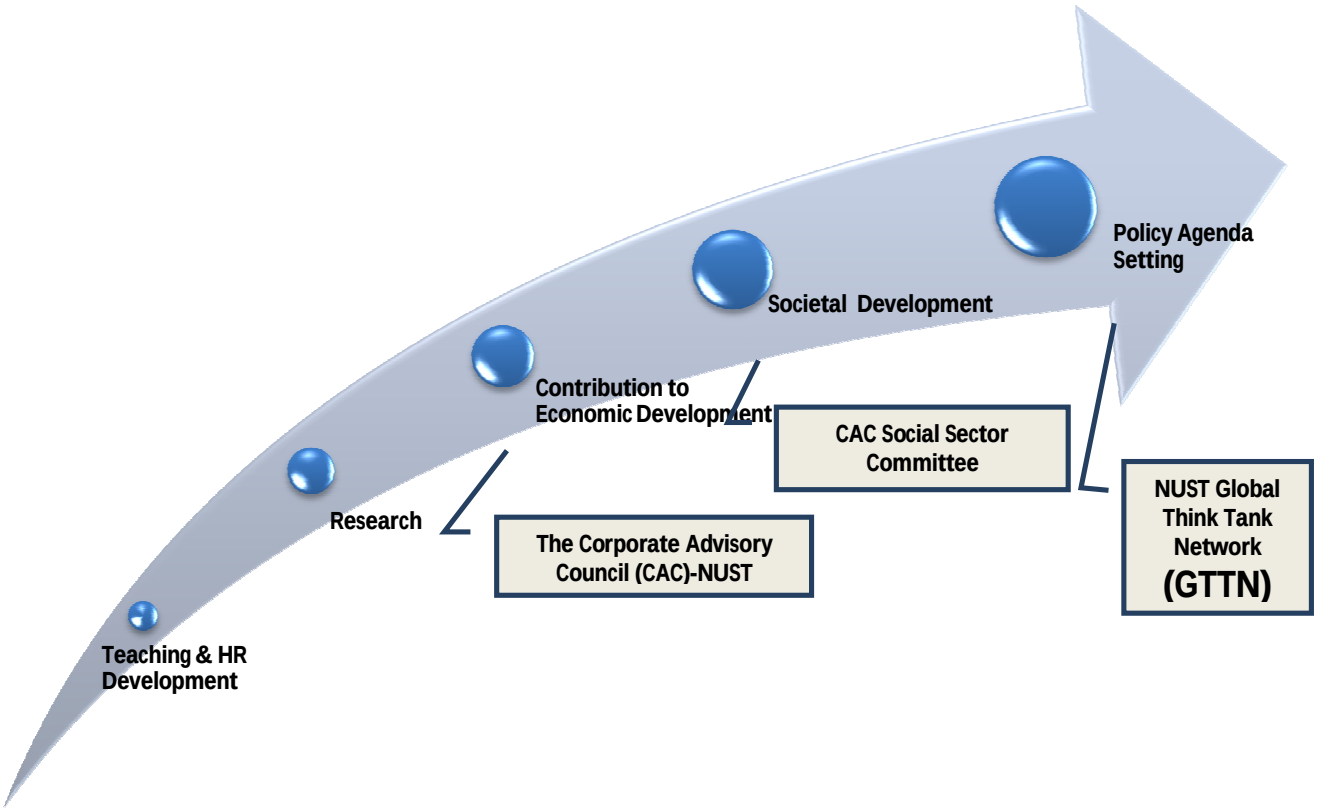

Figure 2: Role of universities as evolved over the period

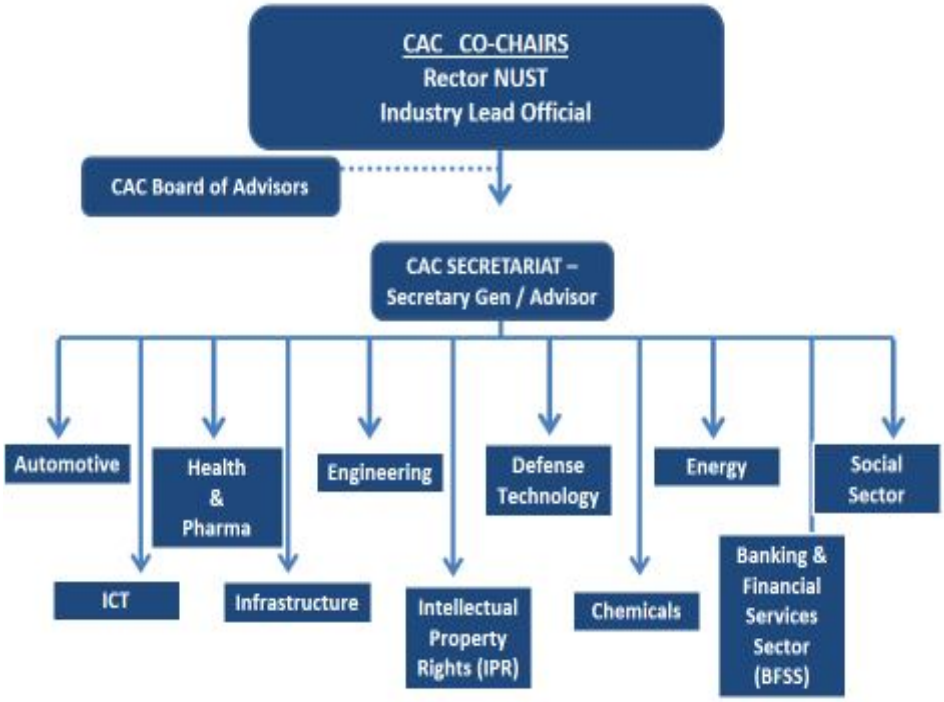

Figure 3: Organizational Structure of CAC

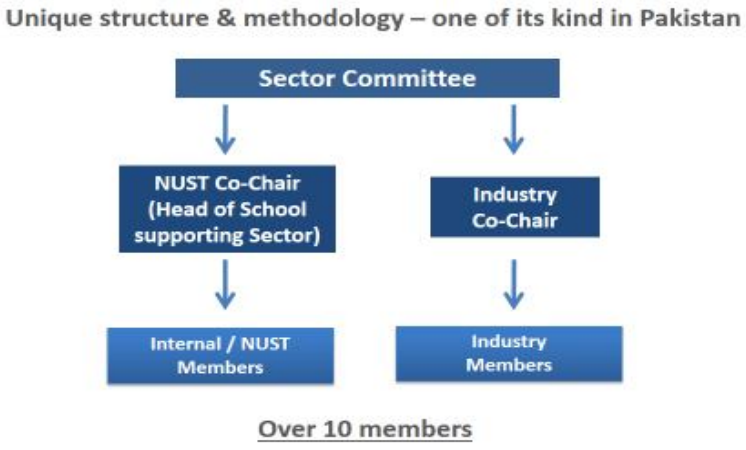

Figure 4: Structure of Sector Committee

Paper ID: KL-07

Implication of Vehicle Aerodynamics on Fuel Savings and the Environment

Firoz Alam and Simon Watkins
School of Aerospace, Mechanical and Manufacturing Engineering, RMIT University, Melbourne, Australia
E-mail: firoz.alam@rmit.edu.au

Abstract

Road vehicles use a large amount of power to overcome aerodynamic resistance (drag) at normal highway speed. The reduction of aerodynamic drag allows not only increasing profit margin of vehicle operation but also reduces energy consumption and greenhouse gas emissions. In order to minimise aerodynamic drag and thereby fuel consumption, streamlining the body shape and minimising flow separations are paramount. Various methods and application of energy saving devices for cars and commercial vehicles are explored and the need for aerodynamic streamlining of commercial vehicles especially truck shapes in developing countries is stressed.

Keywords: Aerodynamics, drag, fuel savings, vehicle, greenhouse gas.

1. Introduction

According to European Regulations, the CO_2 emission from a new vehicle in 2012 cannot be exceeded by 120 grams per km and in 2020 this figure should be limited to 95 grams per km [1]. Additionally, stiff market-competition and rising fuel price force vehicle manufacturers to develop fuel efficient vehicles to be competitive, and economically viable. One way to develop fuel efficient vehicles is the reduction of aerodynamic drag as it accounts for around 80% of the total drag at vehicle cruising speeds over 80 km/h [2]. The reduced drag will not only lower the fuel consumption but also the CO_2 emissions. The major drag reductions have been achieved by optimising vehicle exterior body shapes over four decades. At low speeds the main source of drag is the rolling resistance. Typically, the aerodynamic drag of a medium-sized car accounts for 75-80 percent of the total resistance to motion at 100 km/h, the rest being mainly rolling resistance [2]. Therefore, reducing aerodynamic drag contributes significantly to the fuel economy of a road vehicle. The primary objectives of this paper are to give a broad overview of possible reduction of aerodynamic drag for modern passengers cars, medium and large trucks widely used and to give some insights into the research work that are being undertaken at RMIT University in Australia.

2. Aerodynamic drag of passenger cars and trucks

The aerodynamic shape of passenger cars is greatly dictated by the functional needs of the consumers. The shape of the car should be such that consumers can drive or ride comfortably, can see out of the car and also that the vehicle complies with safety regulations. Drag reduction, more efficient engine technology and weight reduction, became the primary design goals for vehicle engineers and designers around the world in the 1960's to 1980's. Average drag coefficients for typical cars dropped substantially from around 0.5 in the 1960's to typically 0.3 in the late 1980's and mid 1990's [2, 29]. Lowering the drag coefficient for passenger cars below 0.30 will require attention of the underside and internal (cooling) flows. For example, the underneath of many cars is aerodynamically very rough (axles, wheels, muffler, fuel tank, shock absorbers, brake, etc). Streamlining the under-body will not only reduce the drag but also decreases lift. However, this streamlining will create problems for thermal management (exhaust, brake and differential cooling performance). Other adds-on such as side rear view mirrors, roof racks, and antenna do not increase drag significantly but they are the potential sources of aerodynamic noise. In passenger car design, the shape is entirely the domain of the major manufacturers. However, for commercial vehicles where load shapes are determined by the operators, changes can be affected by the operators, including the fitment of shape-changing devices generally known as drag-reducing or add-on aerodynamic devices.

2.1 Drag reduction of passenger cars

The aerodynamic efficiency indicator (drag coefficient) started to fall from around 0.50 for a typical passenger car in 1960s to 0.28 in 2012 (see Fig. 1. The future drag reduction areas that will come from sources other than upper body shape are the smooth under-body, wheel and wheel wells and convoy driving. However, it is not easy to achieve the drag optimisation in these areas as they are interrelated with vehicle cooling performance. The major drag reductions have been achieved so far by optimising vehicle exterior body shapes over four decades. Further reduction can affect the vehicle styling – an important factor for customer perception (aesthetics) and marketing. The only areas left for further reduction of drag without affecting the styling are the vehicle under body, wheels and wheel wells and cooling drag. However, these areas are very sensitive to vehicle cooling needs. The overall drag generated by various body parts of a typical passenger car is shown in Fig. 3. The figure shows that a significant portion (55% of the total drag) of aerodynamic drag is produced by the lower section of the vehicle body. Only 45% of the aerodynamic drag is produced by the upper portion of the body. The wheels and wheel wells, and under body drag are generated by the lower portion of a car. The breakdown of drag of a typical family size passenger car clearly indicates the potential areas that can be targeted for possible aerodynamic drag reduction.

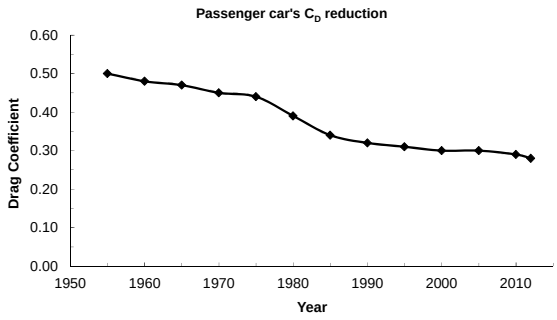

Fig. 1. Passenger car drag reduction chronology [29]

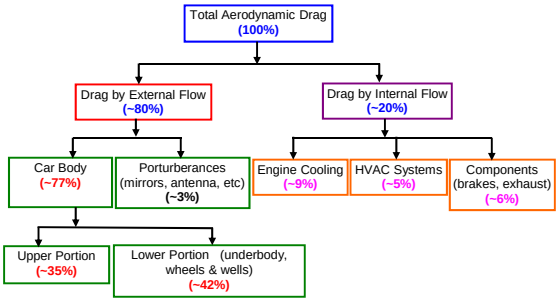

Fig. 2. Breakdown of passenger car aerodynamic drag [29]

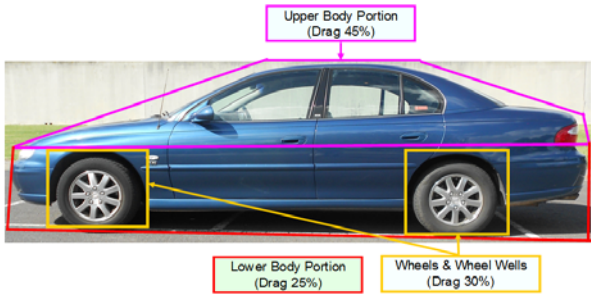

Fig. 3. Aerodynamic drag from external flow over the body [29]

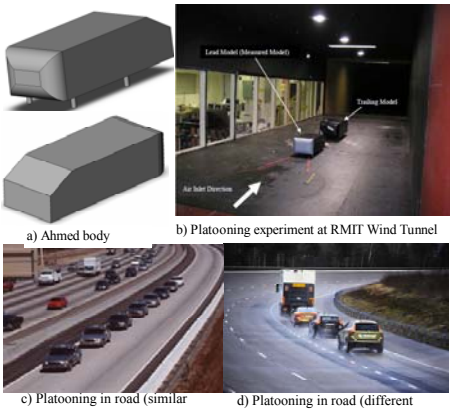

Fig. 4. Vehicles platooning [11, 29]

Freight movement by road vehicles especially by trucks has been gaining momentum world-wide, especially in the developing countries, due to faster road infrastructure development than rail network. Commercial road vehicles (trucks, buses, vans etc) are competing well with traditional rival rail systems thanks to increasingly better road infrastructures, engine and aerodynamic efficiencies and improved payload capacity. However, escalating fuel prices, the need for profitable operation and the greenhouse gas reduction strategy have forced commercial vehicle manufacturers and operators to explore all possible areas for reducing operating costs. The minimum fuel consumption leads to lowering the operating cost which can be achieved by reducing aerodynamic drag. Most high bodied commercial trucks and delivery vans are box type rectangular shape due to load carrying requirement. The box shape generates significantly higher aerodynamic drag compared to streamlined passenger cars. The frontal shape of an un-streamlined truck/van generates most of the drag due to the flow separations and an associated large wake. For un-streamlined trucks or vans, it is estimated that almost 67% of the total drag is exerted on these forward faces, with the remainder 33% coming from the back and the sides due to the complex flow pattern (eg, a combination of separation, reattachment and vortices) [27-28]. For a typical truck at a steady head wind velocity of 80 km/h, nearly 50% of the consumed fuel is used to overcome

aerodynamic drag. It may be noted that with an increase of the velocity, the drag force will rise with the square of the velocity as shown in eq. (1).

$$F_D = C_D \tfrac{1}{2} \rho A V^2 \quad (1)$$

Where, C_D, ρ, V, A are the drag coefficient, air density, velocity and projected frontal area of the truck respectively. The frontal areas of a high-bodied truck, bus, light van, and car are in the ratio of approximately 9: 7: 2.

In order to correctly related the drag coefficient (C_D) with the fuel consumption reduction of a particular vehicle, detailed information about vehicle speed cycle, annual mileage (distance travelled), and baseline engine fuel consumption is required. This is generally being done for a specific vehicle (e.g. [26]). Therefore, discussions in this paper are limited to the reduction of drag coefficient. The reduction of fuel consumption stemming from the decreased C_D value can be determined for specific vehicles if the vehicle's operating environment is known. Vehicle-specific influences on drag coefficient of truck are a) tractor design (classic/aero-style, day-cab/sleeper), b) trailer configuration (dry box, flatbed, tanker), c) gap region between tractor and trailer; and d) appendages (mirrors, deflectors, external air filters, lights, skirts). The environmental influences on truck C_D are a) air properties (barometric pressure, temperature, humidity), b) terrestrial winds (Speed; turbulence intensity, gustiness, wind direction).

2.1.1 Aerodynamic drag associated with cooling flows

The cooling drag associated with the radiator of internal combustion (IC) cars is around 10% of the total aerodynamic drag [2, 5, 29]. The airflow passing through the front end grille and radiator is responsible for the generation of cooling drag. Generally the velocity of the airflow going through the radiator is a function of the vehicle speed and the heat transferred by a radiator is a function of the airflow rate across the radiator [6]. However, the air flow is not uniformly distributed over the entire radiator due to the wake of the bumper bar, etc. which can deteriorate the radiator heat transfer effectiveness due to non-uniform flow on both the air and coolant sides. It is extremely hard to study the complex air flow through the radiator either experimentally and computationally. The RMIT Vehicle Aerodynamics Research Group has developed a special methodology (Specific Heat Dissipation) that can be used to assess the radiator cooling performance as well as cooling drag measurement. Therefore, an experimental program was designed that investigated methods of reducing the airflow through the radiator and engine compartment by shielding the front-end of a passenger vehicle and also measures cooling effectiveness. The velocity distributions as well as the non-uniformity of the cooling airflow across the radiator were measured. In order to investigate the correlation between drag and cooling performance of front grille configurations, an Australian made Ford Falcon AU was selected. This vehicle is a large range family vehicle with a four-speed automatic transmission fitted as standard equipment. The air conditioning and engine cooling components consisted of an air conditioning condenser fitted in front of the radiator, a mechanically driven centrifugal water pump, dual electric fans with shroud combination and an air dam. The air dam aids in engine cooling by creating a favourable pressure gradient for the cooling airflow. The front-end cooling air intakes consist of a decorative grille and a lower intake area. To study the variable front-end geometry, four front-end shielding methods were employed. In each of the methods the front-end cooling air intakes were shielded by an area of ¼, ½, ¾ and totally shut as shown in Fig. 5. The shielding methods employed were vertical, horizontal, side-to-side and side-to-centre. More details about the experimental set up can be found in [7].

The cooling performance and drag were measured using the RMIT University Industrial Wind Tunnel. It is a closed return circuit wind tunnel with a rectangular test section (3 m width, 2 m height and 9 m length). The maximum air speed of the tunnel is approximately 150 km/h. More details about the tunnel can be found in [8]. The solid blockage ratio for the test vehicle is approximately 30%. Despite the high blockage ratio, the tunnel can be used for evaluating cooling performance of a passenger vehicle with confidence using RMIT developed methodology [9-10]. The methodology comprised of 24 pairs of hypodermic tubes inserted into the radiator and condenser assembly, a pressure measuring unit, a computer and the associated software. The system is relatively cheap, reliable, and suitable for measuring complex airflow both in wind tunnel and on-road testing. A detailed description about the system can be found in [10].

In the vertical shielding method evenly-distributed vertical strips were used. The underlying principle for this type of shielding is that many vehicles already have vertical strips as part of their decorative grille and lower cooling intakes. To implement this type of shielding one could envisage plates sliding behind each other that would change the area of the cooling air intakes. However, other vehicles exhibit the opposite by having decorative grilles and lower cooling air intake openings that are covered by horizontally placed strips. The analogous method of shielding that is envisaged is that of having horizontal plates sliding behind each other. The other configuration investigated was closing the intake opening from one side to the other. This

configuration was chosen as it can be applied to small vehicles that have very small radiators and even smaller A/C condensers placed in front of these radiators.

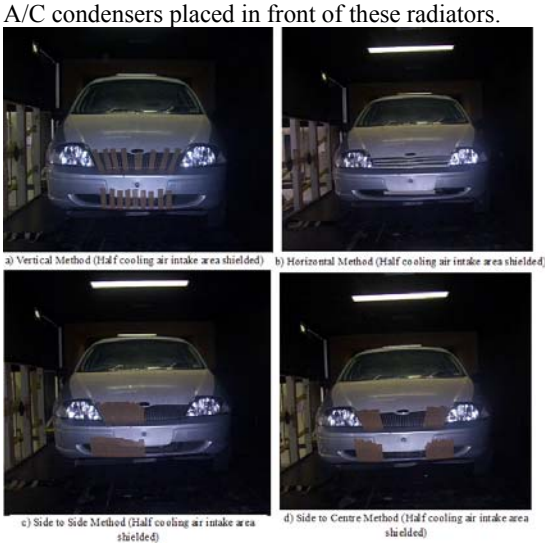

Fig. 5. Test vehicle at RMIT Industrial Wind Tunnel [7, 29]

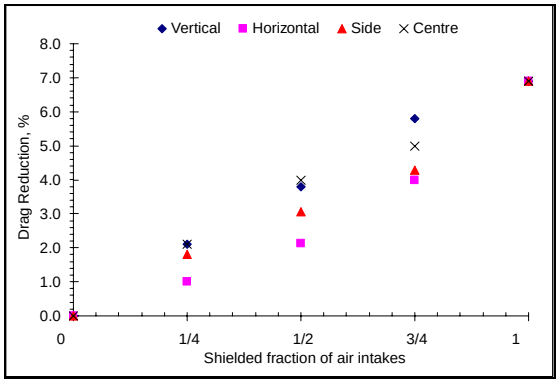

Fig. 6. Drag reduction with shielding at 100 km/h [7, 29]

Instead of this normal arrangement, it was envisaged that the condenser could be placed besides the radiator. Then, in periods of extended non-operation of the condenser (e.g. winter), one could entirely block off the condenser side to the cooling airflow. The last option considered is to symmetrically shield both the grille and lower cooling air intake from both sides to the centre. This last method was used to investigate the interaction between external and internal flows. A/C condensers placed in front of these radiators. Figs 5 and 6 show the effects of shielding on the reduction in drag and heat rejection. The drag reduction was measured on a six-component force and moment balance in the full size open jet wind tunnel at Monash University, Australia. Further details of the test methodology and the influence of shielding on other coefficients (e.g. lift) can be found in [7]. It can be seen that a maximum of 7% drag reduction was achieved by completely shielding the radiator and that the horizontal method gave the least drag reduction when partially shielded. However, the method of shielding made negligible difference to the heat dissipated.

2.1.2 Drag from vehicle under-body

In spite of obvious progress made by production car aerodynamics over the decades, the area of under-body airflow of passenger vehicles still demands detailed investigation and analysis. There are few known published works related to the area of under-body and wheel well airflow. Regarding the under-body of a passenger car, designers look at cooling of under-body components (exhaust, differential, brakes and engine), ground clearance and ramp angle, and simplicity of maintenance. Researchers are trying to find a compromise between these important parameters thus it requires in-depth understanding of all aerodynamic and heat transfer parameters and features of complicated three dimensional under-body airflow. Most vehicle manufacturers are putting emphasis on under-body streamlining and developing special vents or channels for directing air to cool the exhaust, differential and brakes. A significant reduction of drag was achieved without compromising the cooling performance.

2.1.3 Drag reduction from platoons (convoys)

Today's increasing traffic density and Intelligent Transport Systems (ITS) make the formation of platooning (convoys) of vehicles much easier than a decade ago. Under such compact driving conditions (see Fig. 4) considerable favourable interference can occur between vehicles, with potentially drag reductions for both leading and trailing vehicles. The reduced dynamic pressure in the wake of the first vehicle influences the drag coefficient of the vehicle behind (trailing vehicle). Consequently, notable improvement in aerodynamic drag can be achieved even when the distance between the vehicles may be relatively great [14-16]. The reduction of drag by platooning was first exploited in motor racing [2]. The effects of platooning for commercial vehicles have well studied by Hucho [2]. The study showed when a convoy of commercial vehicles is driven at speeds of 80 km/h with an inter-vehicle spacing of 40 m, a drag reduction of 20% can be achieved for the second vehicle and around 30% for the third and every additional vehicle in the platoon for commercial vehicles. However, this

drag reduction will be very shape specific. Since 2004, a series of studies, both experimentally and computationally, was undertaken on platooning effects at RMIT University [16-19].
In order to study the influence of the basic vehicle shape on potential drag reduction the Ahmed body was selected. This is the most researched generic vehicle shape and it features a variety of rear slant angles which can replicate the essence of flows associated with a wide range of vehicle geometries. In particular with a rear slant angle (measured from the horizontal) of 25 degree, the flow is attached down the rear of the model and due to the high levels of lift and associated induced drag the total drag coefficient is high. When the angle is increased to greater than 30 degree the flow does not attach down the rear of the model and the lift and associated induced drag falls. Figure 7 shows the variation of drag with rear slant angle for an isolated Ahmed body. To investigate how the rear slant angle influences two vehicles of similar size in convoy, a series of experiments were undertaken where 25 degree and 35 degree slant models were placed at various inter-vehicle spacing. The drag reduction varies strongly as a function of vehicle spacing with negligible reduction for spacing greater than 2L (see Fig. 7). Further details of this effect and mapping of the wake flow can be found in [19].

In order to study the influence of different size vehicles a similar experiment was conducted but with Ahmed body of 30 degree rear slant angle and of different scale. The leading vehicle was 75% scale of the trailing and the experimental set up can be seen in Fig. 4b. Figure 7 shows the variation of drag coefficient of the leading Ahmed model with vehicle spacing. The reductions in drag coefficients for very close coupling vehicles varied widely and this is dependent on rear slant angle. Surprisingly for some geometries a small drag increase is noted for the trailing vehicle. More details can be found in [17]. Fundamental considerations indicate very significant reductions are possible for extremely closely coupled vehicles, as demonstrated by the very low drag coefficients (per unit volume) for streamlined train shapes. Since the increasing use of intelligent transport systems permit very close coupling it is recommended that further attention be paid to this aspect.

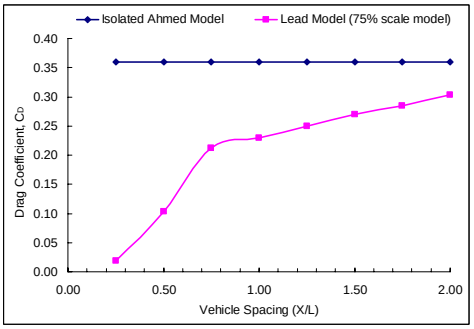

Fig. 7. Effects of platooning on drag coefficient for two different scale Ahmed models [29]

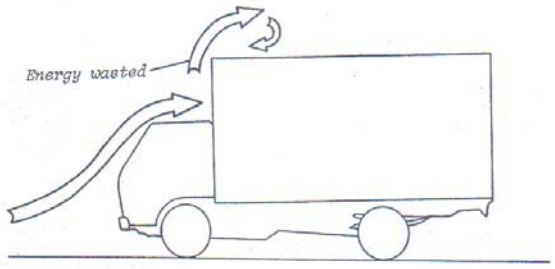

Fig. 8. Flow pattern around a bread delivery van [26-28]

2.1.4 Drag reduction from wheels and wheel wells

Passenger car's wheels and wheel wells generate a significant amount of aerodynamic drag (~25%). Part of the drag originates from the wheels and wheel wells directly, but also due to notable interactions with surrounding flow fields. The high level drag contribution by wheels and wheel wells is primarily due to extremely un-streamlined wheels, the oblique approach of wind (under yaw), and rotation of wheels within wheel wells [2]. Our aerodynamic understanding is limited for both stationary and rotating wheels even without the presence of wheel wells. At present no consistent physical model for the flow around a wheel within a wheel well is available apart from limited data [18, 20-23]. Only the phenomenological data are available which indicate that the smaller the volume of a wheel housing relative to the wheel's volume, the smaller the drag and lift of a wheel; the effect on drag, however, is comparatively small. Considering the huge effort spent on optimising vehicle upper body and under-body, despite being the large drag contributor by wheels and wheel wells, it is time now to look into more closely the aerodynamics of wheels.

The aerodynamic study on wheels and wheel wells at RMIT indicated that the clearance gap around the front wheel and well, except on top reduces aerodynamic drag and lift. The aerodynamic performance of the total vehicle can be improved further using skirt around the front wheel well. The larger diameter front wheel reduces drag but increases lift. A smaller gap on top of the rear wheel or the wheel being shifted into the rear wheel-well caving is the most effective way to reduce aerodynamic drag. The larger rear wheel diameter similar to front wheel reduces the drag. The larger gap around the rear wheel and wheel well increases drag therefore it is not recommended to use. The effects of cooling were not considered in these studies. However, a combined study

on aerodynamics and brakes cooling is needed to optimise the aerodynamic parameters and cooling performance. Further details can be found in [18].

2.2 Drag reduction of trucks

A decisive factor is the aerodynamic quality of the vehicle shape is the drag coefficient (C_D). Due to varied shapes and sizes, commercial vehicles have a wider range of drag coefficients than cars. Buses have drag coefficients about 1.5 times those of cars, and tractor-semi-trailers units, and trucks and trailers units about double. Only light vans, which are more aerodynamically efficient, have the drag coefficients close to passenger cars [2]. Drag coefficients of various commercial vehicles are shown in Fig. 9. Heavy commercial vehicles are considered aerodynamically inefficient compared to other ground vehicles due to their un-streamlined body shapes. As mentioned earlier, a large commercial vehicle travelling at 100 km/h consumes about approximately 52% of the total fuel to provide power to overcome the aerodynamic drag [1-2]. In contrast, a passenger car under the same driving conditions, consumes approximately 4 times less to overcome drag. Generally, a heavy commercial vehicle's annual mileage can vary between 100,000 km and 160,000 km. Therefore, any reduction of aerodynamic drag will result in huge fuel savings and reduction of greenhouse gas emission. Although a significant effort was made by researchers over the decade to develop various fuel saving devices for commercial vehicles [2], there is still scope to further reduce the aerodynamic drag.

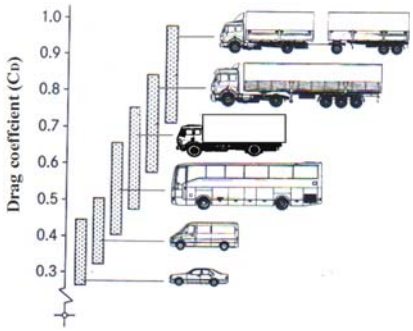

Fig. 9. Drag coefficients of different commercial vehicles [2]

The fuel consumption in litre (L) as a function of the total drag (F_D) for a petrol engine powered truck is given as [38]:

$$\frac{L}{100} = 0.01264 \times F_D \qquad (2)$$

While for a diesel engine powered truck:

$$\frac{L}{100} = 0.008051 \times F_D \qquad (3)$$

As discussed earlier, the external shape of a commercial vehicle (truck, bus, van etc) is determined mainly by the cargo space (trailer box).

Therefore, the main option for drag reduction is to improve the aerodynamic shape of the front end of the vehicle (cab or cabin) using various devices in front of the trailer to minimise the aerodynamic drag.

Commercial vehicle manufacturers are looking for every opportunity to minimise the fuel consumption by improving aerodynamic efficiency (i.e., lowering the drag force). Fuel savings through aerodynamic refinements of the tractor (cab) and the trailer, the development of electronically controlled engines, training drivers to drive for fuel economy, and developing more efficient transmissions offer opportunities to increase the efficiency of trucks and cars significantly. This will not only reduce operating costs (increase greater profitability) but also reduce dependency on fossil fuel and save environment from exhaust pollution. Researchers in various countries including Australia have been working hard to refine the commercial vehicle body-shape (cab and trailer) in order to reduce the aerodynamic drag.

Visualised airflow over a truck model without any drag-reducing devices shows the complex nature of airflow over the cabin and the body (Fig. 8). Usually, airflow passes over the cabin and hits the trailer if the trailer height is greater than cab height. Depending on the trailer height, gap (measured from the cabin rear end to the body front) and magnitude of crosswinds, the airflow may negotiate the sharp-edged corner of trailer or forms a reverse flow below the stagnation line in the gap or on the trailer and cabin-top. The separated flow generates significant aerodynamic drag. In order to avoid this unwanted flow separation, various devices can be used on commercial vehicles.

Many trucks are equipped with various fuel saving devices or add-ons using aerodynamic shapes in front as well as different parts of the truck to minimize drag. Without out changing the projected frontal area of the truck, it is possible to modify the shapes of the truck including the container box in a more streamlined way. These external attachments can minimize aerodynamic drag based on their external shapes, sizes and placements. The aerodynamic effects on current designs of aerodynamic fairings (front and side) and their combinations were not well studied and documented. As the number of trucks have been increased significantly worldwide due to increased logistic transportation, it is utmost important to study the effectiveness of fuel saving devices on existing trucks in order to minimize aerodynamic drag. Although a series of research on truck aerodynamics has

been undertaken in 1970s, 1980s and early 1990s (see Copper [25], Saunders et al. [26], Watkins et al. [27-29]), there is significant scope to improve aerodynamic efficiency further. Most of these studies focussed on fore-body of the cab and cabins and the use of various fuel saving devices. Recently we have undertaken several aerodynamic studies to look for possibilities for further reduction of aerodynamic drag using aerodynamic fairings with various combinations in order to increase its effectiveness. The RMIT Wind Tunnel was used to measure the aerodynamic drag on the experimental model. The maximum speed of the tunnel is approximately 145 km/h. Details of this tunnel can be found in [8]. In order to keep the airflow around the test vehicle as practical as possible, a 10% scale model of a semi-trailer truck was used. The experimental truck model was connected through a mounting strut (see Fig. 10) with the JR3 multi-axis load cell, also commonly known as a 6 degree of freedom force-torque sensor made by JR3, Inc., Woodland, USA. The sensor was used to measure all three forces (drag, lift and side forces) and three moments (yaw, pitch and roll) at a time. Each set of data was recorded for 10 seconds time average with a frequency of 20 Hz ensuring electrical interference is minimized. Multiple data sets were collected at each speed tested and the results were averaged for minimizing the further possible errors in the raw experimental data.

All three forces (drag, lift and side force) and their corresponding moments were measured. Tests were conducted at a range of wind speeds (40 km/h to 120 km/h with an increment of 10 km/h) under four yaw angles (0º, 5º, 10º and 15º) to simulate the crosswind effects. Yaw angle (ψ) can be defined as the angle between the vehicle centerline and the mean direction of airflow experienced by the vehicle as indicated in Fig. 10a. Various fuel saving devices (front and side faring) were designed and manufactured for attaching on the base truck model. These add-ons were 10% scale of their full-size to match the scale model. Figure 11 shows different add-ons used in this study

The C_D as a function of speed for various configurations of fairing at 0º yaw angle is presented in Fig. 12. The figure shows that the baseline model has almost constant C_D value about 0.8. Similar results were found by Watkins et al. [27-29]. Generally, C_D values for a semi-trailer truck are ranges from 0.5 to 0.9 depending on the aerodynamic design of the truck. The baseline model has the highest C_D value whereas the model with any fairing attached has lower C_D values. Experimental data also indicate a decrease of C_D values with the increase of speed for the baseline model with any fairing attachment. The baseline model with the front and side fairing, and gap filled (i.e., configuration–a) as shown in Fig. 12 has the minimum C_D value among all other configurations tested.

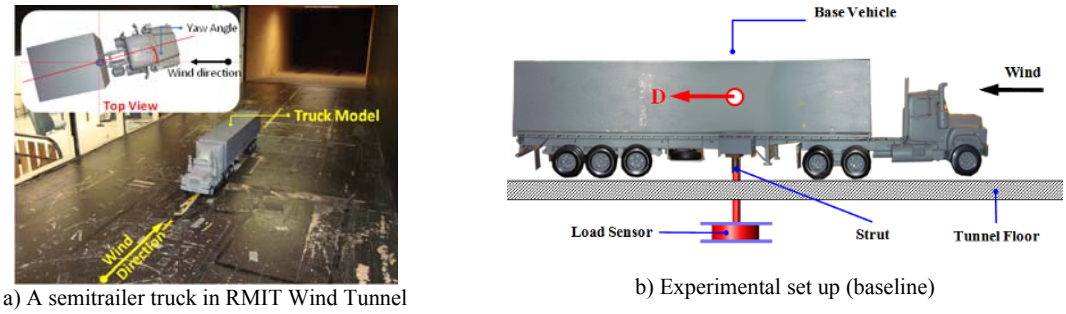

a) A semitrailer truck in RMIT Wind Tunnel

b) Experimental set up (baseline)

Fig. 10. Test vehicle in RMIT Industrial Wind Tunnel [31]

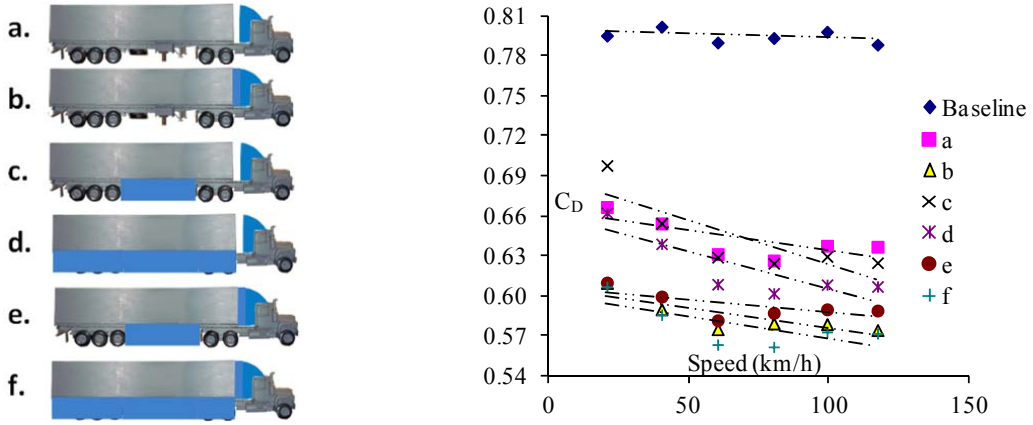

Fig. 11. Different combinations of fairing on the baseline semi-trailer truck model [31]

Fig. 12. Drag coefficient as a function of speed for different test configurations at ψ = 0º base line [31]

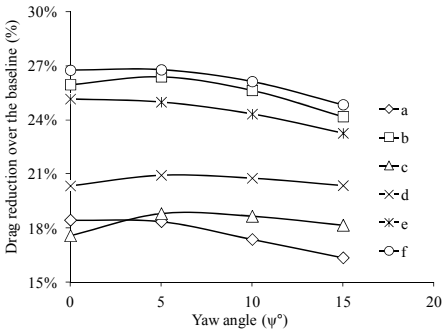

Fig. 13. Drag increase over base vehicle in percentage as a function of yaw angle [31]

Table 1. Percentage reduction of drag on yaw angle variation from 0º to 15º over the baseline [31]

Configuration	Average drag reduction
a	17.6%
b	25.5%
c	18.3%
d	20.6%
e	24.4%
f	26.1%

As mentioned earlier that the base vehicle model has also been tested alone with all attachments with different combinations at other yaw angles (ψ = 5º, 10º and 15º) to study the cross wind effect. The percentage of aerodynamic drag decrease over the base vehicle is shown in Fig. 13 for four yaw angles (ψ = 0º, 5º, 10º and 15º). The yaw angles have different effects on different combinations on the baseline model. For example, aerodynamic drag decreases with the increase of yaw angles for configuration a, e and f. However, the drag increases with the increase of yaw angle up to 5º and thereafter drag decrease with further increase of yaw angle for configurations b, c and d. Table 1 represents the percentage reduction of average drag over the baseline on yaw angle variation from 0º to 15º. The results show that the about 17.6% drag decreased with the "configuration a" and about 26.1% drag reduction with "configuration f".

2.3 Fuel savings for General Trucks in Bangladesh

Road transport is a very fast growing sector in many developing countries. The average annual growth rate of motor vehicles in Bangladesh alone is 10%. Recent studies showed that an average growth of freight and passenger traffics in Bangladesh is approximately 7.7 and 8.3 percent respectively since 199. Over 73% of passenger-km and 66% of freight (ton-km) are now moved by commercial road vehicles.

According a report published by the Bangladesh Road Transport Authority (BRTA), the number of registered motor vehicles rose to 1,899,193 in May 2013 compared to 300,000 in 1995 (over 6.33 times). Currently the number of registered trucks is 96,348 (see Table 2). However, the number would be significantly higher if the unregistered trucks included. The majority trucks in Bangladesh are powered with imported engines and chassis mainly from India (over 90%) and UK (less than 10%). Typical trucks operated in Bangladesh are shown in Fig. 14. Rapid expansion, improved road infrastructures and globalisation will increase the volume of freights significantly in the near future. Commercial vehicles such as trucks will play a dominant role in future transportation in Bangladesh. It is worthwhile mentioning that the total length of paved road network in Bangladesh has been increasing rapidly. There was only 600 km of paved road in 1947, 4000 km in 1971 and over 21,481 km (National Highways – 3,544 km, Regional Highways – 4,278 km & Local or country Road – 13,659 km) in 2013 [32].

At present, the average speed on national highways in Bangladesh is approximately 40 to 50 km/h due to traffic congestion, roadside obstructions, pedestrians and non-motorised transports and lack of traffic rules. However, this cruising speed will be increased significantly with the implementation of traffic rules, construction of double or more lane freeways, segregation of various modes of vehicles, pedestrians, and the expansion of road width. As discussed earlier, with the increase of speeds, the aerodynamic drag will increase and fuel saving will be a required criterion for profitable operations of truck fleet in Bangladesh. Currently locally made cab and body are not at all aerodynamically efficient as shown in Fig. 14. Most body (cab) makers in Bangladesh have no expertise in aerodynamics of vehicles. Streamlining fore-body and various aerodynamic devices will reduce the aerodynamic drag which will intern reduce fuel consumption and greenhouse gas emission. It will also reduce the dependency fuel import and save import bills. The cab shape can be designed in more aerodynamically efficient ways using indigenous and modern technologies if the cab makers are appropriately trained and skilled. It is no doubt that current vehicle body shape (cab and trailer) consumes more fuel per km than it supposed to be. The total fuel consumption by truck fleet in Bangladesh is not known yet as no study was undertaken on this important issue. Truck fleets in Bangladesh are old and smaller in type. In order to obtain a

comprehensive fuel saving characteristics of a particular aerodynamic device, truck specific wind tunnel, on-road tests and computational fluid dynamics (CFD) modeling are required.

Table 2. Various motorized registered vehicles in Bangladesh till May 2013, adapted from [33]

Types of Vehicles	Prior 2010	2010	2011	2012	Till May 2013	Total Till May 2013
Ambulance	2506	287	219	181	83	3276
Auto Rickshaw	108436	18327	20423	23545	6909	177640
Auto tempo	13977	289	175	626	126	15193
Bus	26016	1762	1761	1439	474	31452
Cargo Van	2911	611	489	282	188	4481
Covered van	3760	1898	2354	1421	797	10230
Delivery Van	15564	1499	1004	774	325	19166
Human Hauler	5846	674	1152	715	197	8584
Jeep	30162	2124	2134	1569	507	36496
Microbus	59404	6975	4051	3044	998	74472
Minibus	24749	895	276	249	77	26246
Motorcycle	**650147**	**109110**	**114616**	**101588**	**34664**	**1010125**
Pick Up (Utility Vehicle)	23273	8967	10460	7625	2686	53011
Passenger Car	**196870**	**22960**	**12950**	**9224**	**3393**	**245397**
Special Purpose Vehicle	5900	471	396	226	91	7084
Tanker	2379	327	317	195	113	3331
Taxicab	44361	19	75	172	42	44669
Tractor	16855	3745	5200	3494	945	30239
Truck	**73336**	**9535**	**7327**	**4335**	**1815**	**96348**
Other	934	383	7	1	428	1753
Total	**1307386**	**190858**	**185386**	**160705**	**54858**	**1899193**

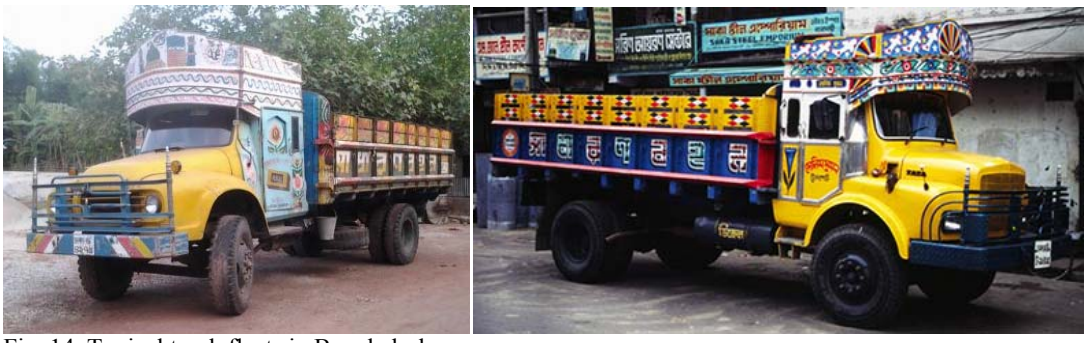

Fig. 14. Typical truck fleets in Bangladesh

3. Concluding Remarks

The reduction of aerodynamic drag is vital to achieve higher vehicle fuel economy and lower greenhouse gas emission. Platooning offers a reduction in aerodynamic drag on all vehicles (cars, trucks and buses) in the platoon, even the lead vehicle. In order to achieve the full benefit of platooning, smart technology and specially developed roads are required to form or leave the platoon, keep optimal spacing and interact between the platoon vehicles and non-platoon vehicles.

An average 5 to 25% fuel consumption reduction can be achieved using various aerodynamic devices and forebody streamlining. The aerodynamic fairings have notable impact on aerodynamic drag. The front fairing alone can reduce around 17% of drag. Further drag reduction up to 26% is possible using various combinations of aerodynamic fairings in different parts of the truck body. The baseline model with the front fairing and side covering including filling the gap between the truck and container box exhibits maximum drag reduction among all configurations tested.

Fuel savings are more relevant for developing countries like Bangladesh than oil rich Middle East. However, the reduction of fuel consumption reduces greenhouse gas production. Many developing countries' truck fleets are old and smaller in type. There are opportunities for incremental decreases on passenger cars and trucks drag. A comprehensive study is needed on goods trucks used in Bangladesh to determine fuel saving characteristics of a particular aerodynamic device.

Acknowledgement

The authors express their sincere thanks to former research associates and members of Vehicle Aerodynamics Research Group: Harun Chowdhury, Giaccino Vino, Hussain Jama, Riccardo Pagliarella, Eton Ng, Satya Prasad Mavuri, Gokul Krishna Rajamani for obtaining data used in this paper.

References

[1] European Automobile Industry Report 2009/2010. ACEA: www.acea.be, accessed on 10 December 2011.
[2] Hucho, W.H., "Aerodynamics of Road Vehicles". Fourth ed., 1998, SAE International, ISBN 0-7680-0029-7, p. 1-918.
[3] Alam, F., Chowdhury, H., Moria, H. and Watkins, S., Effects of Vehicle Add-Ons on Aerodynamic Performance, Proceedings of the 13th Asian Congress of Fluid Mechanics, ISBN: 978-984-33-22214-2, 17-21 December 2010, Dhaka, pp. 186-189,
[4] Wikipedia: http://en.wikipedia.org/wiki/Automotive_aerodynamics, accessed on 12 February, 2012
[5] Carr, G. W., "Potential for aerodynamic drag reduction in car design, Impact of Aerodynamics on Vehicle Design", Int. Journal of Vehicle Design, 1983. SP3: pp. 44-56.
[6] Lee, Y.L. and Hong, Y.T, "Analysis of Engine Cooling Airflow including Non-uniformity over a Radiator", Int. Journal of Vehicle Design, 2000. 24 (1): pp. 121-135.
[7] Jama, H., Watkins, S. and Dixon, C., "Reduced Drag and Adequate Cooling for Passenger Vehicles Using Variable Area Front Air Intakes", SAE Technical Paper 2006-01-0342, 2006.
[8] Alam, F., Zimmer, G. and Watkins, S., "Mean and time-varying flow measurements on the surface of a family of idealized road vehicles", Experimental Thermal and Fluid Sciences, 2003. 27(5): pp. 639-654
[9] Lin, C.H., "Specific Dissipation as a Technique for Evaluating Motor Car Radiator Cooling Performance", PhD thesis, 1999, RMIT University, Melbourne.
[10] Ng, E., Watkins, S., Johnson, P.W., and Grant, L., "Wind Tunnel Tests of Vehicle Cooling Performance at High Blockage", SAE 2000-01-0351, 2000, SAE World Congress, Detroit, USA.
[11] http://green.autoblog.com/2010/08/11/, accessed on 23 January 2012
[12] Landman, D., "Flow field features and aerodynamic drag of passenger cars", Lecture Note, Department of Aerospace Engineering, Old Dominion University, Norfolk, USA.
[13] MotoIQ: http://photos.motoiq.com, accessed on 22 March 2012.
[14] Barnard, R.H., "Road Vehicle Aerodynamic Design", Third ed. 2010. Mechaero Publishing, ISBN-13: 978-0954073473, p. 276.
[15] Azim, A.F., "An Experimental Study of Aerodynamic Interference between Road Vehicles", SAE Paper 940422, 1994.
[16] Watkins, S. and Vino, G., "On Vehicle Spacing and its Effect on Drag and Lift", Proceedings, Fifth International Colloquium of Bluff Body Aerodynamics & Applications (BBAA5), July 2004, Ottawa, Canada.
[17] Rajamani, G K, "CFD Analysis of Air Flow Interactions in Vehicle Platoons", M.Eng Thesis, 2006, RMIT University.
[18] Mavuri, S.P and Watkins, S., "The influence of wheel-housing shape on vehicle aerodynamic performance", Int. Journal of Vehicle Design, 2011. 57 (2/3): p. 275-291.
[19] Pagliarella, R., Watkins, S., and Tempia, A., "The Effect of Rear Slant Angle on Vehicle Wakes and Implications for Platoons", SAE Technical Paper 2006-01-0341, 2006.
[20] Cogotti, A., "Aerodynamic characteristics for car wheels", Int. Journal of vehicle Design, SP3, 1983. p. 173-196.
[21] Jerhamre, A. and Bergström, C., "Numerical Study of Brake Disc Cooling Accounting for Both Aerodynamic Drag Force and Cooling Efficiency", SAE Technical Paper 2001-01-0948, 2001,USA
[22] Wiedemann, J., "The influence of ground simulation and wheel rotation on aerodynamic drag optimisation-potential for reducing fuel consumption", SAE Paper No. 960672, 1996, USA.
[23] Le Good and Garry, K., "On the Use of Reference Models in Automotive Aerodynamics", SAE Technical Paper 2004-01-1308, 2004.
[24] Ahmed S.R. and Ramm G., "Salient features of the time-averaged ground vehicle wake", SAE-Paper 840300, 1984.
[25] Cooper, K.R., "Commercial Vehicle Aerodynamic Drag Reduction: Historical Perspective as a Guide", Canadian Research Council, Ottawa, Canada, p.1-29, 2004
[26] Saunders, J. W., Watkins, S., Hoffmann, P. H. and Buckley, F. T., "Comparison of On-Road and Wind Tunnel Tests for Tractor-Trailer Aerodynamic Devices and Fuel Savings Predictions", SAE Paper No. 850286 (1986), Detroit, USA
[27] Watkins, S., Saunders, J. W. and Hoffmann, P. H., "Wind Tunnel Modelling of Commercial Vehicle Drag Reducing Devices: Three Case Studies", SAE Paper No. 870717, Detroit, USA, 1987
[28] Watkins, S., Saunders, J. W. and Hoffmann, P. H., "Comparison of Road and Wind Tunnel Drag Reductions for Commercial Vehicles", Journal of Wind Engineering and Industrial Aerodynamics, 49 (1993), pp 411-420, 1993
[29] Watkins, S. and Alam, F., Future Vehicle Thermal Cooling and Aerodynamic Drag Savings: Where will they come from?, Proceedings of 2012 International Conference on Advanced Vehicle Technologies and Integration (VTI2012-SS2006), pp. 775-782, 16-19 July, Changchun, China, 2012.
[30] Patten, J., McAuliffe, B., Mayda, W. and Tanguay, B. "Review of Aerodynamic Drag Reduction Devices for Heavy Trucks and Buses", National Research Council Technical Report, pp.1-100, Ottawa, Canada, 2012
[31] Chowdhury, H., Moria, H., Ali, A., Khan, I., Alam, F. and Watkins, S., A study on aerodynamic drag of a semi-trailer truck, Procedia Engineering, Elsevier, Vol. 56, pp. 201-205, 2013
[32] Roads & Highways Department, Ministry of Communications, Bangladesh, retrieved on 16 August, 2013 from http://www.rhd.gov.bd
[33] Bangladesh Road Transport Authority (BRTA), retrieved on 16 August, 2013 from http://www.brta.gov.bd